Volume 72A
Number 3
May–June 1968

Physics and Chemistry

U.S. DEPARTMENT OF COMMERCE

SECTION A

JOURNAL OF RESEARCH

NATIONAL BUREAU OF STANDARDS

Journal of Research

of the

National Bureau of Standards

A. Physics and Chemistry

May–June • 1968

VOLUME • 72A

NUMBER • 3

Editor: C. W. Beckett

Associate Editors: D. D. Wagman
J. M. Richardson

Publication dates:
Feb. 1, Apr. 1, June 1, Aug. 1, Oct. 1, Dec. 1, 1968

JOURNAL OF RESEARCH

The National Bureau of Standards Journal of Research reports research and development in the fields of activity shown at right. Also included from time to time are survey articles on topics closely related to the Bureau's scientific and technical program.

The Journal is published in three separate sections as follows:

A. Physics and Chemistry

Contains papers of interest primarily to scientists working in these fields. Issued six times a year. Annual subscription: domestic, $5.00; foreign, $6.00. Single copy, $1.00.

B. Mathematical Sciences

Presents studies and compilations designed mainly for the mathematician and the theoretical physicist. Issued quarterly. Annual subscription: domestic, $2.25; foreign, $2.75. Single copy, 75c.

C. Engineering and Instrumentation

Reports research and development results of interest chiefly to the engineer and the applied scientist. Issued quarterly. Annual subscription: domestic, $2.75; foreign, $3.50. Single copy, 75c.

The National Bureau of Standards is a principal focal point in the Federal Government for assuring maximum application of the physical and engineering sciences to the advancement of technology in industry and commerce. Its responsibilities include development and maintenance of the national standards of measurement, and the provision of means for making measurements consistent with those standards; determination of physical constants and properties of materials; development of methods for testing materials, mechanisms, and structures, and making such tests as may be necessary, particularly for government agencies; cooperation in the establishment of standard practices for incorporation in codes and specifications; advisory service to government agencies on scientific and technical problems; invention and development of devices to serve special needs of the Government; assistance to industry, business and consumers in the development and acceptance of commercial standards and simplified trade practice recommendations; administration of programs in cooperation with United States business groups and standards organizations for the development of international standards of practice; and maintenance of a clearinghouse for the collection and dissemination of scientific, technical and engineering information. The scope of the Bureau's activities is suggested in the following listing of its three Institutes and their organizational units.

Institute for Basic Standards. Applied Mathematics. Electricity. Metrology. Mechanics. Heat. Atomic Physics. Physical Chemistry. Radiation Physics. Laboratory Astrophysics.* Radio Standards Laboratory.* Radio Standards Physics & Radio Standards Engineering. Office of Standard Reference Data.

Institute for Materials Research. Analytical Chemistry. Metallurgy. Reactor Radiations. Polymers. Inorganic Materials. Cryogenics.* Office of Standard Reference Materials.

Institute for Applied Technology. Building Research. Electronic Instrumentation. Technical Analysis. Center for Computer Sciences and Technology. Textile and Apparel Technology Center. Office of Weights and Measures. Office of Engineering Standards Services. Office of Invention and Innovation. Office of Vehicle Systems Research. Clearinghouse for Federal Scientific and Technical Information.** Materials Evaluation Laboratory. NBS/GSA Testing Laboratory.

*Located at Boulder, Colo. 80302.
**Located at 5285 Port Royal Road, Springfield, Va. 22151.

U.S. DEPARTMENT OF COMMERCE
C. R. Smith, Secretary
NATIONAL BUREAU OF STANDARDS
A. V. Astin, Director

Order all publications from the Superintendent of Documents
U.S. Government Printing Office, Washington, D.C. 20402
Use of funds for printing this publication approved by the Director of the Bureau of the Budget (June 22, 1966).

JOURNAL OF RESEARCH of the National Bureau of Standards—A. Physics and Chemistry
Vol. 72A, No. 3, May–June 1968

Jump Rates for Point Defects in Special Positions Held by a Trapping Center of Noncubic Symmetry

H. S. Peiser and J. B. Wachtman, Jr.

Institute for Materials Research, National Bureau of Standards, Washington, D.C. 20234

(February 14, 1968)

In a previous paper [J. Phys. Chem. Solids **27**, 975 (1966)] the authors have discussed symmetry conditions for equivalence of jump rates operative in point-defect motion between crystallographically equivalent general sites neighboring a trapping center. The treatment is here extended to equivalent special sites to show that the total number of inequivalent jump rates can be expressed as $(N_t/N_d)-q_e-1$ where N_t and N_d are the orders of the symmetry groups of the trap and defect respectively and where q_e is the number of independently effective pairs of nonself-inverse symmetry operators (paired with their inverses) all in the symmetry group of the trap. The number q_e can be obtained by counting any nonself-inverse operator pair, an element of which, when multiplied by any element of the defect symmetry, equals neither its own inverse nor an element of a pair previously counted.

For thermally activated relaxation processes expressions apply for maximum and minimum numbers of jump frequencies involved in complete and partial relaxation processes. For complete relaxation the maximum number is the number of prime factors in the ratio of the order of the symmetry group of the trap to that of the defect group. The minimum number is the minimum number of generators that will raise the defect position symmetry to that of the trap.

Key Words: Crystal symmetry, equivalent sites, jump rates, point defects, relaxation, trapping center.

1. Introduction

In a recent publication [1] [1] we have discussed symmetry conditions for equivalence of jump rates operative in point-defect motion between crystallographically equivalent sites with a view toward an assessment of the extent to which such motion can account for relaxation and diffusion phenomena observable in crystals. Closely related problems have been treated by A. S. Nowick [2] and in papers referred to by him. Our treatment does not depend on linearity of response to an outside influence and is believed to have rather general applicability. In the quoted paper [1] it was applied to a highly specialized situation governed by four restrictions; the partial removal of the second restriction being the contribution in this paper.

Restriction 1: The point defect, though itself relatively mobile, was held to an immobile trapping center, the defect remaining free only to jump between symmetry-equivalent sites on a shell neighboring the trapping center. The effect of this restriction was to reduce a problem concerned with an infinite number of possible defect sites to one concerned with the finite point groups of the trap, G_t and G_t' in the initial and strained conditions, respectively (all basic notation is summarized in table 1). The corresponding point-group orders are designated N_t and N_t'. Both groups are subgroups of the corresponding crystal space groups, and of the crystal point groups G and G' of order N and N', respectively.

Restriction 2: The point group of the point-defect site in the unstrained crystal, G_d, was restricted to the identity 1. In the strained crystal the point group of the defect, G_d', was necessarily 1, too, because by simple symmetry postulate [1] $G_d' \subseteq G_d$. We here relax this restriction to allow the site symmetry of the defect to differ from the identity and we refer to its symmetry as symmetry of specialization. G_d, of order N_d, must be a noncentrosymmetric subgroup of G_t because the trapping center neighbors the defect on only one side. By the correspondence of the shell of sites around the trap with the construction sphere for a stereographic projection, we deduce that the only permitted G_d are the ten symmetries achievable on the surface of a sphere (see tables 3 and 4 in reference [3]), which in turn are isomorphous with the ten two-dimensional diperiodic point groups [4]. Although in three dimensions the presence of the trap imposed the limitation of lack of a symmetry center, this limitation does not apply to the isomorphous two-dimensional groups.

[1] Figures in brackets indicate literature references at the end of this paper.

TABLE 1. *Symbols used for point groups, their orders as well as for individual operators, defect sites and paths*

Crystal		Point group	Order	Symmetry operator in group
Crystal	Unstrained	G	N	S
	Strained	G'	N'	S'
Trap	Unstrained	G_t	N_t	S_t
	Strained	G'_t	N'_t	S'_t
Defect	Unstrained	G_d	N_d	S_d
	Strained	G'_d	N'_d	S'_d

$$G'_d \subseteq G_d \subseteq G_t \subseteq G \supseteq G' \supseteq G'_t \supseteq G'_d \text{ and } G_t \supseteq G'_t$$

where $\supseteq$ indicates a subgroup relationship of the right group to the one written to the left of that symbol.
An S could be a 1, 2, 3, 4, 6, $\bar{1}$, $\bar{2}$, $\bar{3}$, $\bar{4}$ or $\bar{6}$ axial operator to the first positive or negative power.
S^{-1} is specifically an inverse of an S.
$\tilde{S}$ is specifically an inversion axis operator.
$\tilde{S}$ is specifically a rotation axis operator.
$|S|$ is the order of the axis.
Additional suffixes 1, 2, 3 . . . are used to distinguish different operators.
$[uvw]$ is a direction $\epsilon\langle uvw\rangle$ where ϵ means "an element of."
$S[uvw]$ is the direction $\epsilon\langle uvw\rangle$ to which $[uvw]$ is transformed by operator S.
$S_2S_1[uvw] = S_3[uvw]$ when the successive operations S_1 followed by S_2 is equivalent to the single operation of S_3.
$[uvw] \rightarrow S[uvw]$ is a defined path from a site defined by $[uvw]$ to one defined by $S[uvw]$.
$[uvw]\hat{}S$ is the angle between $[uvw]$ and the direction of S.

Indeed the two-dimensional environment of a defect on the surface of the shell and on its tangent plane may be two-dimensionally centrosymmetric.

There exist alternative ways of expressing all possible symmetry operators S. Most systems commonly used allow, in addition to 1, any of the crystallographically permitted rotation axes 2, 3, 4, or 6. To complete a self-consistent set of distinct possible operators S in G we will use inversion axes $\bar{1}$, $\bar{2}$, $\bar{3}$, $\bar{4}$, and $\bar{6}$. Where the order of the operator, $|S|$, defined by the smallest positive integer for which $S^{|S|} = 1$, is greater than 2 (that is for 3, 4, 6, $\bar{3}$, $\bar{4}$, and $\bar{6}$) the operator is nonself-inverse and its inverse is distinct. Nevertheless, if S is an element of G, S^{-1} is, too, i.e., $S\epsilon G \leftrightarrow S^{-1}\epsilon G$. Of the inversion axes only $\bar{2}$, equivalent to a mirror plane, m, provides a possible $S_d\epsilon G_d$. $\bar{2}$ differs from all rotation-axial S_d, denoted $\tilde{S}_d$, in that $\bar{2}_d$ provides a locus of an infinite number of coplanar directions corresponding to defect sites all of which have $G_d \supseteq \bar{2}$, whereas a crystal can only possess a small number of sites with rotational symmetry of specialization. (It is not implied that a defect with $\bar{2}_d$ has a degree of freedom of motion along the mirror plane perpendicular to $\bar{2}_d$. The sites on $\bar{2}_d$ are not in general symmetry related and so can have differing free-energy characteristics.) The possible G_d are then the five $\tilde{S}_d$ alone plus the same five with a perpendicular $\bar{2}_d$ axis ($\tilde{S}_d/\bar{2}_d$). Thus only ten defect groups can occur: 1, 2, 3, 4, 6, m, $2m$, $3m$, $4m$, and $6m$. The effect of the second restriction imposed in our previous paper [1] was further to reduce consideration to equivalent general sites of the point defect. With $G_d = 1$, necessarily, the number of equivalent defect sites was always N_t.

Each site can be defined by a $[uvw]\epsilon\langle uvw\rangle$ where the u, v, w numbers need not be simple integers. Equality of two directions represented by $[u_1, v_1, w_1]$ and $[u_2, v_2, w_2]$ is assured by the conditions that the magnitude and sign of any two of the three ratios $\frac{u}{v}, \frac{v}{w}, \frac{w}{u}$ be the same in the two cases and that the sign of one of the three symbols u, v, w be the same. Every element of $\langle uvw\rangle$ can be described as $S_t[uvw]$, the direction generated by $S_t\epsilon G_t$ acting on $[uvw]$. A path indicated by $[uvw] \rightarrow S_t[uvw]$ will refer to a path from a defect site $[uvw]$ to another site $S_t[uvw]$. Of the infinite number of such geometric paths a choice can be made to fulfill some specific conditions. If the notation were applied to crystal-chemical networks, it might be adequate to designate the straight-line path. In other applications a great-circle path is satisfactory. In our work here, we mean the path which has the largest jump rate, which, in turn, approximates that of minimum free-energy barrier. The path for largest jump rate need not be straight, nor lie on the surface of the shell containing the sites and has no single geometric representation to justify fully the use of the singular word "path" which, nevertheless, we use. One may think of a path with a finite not-sharply delineated width. The removal of restriction 2 will necessitate a further reexamination of the concept of the path (see sec. 2).

In our previous work [1], for which always $G_d = 1$ and for which the number of sites, consequently, equaled the number of elements in $\langle uvw\rangle$, i.e., N_t, the number of nonzero paths emanating from $[uvw]$ was always $N_t - 1$. Symmetry requires that these paths from $[uvw]$ are fully representative of all paths relevant to $\langle uvw\rangle$. This rule will apply equally for $N_d > 1$.

The aim of the present paper is then to remove this second restriction, but we simplify our task by restricting discussion to noncubic trap sites G_t.

Restriction 3: We have assumed that (in our new nomenclature)

$$[uvw] \rightarrow S_t[uvw] = [uvw] \rightarrow S_t^{-1}[uvw] \qquad (1)$$

even when $|S_t| > 2$ that is when

$$[uvw] \rightarrow S_t[uvw] \neq [uvw] \rightarrow S_t^{-1}[uvw].$$

This eq (1) will hold for most physical models one can invent. In our previous paper [1] we have in fact shown that the equation must hold for all steady-state conditions under which the principle of detailed population balance is applicable. Our treatment, though in some ways complicated by this restriction, would lose likely contact with possible experiments if we

removed it. We, therefore, retain the condition imposed by eq (1) throughout this paper.

In our previous paper [1] we found that for each pair of nonself-inverse operators S and S^{-1}, the number J of nonequivalent paths from $[uvw]$ was reduced by one. If q is the number of such S pairs ($|S| > 2$)

$$J = N_t - q - 1 \tag{2}$$

Even after completely upsetting the population in equivalent sites by an externally imposed influence, relaxation by a thermally activated process does not, in general, require all the nonequivalent jump rates to be activated. It is in general impossible to state a number of needed jump rates even for a given G_t. It was, however, possible [1] to derive simple expressions for the minimum number $J_{\min}$, and the maximum number $J_{\max}$ needed completely to relax a system. The minimum number, $J_{\min}$, of nonequivalent jump rates needed completely to relax a system in which the population of defects over equivalent sites had been completely upset was the rank of G_t (the minimum number of operators whose products and powers constitute that group). In most point groups the experimentally observable number of jump rates could be larger than $J_{\min}$ depending on the relative magnitude of the jump rates. There was, however, a usefully restrictive maximum number $J_{\max}$ of nonequivalent jump rates equal to the number of prime factors in N_t. Similarly, simple rules could be formulated for partially upset populations. If N_t' of the N_t initially equivalent sites remained equivalent through a postulated sequence of influences, the minimum number of jump rates, $J_{\min}$, needed for relaxation, was the minimum number of nonequivalent symmetry operators that would raise G_t' of order N_t' to the initial point group G_t.

The maximum number was the number of prime factors in (N_t/N_t'). We presented [1] tabulations of maximum and minimum numbers of jump rates. Experiments designed to observe these points must be carried out at temperatures high enough so that an adequate number of jump rates are above the level of observation, so that point defects can attain equilibrium distributions in finite time.

Restriction 4: Along paths emanating from a given $[uvw]$ predictable cross-over positions may occur with equivalent paths emanating from other elements of $\langle uvw \rangle$. Some crossings must be exact, some may only be approximate, because of limited variability of the radial distance from the trap. As a result some paths must have equal, approximately equal, or lower free-energy barriers than others also emanating from $[uvw]$. These inequalities have not been discussed in detail, nor are they further discussed in this paper. It should be realized, however, that the effect of these inequalities will be to lower the number of experimentally observable distinct jump rates. Accidental equalities of jump rates under specific conditions and within any given experimental precision need not be discussed in the present context.

2. Consequences of Symmetry of Specialization for the Defect Sites

By analogy with the definition of general position in crystallography as the set of symmetry-related positions each of which is left invariant by no other symmetry operator S than the identity, 1, we will use "general direction" to define the $\langle uvw \rangle$ set if a $[uvw]$ ϵ $\langle uvw \rangle$ is not invariant under any operator S_t other than the identity. Similarly "special direction" will signify the $\langle uvw \rangle$ set if at least one S_t (other than the identity, 1) will leave a given $[uvw]$ invariant. The special direction characterizes the symmetry properties of a special position set of a point defect confined to a trap. The stereographic representation of a special direction set $\langle uvw \rangle$ can easily be visualized with the help of the steoregraphic representation of the general direction set for the given G_t [3]. The positions of the general set $\langle uvw \rangle$ are moved, in conformity with the symmetry requirements, on the stereogram into coalescence on the stereographic representation of the defect symmetry group G_d. $\left(\frac{N_t}{N_d} - 1\right)$ paths will then emanate from any $[uvw]$.

The direction $S_d[uvw] \equiv [uvw]$ so that generally for $S_t \notin S_d$:

$$S_t[uvw] \equiv S_t S_d[uvw] \tag{3}$$

where the product $S_t S_d$ signifies the operation required by S_d followed by that of S_t, a product which must equal an operator $S_{t1} \epsilon G_t$; where $S_{t1} \neq S_t$ unless $S_d = 1$. We, therefore, note that for special positions any one direction of the set $\langle uvw \rangle$ can be written in terms of a given $[uvw]$ in N_d ways. All will be of the type $S_t[uvw]$. A given path $[uvw] \rightarrow S_t[uvw]$ can also be written in N_d ways referring to identically the same path by changing only the operator S_t. This is illustrated for the case $G_t = \bar{6}m2$, $G_d = \bar{2}_\perp$ ($\bar{2}_\perp$ signifies $\bar{2} \perp \bar{6}$) in figure 1 with its accompanying table.

The concept of the path itself needs to be examined once more also by reference to figure 1. Reference is made to the path $[uvw] \rightarrow \bar{2}_{||}[uvw]$ for which $S_d = \bar{2}_\perp$ leaves both $[uvw]$ and $\bar{2}_{||}[uvw]$ invariant. For all models for which the geometric path is permitted to depart from the mirror plane of specialization, there will be symmetrically equal geometric realizations of that path on the two sides of the symmetry plane, $\bar{2}_d$. The $2_{[10\bar{1}0]}$ axis relating $[uvw]$ to $\bar{2}_{||}$ $[uvw]$ has a similar effect on any path not going through the angle bisector. Although we are aware of this plurality of some geometric paths $[uvw] \rightarrow S_t[uvw]$ we feel justified in continuing to use the singular word path giving rise to one jump rate. For a given free-energy barrier a geometric path plurality will slightly increase the jump rate, but that enhanced jump rate will be a characteristic of the system, namely, that appropriate for the path $[uvw] \rightarrow S_t$ $[uvw]$. The geometric plurality of paths does not introduce complexities any more than did the path width discussed in the introduction. In fact a wider path with energetically

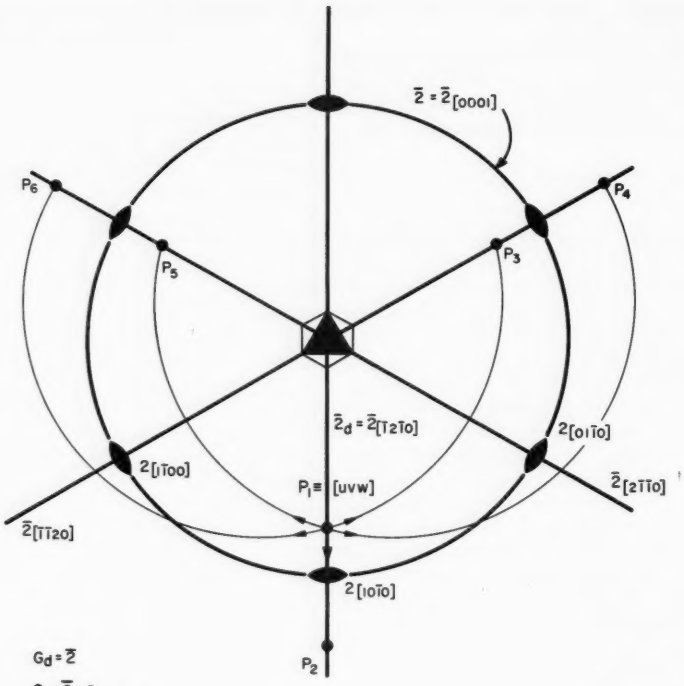

$G_d = \bar{2}$

$G_f = \bar{6}m2$

$N_d = 2$ $\quad \frac{N_f}{N_d} = 6$

$q_e = 2$ $\quad J = 3$

Point	Two Methods of Generation from P_1	Path	Equivalent to Path	Equivalence by Self-inverse Operation	Equivalence by Non Self-inverse Pair
P_1	$1_{[uvw]}$ $\bar{2}_{[1\bar{2}\bar{1}0]\,[uvw]}$	—	—	—	—
P_2	$\bar{2}_{[0001]\,[uvw]}$ $2_{[10\bar{1}0]\,[uvw]}$	$P_1 \rightarrow P_2$	None	—	—
P_3	$\bar{2}_{[2\bar{1}\bar{1}0]\,[uvw]}$ $3_{[uvw]}$	$P_1 \rightarrow P_3$	$P_1 \rightarrow P_5$	$\bar{2}_d$	$3,\ 3^{-1}$
P_4	$2_{[01\bar{1}0]\,[uvw]}$ $\bar{6}^{-1}{}_{[uvw]}$	$P_1 \rightarrow P_4$	$P_1 \rightarrow P_6$	$\bar{2}_d$	$\bar{6},\ \bar{6}^{-1}$
P_5	$\bar{2}_{[\bar{1}\bar{1}20]\,[uvw]}$ $3^{-1}{}_{[uvw]}$	$P_1 \rightarrow P_5$	$P_1 \rightarrow P_3$	$\bar{2}_d$	$3,\ 3^{-1}$
P_6	$2_{[1\bar{1}00]\,[uvw]}$ $\bar{6}_{\,[uvw]}$	$P_1 \rightarrow P_6$	$P_1 \rightarrow P_4$	$\bar{2}_d$	$\bar{6},\ \bar{6}^{-1}$

FIGURE 1. *Equivalence of paths from a special position on a mirror plane in point group* $\bar{6}$m2, *for a defect on a mirror plane,* $m = \bar{2}$.

shallower sides will in the same way lead to lower jump rates.

In the next section we shall obtain the number of independent paths by a procedure involving the counting of the effective number of nonself-inverse operator pairs. We conclude the present section by describing an alternate procedure involving the counting of certain distinct operator product sets; this alternate procedure is perhaps not as easy to apply to specific cases but provides a different point of view. We begin by noting that we need only consider the paths emanating from any one $[uvw]$ and that all paths emanating from a given $[uvw]$ are of the form $[uvw] \rightarrow S_t[uvw]$ where $S_t \not\equiv G_d$ because $[uvw]$ is invariant under all operators in G_d. For two paths to be equal as expressed by $[uvw] \rightarrow S_{t1}[uvw] = [uvw] \rightarrow S_{t2}[uvw]$ the operators must satisfy either of two conditions. First, equality of paths is assured if $S_{t2} = S_{t1}^{-1}$ and S_{t1} is nonself-inverse; this is the only case which can occur for general $[uvw]$ and was previously treated for general sites. Second, if $S_d \epsilon G_d$ and

$$S_{t2} = S_d S_{t1} \text{ or } S_{t2} = S_d S_{t1}^{-1} \tag{4}$$

equality of paths is assured (note that the first condition is contained in the second by taking S_d to be the identity). This second condition holds because an operator S_d which satisfies this condition will leave $[uvw]$ unmoved and will take S_{t1} $[uvw]$ into $S_{t2}[uvw]$. By considering each of the possible operations S_d in turn one can see that each point of the path $[uvw] \rightarrow S_{t1}[uvw]$ is carried into the corresponding path $[uvw] \rightarrow S_{t2}[uvw]$ so that the paths are equivalent and must have equal jump rates. This argument justifies the following procedure for determining the number of independent paths, J: list all of the $S_t \notin G_d$. For each S_t form the set of operator products $S_d S_t$ and $S_d S_t^{-1}$ using all $S_d \epsilon G_d$. J is equal to the number of distinct sets.

3. The Number of Distinct Jump Rates in Terms of the Effective Number of Nonself-Inverse Operators

In this section we shall first show that only nonself-inverse operators need be considered in determining the number of equivalent paths because even though self-inverse operators do in certain instances relate pairs of paths emanating from special positions their effect is always duplicated by the action of nonself-inverse operators. We then consider the fact that distinct pairs of nonself-inverse operators sometimes coincide in their effect on paths emanating from special positions or fail to relate distinct paths so that the effective number of nonself-inverse operator pairs is sometimes less than the total number of distinct pairs.

Two physically distinct paths emanating from $[uvw]$ may be equalized by self-inverse elements of G_d acting directly on the paths or by the demands of nonself-inverse symmetry operators in G_t (compare restriction 3 in the introduction). We can easily cite examples of the second kind of cause without the first being applicable (e.g., $G_t = 4/m$; $G_d = \bar{2}$; $[uv0] \rightarrow 4^{-1}[uv0] = [uv0] \rightarrow 4[uv0]$).

The two paths related by nonself-inverse operators (eq. (1)) need not be related by any element of G_d. Conversely, however, we can prove that two paths related by a self-inverse element of G_d are necessarily also related by a nonself-inverse operator as in eq. (1). Let S_{d1} be a self-inverse operator of G_d which leaves $[uvw]$ invariant; the path $[uvw] \rightarrow S_t[uvw]$ must be equivalent to the path $[uvw] \rightarrow S_{d1} S_t[uvw]$. If $S_t[uvw]$ is also on S_{d1} then two paths connect the same directions and so are considered together as a single path as previously discussed and no equivalence of different paths results. If $S_t[uvw]$ is not on S_d then we can show that either S_t is nonself-inverse or $S_{d1} S_t$ is nonself-inverse. To prove this statement the four possibilities of self-inverse operators 1, 2, $\bar{1}$, $\bar{2}$ for S_{d1} must be considered in turn. The possibilities 1 and $\bar{1}$ can be dismissed at once because the former has no effect and the latter cannot be an element of any G_d. For $S_{d1} = 2$ any mirror plane whose normal is $\|$ to S_{d1} will leave $[uvw]$ invariant; a center, mirror plane, or other 2 axis $\perp S_{d1}$ will generate $[\bar{u}\bar{v}\bar{w}]$ still on S_{d1}. Thus the only self-inverse operators S_t which will move $S_t[uvw]$ off S_{d1} are 2 or $\bar{2}$ axes inclined to S_{d1} whose product with S_{d1} is a nonself-inverse operator. An exactly analogous argument applies for $S_{d2} = \bar{2}$. Note also that if any $|S_d| > 2$ for noncubic G_t all elements of $\langle uvw \rangle$ are coincident with S_d. No $S_d \epsilon G_d$ can then repeat any path $[uvw] \rightarrow S_t[uvw]$ other than into its inverse (i.e., the same path with the direction of motion reversed). We are, however, only concerned with the number of paths emanating from $[uvw]$. We conclude that any pair of paths related by a self-inverse operator is also related by a pair of nonself-inverse operators as in equation 1 and so turn our attention to examining the latter.

If G_t contains no $|S_t| > 2$, i.e., when $q = 0$, no distinct paths can be equal, so $J = \dfrac{N_t}{N_d} - 1$. The total number of nonself-inverse operator pairs may not be effective in relating distinct paths when the $\langle uvw \rangle$ is a special direction set. For a general direction set $\langle uvw \rangle$: $S_{t1}[uvw] \not\equiv S_{t2}[uvw]$. However, for a special direction $\langle uvw \rangle$ it could be that $S_{t1}[uvw] \equiv S_{t2}[uvw]$. Two cases arise: (1) $S_{t1} = S_{t2}^{-1}$ and $S_{t2}^2[uvw] = 1$. This will apply if and only if $[uvw] \| S_t$ $(|S_t| > 2)$. For noncubic G_t all $S_t (|S_t| > 2)$ must be parallel to each other, and for $\langle uvw \rangle \| S_t (|S_t| > 2)$ the number q_e of independently effective pairs of nonself-inverse operators is always zero. (2) The other special case is that in which S_{t1} and S_{t2} are not a mutually inverse pair, yet generate the same path emanating from $[uvw]$. Equation 3, however, expresses all N_d possible ways of expressing a given path. It follows that the condition for this special case is:

$$S_{t1} = S_{t2} S_d.$$

However, for $S_{t1} \| S_{t2}$, all 2 and $\bar{2} \perp S_t$ relate all S_t to $S_{\bar{t}}^{-1}$ only. For $\bar{2} \| S_t$, i.e., a mirror plane perpendicular to S_t, will relate:

$$4 \rightleftarrows \bar{4}^{-1},$$

$$3 \rightleftarrows \bar{6}^{-1},$$

$$\text{and } 6 \rightleftarrows \bar{3}^{-1}.$$

For $\langle uvw \rangle \perp S_t$ therefore $q = q_e$ if $G_d = 2$ and $\frac{q}{2} = q_e$ if $G_d = m$ or $mm2$.

In summary, therefore,

$$J = \frac{N_t}{N_d} - q_e - 1 \tag{5}$$

where $q_e \leqslant q$.

For noncubic G_t and $|S_t| > 2$.

If $S_t \parallel \langle uvw \rangle$	$q_e = 0$
If $S_t \perp \langle uvw \rangle$ and $S_t \parallel \bar{2}$	$q_e = 2$
If $S_t \perp \langle uvw \rangle$ and S_t not $\parallel \bar{2}$	$q_e = q$
If $S_t \wedge \langle uvw \rangle \neq n\pi/2$	$q_e = q$.

The value of q_e can be expressed in words as the following count taken from the q nonself-inverse operator pairs: A pair is counted if neither of its elements multiplied by any element of the defect symmetry equals either its own inverse or an element of a pair previously counted.

4. Jump Rates for Special Defect Directions in Noncubic Point Groups of the Trap Site

For special defect directions $\langle uvw \rangle$ in noncubic trap point groups G_t an exhaustive list of the total number J, of distinct paths, is given in tables 2 and 3 relating to centrosymmetric and other G_t, respectively. The maximum and minimum number of jump rates needed for relaxation is also given in these tables. If the concepts involved are not adequately clarified in the introduction of this paper, the reader is referred to our previous publication [1]. It is noteworthy that for special positions in noncentrosymmetric point groups, $J_{\min} > 2$ occurs only for $G_t = \bar{6}m2$ and $G_d = m_{[0001]}$.

The last two columns of table 2 show additional figures in parentheses corresponding to relaxation jump rates needed after the population has been upset by an influence that itself was centrosymmetric such as homogeneous mechanical strain. For general positions these numbers are always one less than the corresponding one for noncentrosymmetric influences as previously discussed [1], except for the minimum number of paths in point groups having a $\bar{3}$ axis, for which the numbers in parentheses did not differ from

TABLE 2. *Paths for centrosymmetric noncubic trap symmetries; all special positions of point defects*

G_t	N_t	G_d	N_d	$\frac{N_t}{N_d}$	q_e	J	J_{Min}	J_{Max}
							Figures in parentheses refer to limitations for centrosymmetric influence	
$\bar{1}$	2	1	1	2	0	1	1(0)	1(0)
$2/m$	4	2	2	2	0	1	1(0)	1(0)
		m	2	2	0	1	1(0)	1(0)
mmm	8	m	2	4	0	3	2(1)	2(1)
		$mm2$	4	2	0	1	1(0)	1(0)
$\bar{3}$	6	3	3	2	0	1	1(0)	1(0)
$\bar{3}m$	12	m	2	6	2	3	1(1)	2(1)
		2	2	6	2	3	1(1)	2(1)
		$3m$	6	2	0	1	1(0)	1(0)
$4/m$	8	m	2	4	1	2	1(1)	2(1)
		4	4	2	0	1	1(0)	1(0)
$4/mmm$	16	$m_{[100]}$ or $m_{[110]}$	2	8	2	5	2(1)	3(2)
		$m_{[001]}$	2	8	1	6	2(2)	3(2)
		$mm2$	4	4	1	2	1(1)	2(1)
		$4mm$	8	2	0	1	1(0)	1(0)
$6/m$	12	m	2	6	2	3	1(1)	2(1)
		6	6	2	0	1	1(0)	1(0)
$6/mmm$	24	$m_{[10\bar{1}0]}$ or $m_{[2\bar{1}\bar{1}0]}$	2	12	4	7	2(1)	3(2)
		$m_{[0001]}$	2	12	2	9	2(2)	3(2)
		$mm2$	4	6	2	3	1(1)	2(1)
		$6mm$	12	2	0	1	1(0)	1(0)

TABLE 3. *Paths for noncentrosymmetric noncubic trap symmetries; all special positions of point defects*

G_t	N_t	G_d	N_d	$\frac{N_t}{N_d}$	q_e	J	J_{Min}	J_{Max}
1	1	1	1	1	0	0	0	0
2	2	2	2	1	0	0	0	0
m	2	m	2	1	0	0	0	0
222	4	2	2	2	0	1	1	1
$mm2$	4	m	2	2	0	1	1	1
		$mm2$	4	1	0	0	0	0
3	3	3	3	1	0	0	0	0
32	6	2	2	3	1	1	1	1
		3	3	2	0	1	1	1
$3m$	6	m	2	3	1	1	1	1
		$3m$	6	1	0	0	0	0
4	4	4	4	1	0	0	0	0
$\bar{4}$	4	2	2	2	0	1	1	1
422	8	2	2	4	1	2	1	2
		4	4	2	0	1	1	1
$4mm$	8	m	2	4	1	2	1	2
		$4m$	8	1	0	0	0	0
$\bar{4}2m$	8	2	2	4	1	2	1	2
		m	2	4	1	2	1	2
		$mm2$	4	2	0	1	1	1
6	6	6	6	1	0	0	0	0
$\bar{6}$	6	m	2	3	1	1	1	1
		3	3	2	0	1	1	1
622	12	2	2	6	2	3	1	2
		6	6	2	0	1	1	1
$6mm$	12	m	2	6	2	3	1	2
		$6m$	12	1	0	0	0	0
$\bar{6}m2$	12	$m_{[10\bar{1}0]}$	2	6	1	3	1	2
		$m_{[0001]}$	2	6	1	4	2	2
		$mm2$	4	3	1	1	1	1
		$3m$	6	2	0	1	1	1

that corresponding to noncentrosymmetric influences. For special positions, however, there are additional causes for equalities of numbers in and out of parenthesis while in point groups containing a $\bar{3}$ axis a difference in minimum numbers of paths is obtained when the special direction is parallel to that $\bar{3}$-axis.

5. References

[1] J. B. Wachtman, Jr., and H. S. Peiser, Symmetry conditions on jump rates occurring in relaxation times associated with point defect motion between equivalent general sites in crystals, J. Phys. Chem. Solids **27,** 975 (1966).

[2] A. S. Nowick, Dielectric and anelastic relaxation of crystals containing point defects, II. Adv. in Phys. (Phil. Mag. Suppl.) **16,** 1 (1967).

[3] H. S. Peiser and J. B. Wachtman, Jr., Reduction of crystallographic point groups to subgroups by homogeneous stress, J. Res. NBS **69A** (Phys. and Chem.) No. 4, 309 (1965).

[4] N. F. M. Henry and K. Lonsdale, Eds., International Tables for X-ray Crystallography (Kynoch Press, Birmingham, England, 1952).

(Paper 72A3–496)

JOURNAL OF RESEARCH of the National Bureau of Standards—A. Physics and Chemistry
Vol. 72A, No. 3, May–June 1968

The Thermodynamics of the Ternary System: Water-Potassium Chloride-Calcium Chloride at 25 °C

R. A. Robinson [1] and A. K. Covington [2]

Institute for Materials Research, National Bureau of Standards, Washington, D.C. 20234

(January 26, 1968)

Isopiestic vapor pressure measurements have been made on the system: water-potassium chloride-calcium chloride at 25 °C. The osmotic coefficients of the mixed salt solutions and the activity coefficients of each salt in the presence of the other have been evaluated.

Key Words: Activity coefficient, calcium chloride, isopiestic measurements, mixed salt solutions, osmotic coefficients, potassium chloride, vapor pressure.

1. Introduction

Isopiestic vapor pressure measurements have been reported for the systems: water-sodium chloride-barium chloride [1],[3] water-potassium chloride-barium chloride [2], and water-sodium chloride-calcium chloride [3]. Results for the system: water-potassium chloride-calcium chloride are now described.

2. Definitions

M_B is the molality (moles per kilogram of water) of a solution containing only potassium chloride; it is the "reference" from which isopiestic data are calculated.

m_B, m_C, are the molalities of potassium chloride and calcium chloride, respectively, in a solution containing both these salts and in isopiestic (vapor phase) equilibrium with the potassium chloride solution of molality M_B.

$m = m_B + 1.5\ m_C$.

$R = M_B/m$ is the isopiestic ratio.

$x_C = 1.5\ m_C/m$.

$I = m_B + 3m_C$ is the total ionic strength of the solution.

$y_B = m_B/I$.

$y_C = 3m_C/I$.

γ_B, γ_C, are the activity coefficients of potassium chloride and calcium chloride, respectively, in the mixed salt solution.

γ_B° is the activity coefficient of potassium chloride in a solution containing potassium chloride only at the same total ionic strength $I = m_B + 3m_C$ as the mixed solution.

γ_C° is the activity coefficient of calcium chloride in a solution containing only calcium chloride at the same total ionic strength, I.

$\varphi = -55.51\ \ln\ a_w/(2m_B + 3m_C) = -55.51\ \ln\ a_w/[(y_B+1)I]$ is the osmotic coefficient of the mixed salt solution.

φ_B° is the osmotic coefficient of the solution containing potassium chloride only at the same total ionic strength as that of the mixed salt solution.

φ_C° is the osmotic coefficient of the solution containing calcium chloride only at the same total ionic strength as the mixed salt solution.

3. Experimental Procedure and Results

The salts were portions of those used in earlier work [2, 3]. Isopiestic vapor pressure measurements were made in the manner described previously [1]. The results are given in table 1.

4. Discussion

The immediate result of an isopiestic measurement is the information that a solution containing two salts of known molality has the same aqueous vapor pressure as a solution of one of the salts, again at a known molality. Such information is readily transformed into osmotic coefficient data. Activity coefficient data,

[1] Present address: Department of Chemistry, State University of New York at Binghamton, N.Y. 13901.
[2] Guest worker (1966) on leave from the University of Newcastle upon Tyne, England.
[3] Figures in brackets indicate the literature references at the end of this paper.

TABLE 1. *Isopiestic data for the system: potassium chloride* (B)– *calcium chloride* (C)

Set	M_B	m_B	m_C	$\varphi_{(obs.)}$	$\varphi_{(calc.)}$	Set	M_B	m_B	m_C	$\varphi_{(obs.)}$	$\varphi_{(calc.)}$
1	0.7560	0.5219	0.1564	0.8964	0.8942			0.6726	1.2065	1.1193	1.1182
		.2903	.3087	.9002	.8990			.....	1.5264	1.2136	1.2109
		.1347	.4072	.9095	.9055		2.9694	1.8591	0.6052	1.0044	1.0048
		.....	.4948	.9141	.9140			1.0832	1.0040	1.0733	1.0728
	0.7577	0.6384	0.0789	0.8987	0.8944			0.3690	1.3528	1.1588	1.1570
		.4168	.2267	.8980	.8957						
		.1929	.3723	.9047	.9031	7	3.4262	2.8230	0.3250	0.9815	0.9811
								1.7945	.8579	1.0545	1.0552
2	1.1535	0.9288	0.1440	0.9051	0.9041			0.8574	1.3132	1.1494	1.1510
		.5890	.3579	.9204	.9207		3.4611	2.2892	0.6221	1.0196	1.0193
		.2704	.5525	.9427	.9434			1.2082	1.1605	1.1142	1.1151
		.....	.7140	.9675	.9691			0.3930	1.5399	1.2156	1.2153
								.....	1.7164	1.2761	1.2742
3	1.5135	1.3037	0.1310	0.9108	0.9117						
		0.9350	.3559	.9302	.9327	8	3.7176	2.7254	0.5244	1.0125	1.0128
		.5999	.5518	.9571	.9569			1.6537	1.0560	1.0983	1.0982
		.....	.8952	1.0175	1.0180			*0.5957	1.5476	1.2190	.....
	1.5240	1.0898	0.2681	0.9223	0.9240		3.7221	3.1867	0.2866	0.9845	0.9848
		0.7744	.4569	.9427	.9448			2.2269	.7784	1.0489	1.0492
		.4029	.6734	.9740	.9759			1.1373	1.3036	1.1513	1.1529
								.....	1.8128	1.3094	1.3089
4	2.0809	1.2658	0.4755	0.9613	0.9641						
		0.7063	.7865	1.0087	1.0118	9	4.3263	3.7758	0.2844	1.0031	1.0018
		.2483	1.0229	1.0672	1.0600			*2.6197	.8587	1.0784	.....
	2.1530	1.7491	0.2373	0.9370	0.9383			*1.6439	1.3151	1.1653	.....
		1.0520	.6320	.9862	.9881			.....	2.0262	1.3871	1.3859
		0.4806	.9403	1.0431	1.0434		4.3543	3.2196	0.5776	1.0394	1.0380
		.....	1.1896	1.1050	1.1041			*1.9778	1.1736	1.1360	.....
								*0.5997	1.7831	1.2970	.....
5	2.7872	1.9415	0.4654	0.9833	0.9813						
		0.6796	1.1226	1.0982	1.0954	10	4.6033	3.8770	0.3749	1.0188	1.0217
		.3588	1.2791	1.1397	1.1349			*2.4736	1.0524	1.1161	.....
	2.7986	2.3180	0.2674	0.9589	0.9585			*1.0844	1.6724	1.2607	.....
		1.4805	.7194	1.0185	1.0178			.....	2.1195	1.4226	1.4206
		1.0515	.9406	1.0586	1.0567		4.6201	*3.1511	0.7405	1.0656	.....
								*1.5840	1.4625	1.2022	.....
6	2.9689	2.4640	0.2806	0.9632	0.9645			*0.5200	1.9134	1.3396	.....
		1.5330	.7747	1.0310	1.0307						

*Not used in computing values of β_0 in eq (26).

however, have to be obtained indirectly. One method achieves this objective by means of the McKay-Perring procedure [4]. It was shown earlier [1] that if the isopiestic ratios, R, can be expressed in terms of the ionic fraction, x_C, by means of the equation

$$R = 1 + ax_C, \tag{1}$$

the application of the McKay-Perring method is very simple. Even if an additional term is needed,

$$R = 1 + ax_C + bx_C^2, \tag{2}$$

it is still possible to use the method.

Figure 1 shows some of the isopiestic data obtained in the present work. It will be observed that there is considerable curvature in the plots, particularly for those corresponding to solutions of low total ionic strength. It was found that eq (2) was inadequate to represent the experimental results and even the addition of a further term in x_C^3 gave only slightly better agreement. However, even if the equation

$$R = 1 + ax_C + bx_C^2 + cx_C^3 \tag{3}$$

was adequate, it would be difficult to handle the integration needed in the McKay-Perring method.

An alternative, but equivalent, approach, based on the work of Scatchard [5], is now presented. As this should have wide application to the study of mixed salt solutions, it will be described in some detail.

Consider, first, a solution of two salts each of the 1:1 charge type. Let the activity coefficients of the salts in solutions of constant total ionic strength ($I = m_B + m_C$ if the salts are of the 1:1 charge type) be capable of representation by the equations,

$$\ln \gamma_B = \ln \gamma_B^\circ + Q_B y_C + R_B y_C^2 \tag{4}$$

$$\ln \gamma_C = \ln \gamma_C^\circ + Q_C y_B + R_C y_B^2. \tag{5}$$

Here $y_B = m_B/I$, $y_C = m_C/I$ for salts of this charge type. Q_B, Q_C, R_B, and R_C may be functions of I but not of y_B, y_C individually.

It has been shown, by the use of the Gibbs-Duhem equation, [2, 6, 7] that, if eqs (4) and (5) hold, the osmotic coefficient of the solution is given as

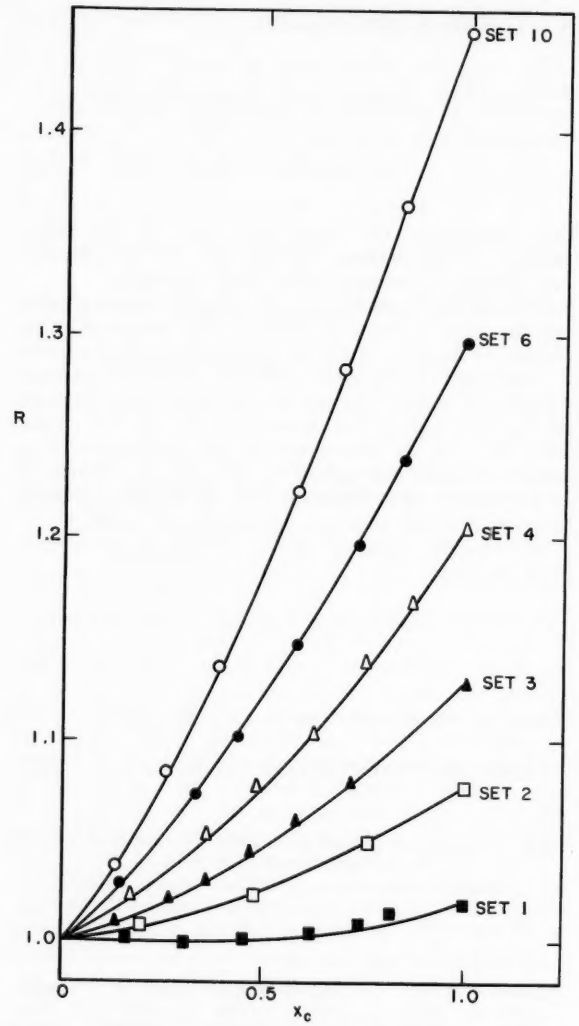

FIGURE 1. *Isopiestic ratio* (R) *versus ionic fraction* (x_C) *of calcium chloride.*

$$\varphi = \varphi_B^\circ + y_C Q_B - \frac{1}{2} y_C^2 (Q_B + Q_C) + y_C^2 \left(1 - \frac{2}{3} y_C\right)(R_B - R_C) \qquad (6)$$

and, by symmetry,

$$\varphi = \varphi_C^\circ + y_B Q_C - \frac{1}{2} y_B^2 (Q_B + Q_C) + y_B^2 \left(1 - \frac{2}{3} y_B\right)(R_C - R_B). \qquad (7)$$

Combining eqs (6) and (7), we get

$$\varphi = y_B \varphi_B^0 + y_C \varphi_C^0 + \frac{1}{2} y_B y_C (Q_B + Q_C) + \frac{1}{3} y_B y_C (y_B - y_C)(R_C - R_B). \qquad (8)$$

Since φ_B^0 and φ_C^0 depend only upon properties of solutions containing a single salt, the departure from ideality on mixing the single salt solutions can be represented as

$$\Delta = 2\varphi - 2y_B \varphi_B^0 - 2y_C \varphi_C^0 = y_B y_C (Q_B + Q_C) + \frac{2}{3} y_B y_C (y_B - y_C)(R_C - R_B). \qquad (9)$$

If $R_B = R_C = 0$ and φ can be described entirely in terms of Q_B and Q_C (the case of the Harned Rule) a plot of Δ against y_C should be symmetrical about the $y_B = y_C = 0.5$ axis. The $(R_C - R_B)$ term allows for a possible skew in the plot.

Figure 2 shows some data for the system: water-sodium chloride (B)–potassium chloride (C) [8]. The value of Δ was calculated using the data in series 6 of this reference. It is true that the values of Δ are taken from data where the total ionic strength varied from 4.0 to 4.5 and, therefore, do not satisfy exactly the condition of constant total ionic strength. However, the figure suffices to show that Δ should be capable of expression by a term in $y_B y_C$ with only a small term in $y_B y_C (y_B - y_C)$.

In Scatchard's equations for a solution containing two 1:1 salts, the osmotic coefficient of the solution is given by the equation

$$2\varphi = 2y_B \varphi_B^0 + 2y_C \varphi_C^0 + y_B y_C \beta_0 + y_B y_C (y_B - y_C)\beta_1 + \ldots \qquad (10)$$

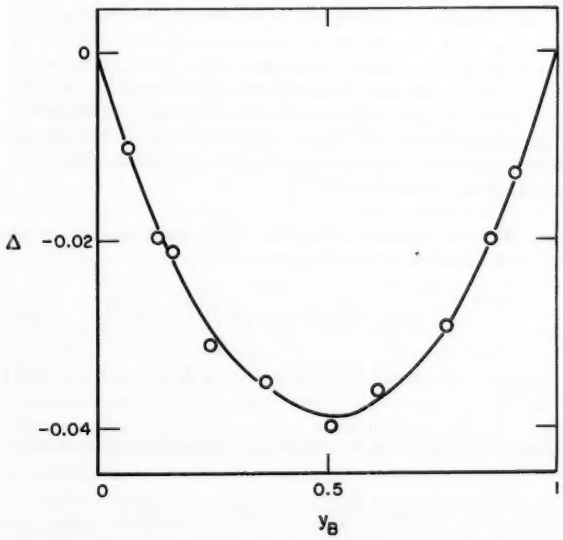

FIGURE 2. *The function* $\Delta = 2\varphi - 2y_B\varphi_B^0 - 2y_C\varphi_C^0$ *for the system: water-sodium chloride* (B)–*potassium chloride* (C) *at 25 °C.*

with

$$\beta_0 = b_{01}m + b_{02}m^2 + \ldots \quad (11)$$

and

$$\beta_1 = b_{12}m^2 + \ldots \quad (12)$$

Unlike the Q and R terms of eqs (4) and (5), b_{01}, b_{02}, and b_{12} are independent of m.

The activity coefficient of salt B is given by the equation

$$2 \ln \gamma_B/\gamma_B^0 = [2(\varphi_C^0 - \varphi_B^0) + \beta_0 + \beta_1]y_C + [(B_0 - \beta_0) + 3(B_1 - \beta_1)]y_C^2 - 2(2B_1 - \beta_1)y_C^3 \quad (13)$$

and that of salt C by the equation

$$2 \ln \gamma_C/\gamma_C^0 = [2(\varphi_B^0 - \varphi_C^0) + \beta_0 - \beta_1]y_B + [(B_0 - \beta_0) - 3(B_1 - \beta_1)]y_B^2 + 2(2B_1 - \beta_1)y_B^3. \quad (14)$$

Here, $B_0 = md\beta_0/dm$ and $B_1 = md\beta_1/dm$. If β_1 does not require terms higher than m^2, then the coefficients of the y_B^3 and y_C^3 terms are zero.

Equation (10) can be written

$$\Delta = 2\varphi - 2y_B\varphi_B^0 - 2y_C\varphi_C^0 = y_By_C(b_{01}m + b_{02}m^2) + y_By_C(y_B - y_C)b_{12}m^2. \quad (15)$$

The procedure then is to use isopiestic data to calculate the osmotic coefficients of mixed salt solutions at all available values of y_B and m. The coefficients b_{01}, b_{02}, and b_{12} are then evaluated by the method of least squares. These, together with the corresponding values of B_0 and B_1, are then substituted in eqs (13) and (14) to get values of the activity coefficients. The application of these equations to the system: water-sodium chloride-potassium chloride has already been considered [9].

For the potassium chloride (B)−calcium chloride (C) system, it is convenient to write

$$2 \ln \gamma_B = 2 \ln \gamma_B^0 + Q_By_C + R_By_C^2 \quad (16)$$

$$\ln \gamma_C = \ln \gamma_C^0 + Q_Cy_B + R_Cy_B^2. \quad (17)$$

The equation for the osmotic coefficient now becomes

$$(y_B + 1)\varphi = 2y_B\varphi_B^0 + y_C\varphi_C^0 + \frac{1}{2}y_By_C(Q_B + Q_C) + \frac{1}{3}y_By_C(y_B - y_C)(R_C - R_B). \quad (18)$$

A convenient deviation function

$$\Delta = (y_B + 1)\varphi - 2y_B\varphi_B^0 - y_C\varphi_C^0 = \frac{1}{2}y_By_C(Q_B + Q_C) + \frac{1}{3}y_By_C(y_B - y_C)(R_C - R_B) \quad (19)$$

now represents the departure from ideality when solutions of potassium chloride and calcium chloride are mixed at constant total ionic strength.

Table 2 gives some values of Δ for this system, utilizing the data of set 6 of table 1. The values of Δ are plotted in figure 3. It will be observed that Δ is smaller for this system than for sodium chloride-potassium chloride mixtures (see fig. 2). The total ionic strength of these solutions lay between 3.3 and 4.4; therefore, they be no means satisfy the condition of constant total ionic strength. The only purpose of figure 3 is to suggest that departures from ideality for solutions of this salt pair are comparatively small.

Scatchard's equations for a system of this charge type become

$$(y_B + 1)\varphi = 2y_B\varphi_B^0 + y_C\varphi_C^0 + y_By_C\beta_0 + y_By_C(y_B - y_C)\beta_1 \quad (20)$$

$$2 \ln \gamma_B/\gamma_B^0 = [(\varphi_C^0 - 1) - 2(\varphi_B^0 - 1) + \beta_0 + \beta_1]y_C + [(B_0 - \beta_0) + 3(B_1 - \beta_1)]y_C^2 - 2(2B_1 - \beta_1)y_C^3 \quad (21)$$

TABLE 2. *Osmotic coefficients of solutions of potassium chloride* (B) *+ calcium chloride* (C) *at 25 °C*

m_B	m_C	y_B	φ	Δ [a]	$\Delta_{(calc)}$ [b]
2.4640	0.2806	0.7454	0.9632	−0.0030	−0.0029
1.8591	.6052	.5059	1.0044	−.0047	−.0056
1.5330	.7747	.3974	1.0310	−.0059	−.0061
1.0832	1.0040	.2645	1.0733	−.0065	−.0058
0.6726	1.2065	.1567	1.1193	−.0051	−.0043
0.3690	1.3528	.0833	1.1588	−.0022	−.0027

[a] $\Delta = (y_B + 1)\varphi - 2y_B\varphi_B^0 - y_C\varphi_C^0$

[b] $\Delta_{(calc)} = -0.0225y_By_C + 0.0150y_C(y_B - y_C)$

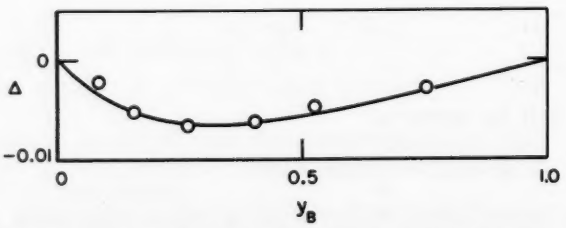

FIGURE 3. *The function* $\Delta = (y_B + 1)\varphi - 2y_B\varphi_B^0 - y_C\varphi_C^0$ *for the system: water-potassium chloride* (B)*−calcium chloride* (C) *at 25 °C.*

$$\ln \gamma_C/\gamma_C^0 = [2(\varphi_B^0 - 1) - (\varphi_C^0 - 1) + \beta_0 - \beta_1] y_B$$

$$+ [(B_0 - \beta_0) - 3(B_1 - \beta_1)] y_B^2 + 2(2B_1 - \beta_1) y_B^3. \quad (22)$$

The osmotic coefficients of solutions of potassium chloride alone [10] were expressed as a polynomial in I by means of the equation

$$2(\varphi_B^0 - 1) = \varphi^{DH} - 2(0.03204I - 0.02622I^2 + 0.00562I^3 - 0.000459I^4) \quad (23)$$

and those for calcium chloride alone [3, 11] by means of the equation

$$(\varphi_C^0 - 1) = \varphi^{DH} + 0.05840I + 0.00553I^2 - 0.000068I^3. \quad (24)$$

Here, φ^{DH} is the Debye-Hückel contribution to the osmotic coefficient and, for aqueous solutions at 25 °C, can be written

$$\varphi^{DH} = -\frac{2.34164}{\rho^3 I}[(1+x) - 2\ln(1+x) - (1+x)^{-1}] \quad (25)$$

where $x = \rho I^{1/2}$ and $\rho = 1.5$ mole$^{-1/2}$ kg$^{1/2}$.

With the values of φ_B^0 and φ_C^0 calculated with the aid of eqs (23) and (24), and the osmotic coefficient data for the mixed salt solutions given in table 1, it was found, by the method of least squares, that a fair approximation to the experimental values could be obtained by putting $\beta_0 = b_{01}I + b_{02}I^2 = 0.03330I - 0.01036I^2$. The fit is perhaps not as good as one might wish, the standard deviation being 0.0021 in φ. The introduction of a further term, however, $\beta_0 = 0.03340I - 0.01045I^2$, $\beta_1 = -0.00035I^2$, did not improve the agreement. It was decided, therefore, that the simpler equation should be adopted. The equations now become

$$(y_B + 1)\varphi = 2y_B\varphi_B^0 + \varphi_C^0 + y_B y_C \beta_0 \quad (26)$$

$$2\ln \gamma_B/\gamma_B^0 = [(\varphi_C^0 - 1) - 2(\varphi_B^0 - 1) + \beta_0] y_C + (B_0 - \beta_0) y_C^2 \quad (27)$$

$$\ln \gamma_C/\gamma_C^0 = [2(\varphi_B^0 - 1) - (\varphi_C^0 - 1) + \beta_0] y_B + (B_0 - \beta_0) y_B^2 \quad (28)$$

with

$$\beta_0 = 0.03330I - 0.01036I^2, \; B_0 = 0.03330I - 0.00518I^2,$$

and

$$(B_0 - \beta_0) = 0.00518I^2.$$

Values of the osmotic coefficients calculated by means of eq (26) are given in the last column of table 1. Some data in table 1 are marked with an asterisk; in these cases the total ionic strength was greater than that of saturated potassium chloride solution and it is doubtful if eq (23) is applicable; these data were not used in calculating values of b_{01} and b_{02} by the method of least squares.

TABLE 3. *Osmotic and activity coefficients of the system water-potassium chloride-calcium chloride at 25 °C*

y_C	φ	$\log \gamma_B/\gamma_B^0$	$\log \gamma_C/\gamma_C^0$
$I=1$			
0	0.8962	0	−0.0251
0.2	.8963	0.0048	−.0204
.4	.8952	.0096	−.0156
.6	.8925	.0146	−.0106
.8	.8874	.0196	−.0054
1.0	.8784	.0248	0
$I=2$			
0	0.9122	0	−0.0375
0.2	.9194	0.0070	−.0314
.4	.9271	.0144	−.0246
.6	.9356	.0221	−.0171
.8	.9452	.0302	−.0089
1.0	.9566	.0387	0
$I=3$			
0	0.9375	0	−0.0519
0.2	.9503	0.0082	−.0447
.4	.9661	.0172	−.0360
.6	.9859	.0270	−.0256
.8	1.0119	.0377	−.0136
1.0	1.0478	.0491	0
$I=4$			
0	0.9644	0	−0.0735
0.2	.9820	0.0089	−.0646
.4	1.0056	.0192	−.0527
.6	1.0378	.0309	−.0380
.8	1.0828	.0441	−.0205
1.0	1.1485	.0587	0
$I=5$			
0	0.9977	0	−0.0980
0.2	1.0184	0.0085	−.0874
.4	1.0489	.0193	−.0723
.6	1.0935	.0323	−.0527
.8	1.1590	.0476	−.0286
1.0	1.2582	.0652	0

Activity coefficients for the mixed salt solutions have been calculated using eqs (27) and (28); values of $\log \gamma_B/\gamma_B^0$ and $\log \gamma_C/\gamma_C^0$ are given in table 3 and plotted in figures 4 and 5. As will be seen from these figures, plots of $\log \gamma_B$ against y_C and of $\log \gamma_C$ against y_B are by no means linear except at the lowest value of the total ionic strength, $I=1$, where the curvature is slight. Moreover, the variation of the activity coefficient is large; thus at $I=4$, $\log \gamma_B^0 = -0.2368$ for potassium chloride in its own solution, whereas $\log \gamma_B^{tr} = -0.1781$ for the "trace" activity coefficient of potassium chloride in the limit when the solution contains only calcium chloride, a difference of 0.0587. The corresponding quantities for calcium chloride are $\log \gamma_C^0 = -0.2502$ and $\log \gamma_C^{tr} = -0.3237$, a difference of 0.0735.

These differences are much larger than those found for other systems of this charge type, as is emphasized by figure 6. It will be seen that the next largest variation is found with barium chloride in potassium chloride solution, where $\log \gamma_C^0/\gamma_C^{tr} = 0.021$. Moreover,

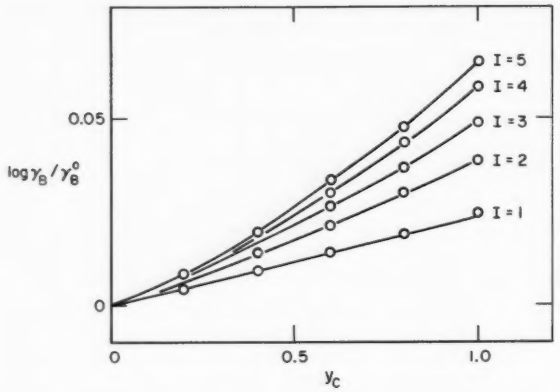

FIGURE 4. *Variation of the activity coefficient of potassium chloride in potassium chloride-calcium chloride mixtures at constant total ionic strength.*

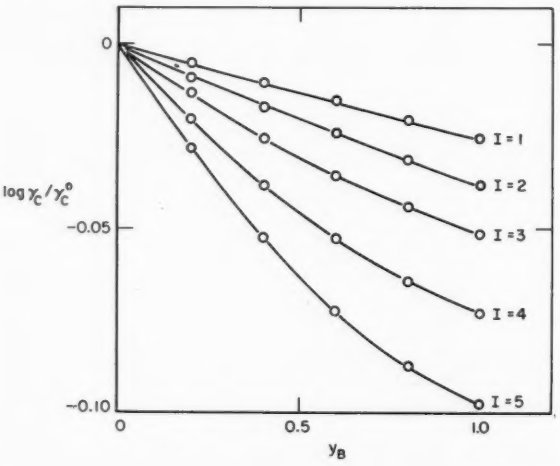

FIGURE 5. *Variation of the activity coefficient of calcium chloride in potassium chloride-calcium chloride mixtures at constant total ionic strength.*

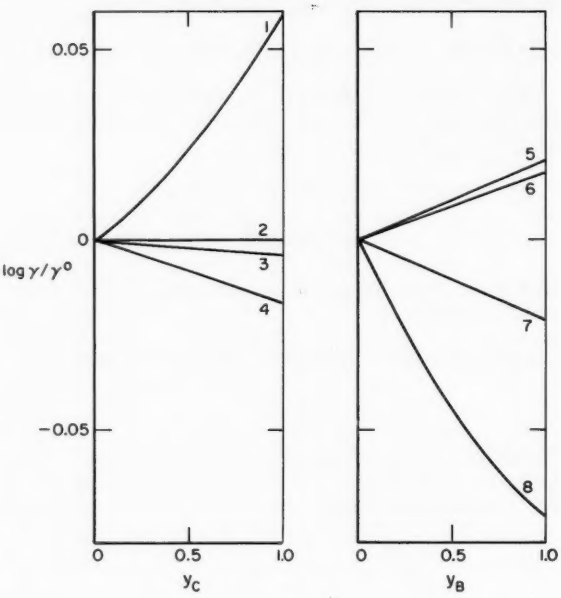

FIGURE 6. *Activity coefficients in solutions at a constant total ionic strength of* I = 4.

1. Potassium chloride in calcium chloride solution.
2. Sodium chloride in calcium chloride solution.
3. Potassium chloride in barium chloride solution.
4. Sodium chloride in barium chloride solution.
5. Barium chloride in sodium chloride solution.
6. Calcium chloride in sodium chloride solution.
7. Barium chloride in potassium chloride solution.
8. Calcium chloride in potassium chloride solution.

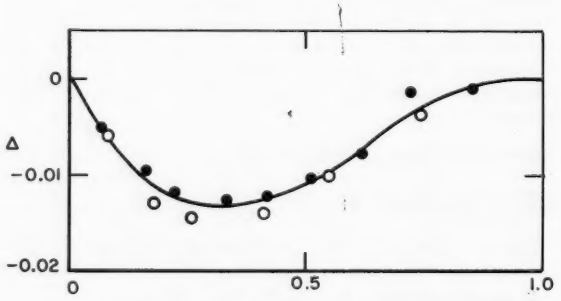

FIGURE 7. *The function* $\Delta = (y_B + 1)\varphi - 2y_B\varphi_B^0 - y_C\varphi_C^0$ *for the system: water-potassium chloride* (B)*—calcium chloride* (C) *at 25 °C.*

○ Present work, set 7 of table 1, $M_B \sim 3.44$
● Kirgintsev and Luk'yanov, [12], $M_B = 3.362$.

there is a marked curvature in the two plots for the potassium chloride-calcium chloride system whereas, for the other three systems, any curvature in the plots must have been small.

Kirgintsev and Luk'yanov [12] have reported isopiestic vapor pressure measurements of this system. They had nine mixed salt solutions of different potassium chloride to calcium chloride ratios and these were equilibrated with six reference potassium chloride solutions of molalities ranging from 1.857 to 4.217*m*.

Their results are in good agreement with ours. This can be illustrated by means of figure 7. We have used our data from set 7 of table 1 for six solutions in equilibrium with either 3.4262 or 3.4611*m* potassium chloride and also the data of Kirgintsev and Luk'yanov for nine solutions in equilibrium with 3.362*m* potassium chloride and calculated the deviation function, Δ, represented by eq (19). As figure 7 shows, the agreement between the two sets of data is good.

These authors had 54 results for mixed solutions but nine of these were for solutions whose total ionic strength exceeded 5. If we exclude these on the ground that our eq (23) is not applicable at such high total ionic strengths, it is found that the remaining 45 results can be well represented by eq (26), with the β_0 values given earlier. The standard deviation is 0.0021 in φ, which is also the standard deviation of our own results.

The excess free energy of mixing is the increase in free energy corresponding to the process

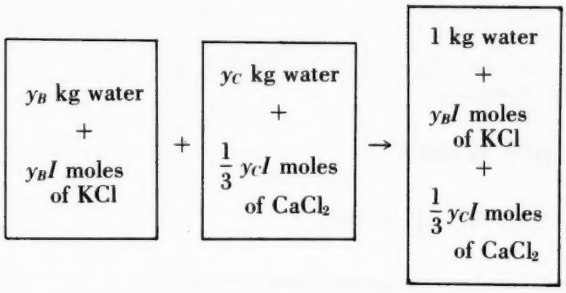

when solutions of potassium chloride and calcium chloride are mixed without change in total ionic strength. As was shown earlier [13], this can be written

$$G^E/RT = y_B y_C I[\tfrac{1}{2}(Q_B + Q_C) + y_B R_B + y_C R_C + \tfrac{2}{3}(y_B - y_C)(R_C - R_B)]. \quad (29)$$

Under the conditions represented by eqs (26), (27), and (28), this reduces to the particularly simple form

$$G^E/RT = y_B y_C I \beta_0. \quad (30)$$

The following values of the excess free energy of mixing in the potassium chloride-calcium chloride system have been calculated by means of eq (30) (in cal per kg of water, 1 cal = 4.1840 J.) for the case when $y_B = y_C = 0.5$:

$I=$	1	2	3	4	5
KCl-$CaCl_2$	3.4	3.7	1.0	−4.8	−13.7
KCl-$BaCl_2$	−2.9	−12.3	−35.3	−73.4	.....
NaCl-$CaCl_2$	3.5	15.3	30.9	50.8	75.9
NaCl-$BaCl_2$	−1.4	−7.1	−16.7	−34.9	−64.4

Some values for other systems of like charge type are included. In general, the excess free energy of mixing is small for the potassium chloride-calcium chloride system; this contrasts with the comparatively large changes in the activity coefficients as shown in table 3. The reason for this is to be found in the magnitudes of the Q_B and Q_C terms in eqs (16), (17), and (29). Assuming, as is the case with this system, that the contribution of the R terms is small compared with that of the Q terms, we see that it is the individual Q_B and Q_C terms which determine the change in the activity coefficients on mixing, whereas it is the sum $(Q_B + Q_C)$ which determines the excess free energy of mixing. It is quite possible that Q_B and Q_C could be very large, with large changes in the activity coefficients on mixing, yet if $Q_B = -Q_C$ there would be no change in free energy on mixing.

We thank Dr. J. S. Johnson and Dr. R. M. Rush for many useful discussions and Dr. Rush for the least square calculations on which this paper is based. Our thanks are expressed to the University of Newcastle upon Tyne for the grant of study leave to one of us (A.K.C.) and to the Office of Saline Water for a grant in partial support of this work.

5. References

[1] R. A. Robinson and V. E. Bower, J. Res. NBS **69A** (Phys. and Chem.), No. 1, 19 (1965).
[2] R. A. Robinson and V. E. Bower, J. Res. NBS **69A** (Phys. and Chem.), No. 5, 439 (1965).
[3] R. A. Robinson and V. E. Bower, J. Res. NBS **70A** (Phys. and Chem.), No. 4, 313 (1966).
[4] H. A. C. McKay and J. K. Perring, Trans. Faraday Soc. **49,** 163 (1953).
[5] G. Scatchard, J. Am. Chem. Soc. **83,** 2636 (1961).
[6] H. S. Harned and B. B. Owen, The Physical Chemistry of Electrolytic Solutions, ch. 14, 3d ed. (Reinhold Publ. Corp., New York, N.Y., 1958).
[7] R. A. Robinson and R. H. Stokes, Electrolyte Solutions, ch. 15, revised ed. (Butterworths Scientific Publications, London, 1965).
[8] R. A. Robinson, J. Phys. Chem. **65,** 662 (1961).
[9] R. M. Rush and R. A. Robinson, J. Tenn. Acad. Sci., **43,** 22 (1968).
[10] Reference [7], p. 476.
[11] Reference [7], p. 478.
[12] A. N. Kirgintsev and A. V. Luk'yanov, Russ. J. Phys. Chem. **40,** 686 (1966).
[13] See appendix to reference [2].

(Paper 72A3–497)

JOURNAL OF RESEARCH of the National Bureau of Standards—A. Physics and Chemistry
Vol. 72A, No. 3, May–June 1968

Force Field for SiF_4

Ira W. Levin* and Stanley Abramowitz

Institute for Basic Standards, National Bureau of Standards, Washington, D.C. 20234

(January 29, 1968)

The force field of SiF_4 has been determined using both Coriolis coupling constants obtained from an investigation of the band contour of ν_3 at 195 °K and isotopic shifts. The force fields are equally well determined using both methods and are in agreement.

Key Words: Band contour, Coriolis constant, force field, infrared, isotopic shift, low temperature, SiF_4.

In determining the general valence force field for silicon tetrafluoride from various sources of molecular information, McKean [1][1] noted a significant discrepancy in the range of values for the stretch-bend interaction force constant characterized separately by the isotopic frequency shift $\Delta\nu_4$ and by the Coriolis constant ζ_4. Since the estimate of ζ_4 from the band shape of ν_4 contains a relatively large uncertainty, as a consequence of an inability to locate precisely the P and R branch maxima, we examine in this communication the contour of the ν_3 fundamental at 195 °K in order to obtain a reliable zeta value for constraining the force field. In addition to confirming the potential function for SiF_4 by comparing the force constants calculated from alternate methods, rotation-vibration interaction data from the two F_2 vibrations provide further tests concerning the utility of the band contour method for estimating Coriolis parameters.

The contours for both infrared active fundamentals, ν_3 and ν_4, were recorded at 310 and 195 °K with a double beam grating spectrophotometer equipped with interference filters to separate the orders. Spectral slit widths varied between 0.7 and 0.9 cm^{-1}. For low temperature measurements, a 5-cm path length copper cell, surrounded by an evacuated glass shell, was in contact with a solid CO_2 and acetone mixture.

Figure 1 displays a representative scan of the ν_3 contour at 310 and 195 °K. A hot band at approximately 1029 cm^{-1} distorts the contour sufficiently at 310 °K to preclude a valid P–R measurement for use in the Coriolis constant determination. The attenuation of the intensity of the hot band transition at 195 °K, however, reveals definite P, Q, and R branch features. Additional absorptions, attributed to the naturally occurring isotopes of ^{29}Si and ^{30}Si, are also observed. These values, summarized in table 1, agree well with Heicklen and Knight's frequencies obtained from isotopically enriched compounds [2].

For ν_3, an average value of 8.3 cm^{-1} for $\Delta\nu_{P\text{-}R}$ was determined from twelve expanded traces, recorded at several spectral slit widths. Repeated determinations of the P and R branch maxima by a second investigator suggests an uncertainty in $\Delta\nu_{P\text{-}R}$ of less than 0.5 cm^{-1}. For the ν_4 vibration, it is more difficult to determine $\Delta\nu_{P\text{-}R}$ owing to the relative broadness of the P and R branch features. Measurements in a 10-cm path length cell at 310 °K, with varying sample pressures and instrumental conditions, give 23.4 ± 1.0 cm^{-1} for

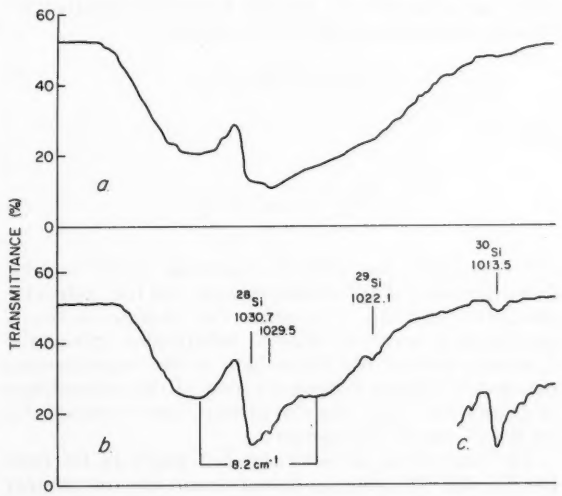

FIGURE 1. *The vibration-rotation band contour for the ν_3 fundamental of SiF_4.*

(a) 310 °K, (b) 195 °K, (c) 195 °K. The frequencies are labeled in cm^{-1}.

*National Institute of Arthritis and Metabolic Diseases, National Institutes of Health, Bethesda, Md. 20014.

[1] Figures in brackets indicate the literature references at the end of this paper.

293-857 O - 68 - 2

$\Delta\nu_{P-R}$, in agreement with Heicklen and Knight's single value of 23.1 cm^{-1}.

TABLE 1. *Observed data for SiF_4*

$\Delta\nu_{P-R}$ represents the $P-R$ separation in cm^{-1}. The frequencies are in cm^{-1}; the ζ_i are dimensionless.

	Frequency (cm^{-1})	Assignment			
	1030.7	$^{28}SiF_4$			
	1029.5	hot band			
	1022.1	$^{29}SiF_4$			
	1013.5	$^{30}SiF_4$			
	Observed frequency (cm^{-1})	$\Delta\nu_{P-R}$ (cm^{-1})	ζ_i	$\Sigma\zeta_i$	Sum rule
ν_3	1030.7	8.3 ± 0.5 [a, c]	0.53 ± 0.03		
ν_4	389.4	23.4 ± 1.0 [b]	-0.07 ± 0.05	0.46 ± 0.06	0.50

[a] 195 °K.
[b] 310 °K.
[c] The estimated uncertainty of 0.5 cm^{-1} represents twice the maximum deviation from the value obtained from averaging twelve traces of the spectrum.

Edgell and Moynihan's expression (3) in terms of the rotational constant B and absolute temperature T, relates the Coriolis constant ζ_i to the measured $\Delta\nu^i_{P-R}$ values. Perturbations to the contour from the ^{29}Si and ^{30}Si isotopes are ignored in this calculation. A summary of the calculated Coriolis constants appears in table 1. The zeta sum of 0.46 ± 0.06 for the two Coriolis values, compared to the theoretical sum of 0.50, supports the consistency of the data determined by the contour method.

The Coriolis coefficients ζ and the isotopic frequency shifts $\Delta\nu$, respectively, provide force field information through analogous expressions; namely

$$\zeta = L^{-1}C(L^{-1})', \tag{1}$$

and

$$\frac{2\Delta\nu}{\nu} = L^{-1}\Delta G(L^{-1})'. \tag{2}$$

L^{-1} represents the normal coordinate vector matrix; C is a function of the atomic masses and the molecular geometry, and ΔG represents the change in the G matrix as a result of isotopic substitution. Since the L matrix relates the force field to the experimental parameters, figure 2 presents plots of the dependence of ζ_i and $\Delta\nu_4$ upon the interaction force constant F_{34} for the F_2 symmetry species.

The use of eq (2) with the L^{-1} matrices for both the ^{28}S and ^{30}Si isotopes demonstrates the uncertainty in the force field fixed by a value for $\Delta\nu_4$. The lower portion of figure 2 displays the relevant plots. The solid circles locate the experimental point for $\Delta\nu_4$ of

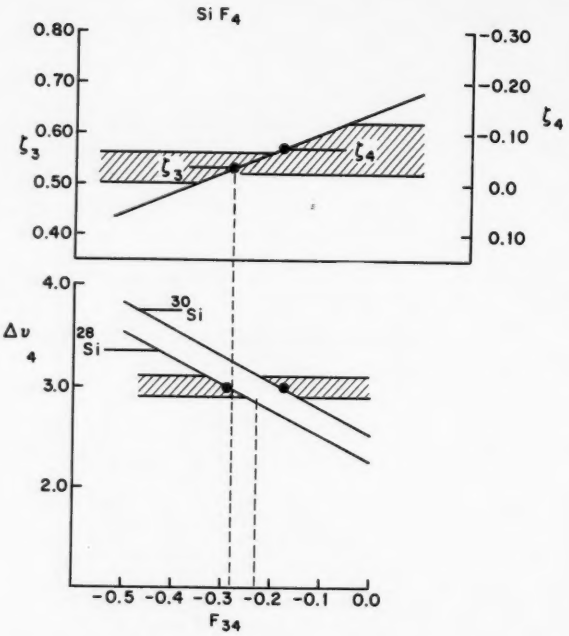

FIGURE 2. *Plots of ζ^2_{33}, ζ^2_{44}, and $\Delta\nu_4$ (in cm^{-1}) as functions of F_{34} for the F_2 symmetry species of SiF_4.*
F_{34} is in millidynes per angstrom.

3.0 ± 0.1 cm^{-1} (1, 2), while the shaded areas represent the uncertainty in the experimental measurement. A vertical dotted line gives the average value for F_{34} from the perturbation calculation. The solid circles and shaded areas in the upper portion of the figure represent the experimental Coriolis constants and their uncertainties, respectively. The vertical line originating from ζ_3 in the plot defines the preferred force field using the more certain Coriolis value. The L^{-1} matrix for the ^{28}Si species formed the basis for the Coriolis plot in the figure. Definitions for the symmetry coordinates, as well as the details of the vibrational calculation, appear in reference [4].

The force constants, constrained by (a) $\Delta\nu_4$, (b) ζ_3 and ζ_4, and (c) ζ_3 alone appear in table 2. The dispersions in the F's are assumed to arise from the uncertainties in the experimental data alone; that is, the errors due to anharmonicity and the uncertainty in

TABLE 2. *SiF_4 force constants constrained by $\Delta\nu_4$, ζ_3 and ζ_4, and ζ_3, respectively*

The units of F are expressed in millidynes per angstrom.

Force constant	$\Delta\nu_4$	ζ_3 and ζ_4	ζ_3
F_{33}	6.28 ± 0.22	6.21 ± 0.31	6.40 ± 0.16
F_{34}	-0.23 ± 0.10	-0.20 ± 0.15	-0.28 ± 0.07
F_{44}	$.44\pm0.01$	$.45\pm0.02$	$.44\pm0.01$

the normal coordinates are neglected. The very good agreement for the force fields between the two types of constraints confirms the potential function for SiF_4. Although the frequency shift method reflects an optimistic estimate of ± 0.1 cm^{-1} uncertainty in the $\Delta\nu_4$ measurement (1, 2), the estimated dispersions in the crucial interaction force constant F_{34} suggest that the Coriolis and the isotopic shift constraints are about equally effective for this molecule.

One of us (S.A.) acknowledges the support of the Air Force Office of Scientific Research, U.S. Department of Defense.

References

[1] D. C. McKean, Spectrochim. Acta **22**, 269 (1966).
[2] J. Heicklen and V. Knight, Spectrochim. Acta **20**, 295 (1964).
[3] W. F. Edgell and R. E. Moynihan, J. Chem. Phys. **27**, 155 (1957).
[4] I. W. Levin and S. Abramowitz, J. Chem. Phys. **44**, 2562 (1966).

(Paper 72A3–498)

JOURNAL OF RESEARCH of the National Bureau of Standards—A. Physics and Chemistry
Vol. 72A, No. 3, May–June 1968

Blemish Formation in Processed Microfilm

C. I. Pope

Institute for Basic Standards, National Bureau of Standards, Washington, D.C. 20234

(January 9, 1968)

Oxidizing and reducing agents generated by paper cartons during storage may react with the image silver to form blemishes. The type of fixing bath, concentration of chlorine in the wash water, washing time and composition of the storage cartons can be factors that accelerate or retard the attack of the peroxide on the image silver. Microfilm washed after fixation in distilled water or chlorine-free tap water formed blemishes when exposed to peroxide paper. A trace of silver chloride in the image silver of processed microfilm augmented the formation of the natural type blemishes when exposed to peroxide paper, but high concentrations of residual silver chloride inhibited blemish formation. During storage, some storage cartons evolved formaldehyde, formic acid, and ammonia which created a chemical environment favorable for blemish formation in microfilm in the presence of peroxide. A correlation was found between the incidence of blemishes and the brand of paper storage cartons. A procedure was developed for testing processed microfilm to determine its susceptibility to blemish formation. According to the present theory, peroxide reacts with the silver in the image, forming colloidal silver which imparts a yellowish or reddish color to the blemishes.

Key Words: Archival record film, blemishes due to aging, colloidal silver, microfilm, microfilm storage cartons, permanent record film, peroxides.

1. Introduction

Blemish formation in stored microfilm has been under investigation for some time [1, 2, 3].[1] The nature of the problem and the types of blemish formation have been described [1, 2]. It has been shown that oxidizing and reducing agents, probably peroxides, emitted by paper cartons in which the microfilm is stored attack the silver in the image, causing yellowish or reddish blemishes [4]. In the present study, the processing procedure was investigated to determine its effect on blemish formation. In this paper the term "blemish" includes various types of spots and edge attack on characters and other image boundaries.

2. The Role of the Processing Procedure in Blemish Formation in Microfilm

In the investigation of processing variables, four fine grain 16 mm microfilms, made by three manufacturers, were used. The processing solutions and times of developing, stopping, and fixing are given in the appendix. The microfilm samples were processed in beakers and agitated with a glass rod. The chlorine concentration of the wash water was determined by a Taylor chlorine analyzer [7] using the *o*-tolidene dihydrochloride reagent.

[1] Figures in brackets indicate the literature references at the end of this paper.

The peroxide source for testing the microfilm was a chromatographic paper, 0.03 cm thick, which had been treated in aqueous hydrogen peroxide. The test procedure is described in section 5. From 2 to 4 cm^2 of the peroxide paper formed spots in areas of microfilm containing natural spots. All microfilms were dried at least 1 day after processing or other treatment before exposure to peroxide paper.

2.1. Effect of the Fixing Bath and Wash Water

A study was made to determine if processed microfilm formed blemishes when the thiosulfate was removed by washing in chlorine-free water. The fixing baths tested were a neutral bath, a nonhardening acid bath, and an acid hardening bath. The wash waters were distilled water and chlorine-free tap water which had a *p*H of about 8. Chlorine-free tap water was obtained by storing cold tap water until the chlorine disappeared or by adding sodium sulfite to the tap water to neutralize the chlorine. For a chlorine concentration of 1.2 ppm, 50 ml of a sodium sulfite solution containing 0.500 g per liter was sufficient for 4 liters of tap water. About 50-cm lengths of the microfilms were exposed to a test pattern having various kinds of information, developed, fixed and washed in 1-liter baths of the wash water in 1.5-liter beakers. Three baths of the wash water were used for a 3-min wash and for longer washes a bath was used for each additional 5 min of washing. The sample was trans-

ferred from beaker to beaker and agitated with a glass rod. The temperature of the processing solutions and wash water was 26 °C.

The processed microfilms developed spots and, in some cases, edge attack when exposed to peroxide paper. The microfilm fixed in the neutral and the nonhardening baths and washed in distilled water developed much larger spots than microfilm fixed in the nonhardening and the acid hardening baths and washed in chlorine-free tap water. The spots in the latter two fixing procedures were more numerous and had sharper edges than those for the first two fixing procedures with distilled water washing. The spots were almost contiguous to each other for microfilm fixed in the acid hardener bath. The spots from all fixing baths appeared white when they first developed but turned yellow or yellowish as the peroxide attack continued. The edges of the spots were slightly fuzzy. No significant differences were observed between blemishes formed after a 3-min wash and a 15-min wash.

The results of the tests are shown in table 1, where the observed effect for each processing procedure and the amount of peroxide paper necessary to induce blemish formation are indicated. The residual thiosulfate in the microfilm samples that formed blemishes ranged between 0 and 3 μg per 6 cm^2 of the image area. Microfilm D retained more residual thiosulfate than the other microfilms and exhibited only slight blemish formation for the neutral and the nonhardening baths and none for the acid hardening bath when washed in chlorine-free water. Microfilm A, fixed in the acid hardening bath and washed in distilled water, had a residual thiosulfate concentration of 10 μg per 6 cm^2, making it resistant to peroxide attack. The results show that microfilm developed blemishes when exposed to peroxide paper if the processing procedure was such that the residual thiosulfate was reduced to a very low level. A higher concentration of residual sodium thiosulfate would form additional silver sulfide in the image silver, protecting it from oxidation. The thiosulfate was more difficult to wash from the microfilm after fixation in the acid hardener bath than in the neutral or nonhardening acid bath, but chlorine-free tap water still removed the thiosulfate sufficiently to permit blemish formation. The tap water, being slightly alkaline, acted as a thiosulfate eliminator.

2.2. Effect on Blemishes of Silver Chloride Formed in Microfilm by Chlorine in Tap Wash Water

It was found that silver chloride formed in processed microfilm during processing is a factor in blemish formation. Trace amounts of silver chloride enhance blemish formation but larger concentrations inhibit it.

Water from city taps generally contains 0.1 to 1 ppm of chlorine [8]. The chlorine in tap water forms hypochlorous acid (HOCl) which is a powerful oxidizing agent because it liberates oxygen ($HOCl \rightarrow HCl + O$) [9]. The evolved oxygen oxidizes the silver in the image to silver ions which in turn combine with the ever-present chloride ions in tap water to form silver chloride.

Tests were made of the effect of chlorine in the wash water on blemish formation in microfilm A. The microfilm was fixed in an acid hardening bath. Samples were washed for 30 min in running tap water at 27 °C, containing 0.8 ppm of chlorine in one run and 1.2 ppm in a second run, and exposed, respectively, to 6 cm^2 and 8 cm^2 of the peroxide paper. No blemishes developed on the microfilm samples. Other samples were washed at 26 °C for a total of 30 min by placing them in a succession of tap water baths containing 0.3 ppm of chlorine for 2, 3, 5, 10, and 10 min, respectively. Exposure to 4 cm^2 of peroxide paper produced some

TABLE 1. *Blemish formation on exposure to peroxide paper for four microfilms and various processing procedures*

	Processing procedures			
Microfilm	Neutral fix and washed in distilled water for 3 min	Nonhardening acid fix and washed in distilled water or chlorine-free tap water for 3 min	Acid hardening fix and washed in chlorine-free tap water for 3 min	Acid hardening fix and washed in distilled water for 40 min
A	Many spots and edge attack.	Many spots and edge attack.	Many spots but no edge attack.	No spots or edge attack.
B	Many spots and edge attack.	Many spots and edge attack.	Many spots but no edge attack.	
C	Many spots and edge attack.	Many spots and edge attack.	Many spots but no edge attack.	
D	Few spots but edge attack.	Few spots but edge attack.	No spots or edge attack.	
Amount of peroxide paper used.	1 to 2 cm^2	2 cm^2	4 to 8 cm^2	8 cm^2.

spots but a considerable resistance to blemish formation was noted when compared to samples washed in chlorine-free tap water.

After fixation, microfilm A was washed in running tap water at 27 °C, containing 1.2 ppm chlorine for 3, 6, 9, 15 and 30 min. A sample was removed at the end of each washing time. The processed microfilm was exposed to 4 cm^2 of the peroxide paper. The microfilm samples fixed in the acid hardening bath developed a high incidence of yellow spots for the 3-min wash, a few in the 6-min wash, and none in the 9, 15, and 30-min washes. The microfilm samples fixed in the nonhardening bath developed many light yellow spots for the 3-min wash, with slight yellowing of the image silver, a decrease in number of spots and no yellowing for the 6-min wash, a few spots for the 9-min wash, and none for the 15 and 30-min washes.

Thus a high concentration of chlorine in the wash water formed silver chloride in the image silver making it resistant to yellowing and spot formation when exposed to peroxide. Furthermore, resistance to blemish formation increased with the washing time for 1.2 ppm of chlorine in the tap wash water and 10 to 15 min was required to impart complete resistance. At the end of the 3-min wash, the thiosulfate had reached a low concentration and the chlorine began to form silver chloride. As the washing progressed, more silver chloride was formed and it finally reached a concentration which inhibited blemish formation. The spots which formed after fixation in the acid hardening bath and a 3-min wash were more yellow than those obtained from the nonhardening bath and a 3-min wash. This would be the expected effect of acid carried over into the wash water from the acid bath, since chlorine reacts more rapidly in the presence of acid to form silver chloride. Since the tap water had a *p*H of about 8, a high concentration of chlorine and a considerable washing time was necessary to form sufficient residual silver chloride to inhibit blemish formation. Tap water containing low concentrations of chlorine, such as 0.3 ppm, may not form a sufficient amount of silver chloride to inhibit blemish formation even after a 30-min wash but the tests described above for 0.3 ppm of chlorine in wash water showed that some resistance to blemish formation was obtained.

Microfilm containing sufficient silver chloride to make it resistant to blemish formation loses this resistance if treated for 10 min in a 0.2 percent solution of ammonium hydroxide to remove the silver chloride. Microfilm so treated showed only an even yellowing of the image silver when exposed to 2 to 4 cm^2 of the peroxide paper.

It is not known how long silver chloride formed from chlorine in the tap water will impart resistance to blemish formation from peroxide attack. But in section 3 it is shown that chemicals given off by the storage cartons do react with the image silver, causing blemish formation in the presence of peroxide. Evidently the silver halide, if present, is partially reduced by the peroxide.

2.3. Effect of Iodide in the Fixer

It has been shown [12] that the silver in a photographic image is partially sulfided during fixation. If iodide is added to the fixing bath most of the sulfiding is prevented, leaving a layer of silver iodide on the silver grains.

Henn, Wiest, and Mack [14] have reported that collections of microfilm processed in iodide-containing developers or fixing baths to be relatively free from blemishes. They recommend the use of 0.2 g of potassium iodide per liter of fixing solution to give microfilm greater resistance to blemish formation.

Tests were made on four microfilms by adding 0.2 g of potassium iodide to each liter of the acid hardening fixing solution. After development, the samples were fixed and washed in chlorine-free tap water. The chlorine-free tap water was used to avoid the blemish inhibiting effect of the chlorine. The samples were exposed to 2 to 8 cm^2 of the peroxide paper. The microfilms showed more even yellowing of the image silver than the controls without iodide, indicating that iodide had made the image silver more susceptible to attack by peroxide. (If natural blemishes were caused by peroxide from the boxes, this finding seemed inconsistent with the field observations.) The resistance to spot formation was about the same as the controls. However, if the microfilms fixed with iodide in the fixer were washed in the chlorine-free tap water to which 1 ppm of chlorine was added, they, like the controls, resisted blemish formation and did not show an even yellowing. Old microfilms which had been processed with iodide in the fixing bath formed blemishes when exposed to peroxide at low levels of 2 to 4 cm^2 of the peroxide paper.

To simulate actual practice, a study was then made of the effect of storing processed microfilm in fresh storage cartons. The films in cartons were placed in a desiccator jar for 10 days at 86 percent relative humidity and 26 °C and then the samples were exposed to 2 to 4 cm^2 of the peroxide paper. The samples processed with potassium iodide in the fixer developed a few blemishes but samples processed without potassium iodide in the fixer developed many more. These tests confirmed the field observations and suggested that chemicals in addition to peroxide were generated in the storage carton and played a part in the chemistry of blemish formation.

2.4. Natural-Type Blemishes Obtained With Acid and Silver Chloride in the Image

A small amount of silver chloride was formed in the image silver of old films and freshly processed films. When these films were exposed to peroxide, sharp-edged blemishes formed which resembled very closely those found in nature, even duplicating the ring formation and edge attack. The films were exposed to about 25 cm^2 of the peroxide paper at 76 percent relative humidity and 26 °C. A higher relative

humidity did not produce the natural-type blemishes. Although these tests may not be applicable to microfilm as normally processed and stored they do suggest that a trace of silver chloride contributes to blemish formation under natural storage conditions.

For these experiments, processed films were treated 10 min in a solution containing 0.025 g of sodium chloride and 3 ml of glacial acetic acid per liter, dried and exposed to peroxide paper. (Formic acid may be substituted for the acetic acid.) The 0.025 g of sodium chloride per liter gave a solution containing 15 ppm of the chloride ion which is close to the median value of 13 ppm in the water supplies of large cities [6]. The oxygen dissolved in the sodium chloride-acetic acid solution oxidized the image silver to silver ion which combined with the chloride ion to precipitate silver chloride in the image silver. The silver chloride formed in microfilm by the sodium chloride-acetic acid solution may be removed by treating the film for 10 min in a 0.2 percent solution of ammonium hydroxide. After such treatment, the image silver showed only an even yellowing after exposure to peroxide paper. When microfilm was treated in a solution of 3 ml of acetic acid per liter without the sodium chloride and exposed to peroxide paper, no spot or edge blemishes formed in the image silver, only an even yellowing.

The microfilms A, B, C and D, reported in section 2.1, which readily formed blemishes when exposed to peroxide paper were treated in the sodium chloride-acetic acid solution and dried. Peroxide exposure produced natural type spots, some with ring structure, and edge attack. There was no even yellowing, indicating that silver chloride was formed throughout the image. The edges of the spots were sharp and the spots were deep yellow, showing the effect of silver chloride. The number of spots was much less than before the sodium chloride-acetic acid treatment since too much silver chloride had been formed at most points in the image for spot induction.

Blemish formation was induced in old processed microfilms by treatment in chlorine gas or an acid solution of chlorine and subsequent exposure to peroxide. The films were exposed to chlorine gas by suspending the samples over a chlorine solution in a 1-liter closed glass bottle. The chlorine solution was prepared by dissolving 0.250 g of technical grade calcium hypochlorite containing 70 percent calcium hypochlorite in 1 liter of water and adding 5 ml of glacial acetic acid. Approximately 400 ml of this solution was added to the bottle. The film samples were soaked in distilled water for 10 s, squeegeed with a dry glass rod and suspended immediately in the chlorine gas above the solution for 20 to 60 s, dried overnight and exposed to peroxide paper. This method produced spot and edge attack but each brand of microfilm required a different time of exposure to the chlorine gas.

To determine whether silver chloride was formed in the image silver by the chlorine gas, microfilm samples were treated in a 0.2 percent ammonium hydroxide solution for 5 min to remove any existing silver chloride, dried overnight, treated 10 s in distilled water, squeegeed, treated to the chlorine gas for 30 s and exposed to peroxide paper. These films had spot and edge attack.

Microfilm samples were immersed for 5 s in the chlorine solution described above, dried and exposed to peroxide paper. These microfilms showed spot and edge attack but were more resistant to peroxide because more silver chloride had been formed in the image silver.

The findings with respect to chlorine and chloride ion raised a question about the effects of the other halides, silver bromide and silver iodide. Old processed microfilm samples, blemish free, were treated 10 min in solutions of sodium bromide containing 0.045 g/l and 3 ml of glacial acetic acid, and potassium iodide containing 0.060 g/l and 3 ml glacial acetic acid. Strong spot and edge attack were obtained in most samples when exposed to peroxide paper. The amount of blemish formation decreased as the solubility of the corresponding silver halides decreased.

A method was developed for estimating the free silver in processed microfilm. "Free silver" as here defined includes silver ion, silver oxide and silver halides but the method does not show how much of the silver is in the form of halide salt. This method indicated as much free silver present in old processed microfilm which had been treated in a solution containing 3 ml of acetic acid per liter as in microfilm treated in a solution containing 3 ml of acetic acid and 0.025 g of sodium chloride per liter. However, when they were exposed to peroxide paper, the samples given the acetic acid and sodium chloride treatment resisted background yellowing though they had natural-like spots and edge attack while those given the acetic acid treatment showed only an even yellowing of the image silver. Apparently traces of silver in the image are oxidized by oxygen dissolved in the water, in the presence of acid, and if the chloride ion is present, silver chloride is formed.

The procedure for determining the free silver is outlined as follows. The free silver was extracted from 12 cm^2 of processed microfilm with 10 ml of a 0.2 percent solution of ammonium hydroxide containing 1 g of sodium chloride per liter. Two 6 cm^2 pieces of microfilm were cut, folded emulsion in and placed back to back in a glass vial containing the test solution and allowed to stand 15 min. The samples were removed by a glass rod having a hook at one end and 0.10 ml of a potassium bromide solution containing 100 g/l was added and mixed. Then the solution was acidified by adding 1 ml of concentrated nitric acid diluted 1 to 5 and mixed, allowed to stand 1 hr and the turbidity measured with a nephelometer. A calibration curve was prepared from known amounts of silver added to the standard solution as silver nitrate. One-fourth microgram of silver as silver nitrate gave a measurable turbidity. The values obtained are relative but were helpful in showing changes in the free silver content of microfilm after various treatments. The free silver content of old processed microfilms containing blemishes ranged from 0.2 to 1 μg for 6 cm^2 of film.

3. Formaldehyde, Formic Acid, and Ammonia From Paper Cartons

Microfilms in which blemishes had formed during natural storage were studied to determine if more blemishes would develop in the laboratory peroxide test. Several rolls of microfilm having blemishes on the outer convolutions but none on the remainder of the roll were tested. Samples taken from blemish-free areas were tested and no blemishes developed, but samples from areas where blemishes had formed during storage did develop blemishes like those already present. The blemishes present before the test were ringed with a stylus to differentiate them from blemishes produced by the peroxide. Evidently chemicals in addition to peroxide had evolved from the paper carton during storage and created a chemical environment conducive to blemish formation in the presence of peroxide.

Formaldehyde, formic acid, and ammonia have been detected in the atmosphere within many of the paper storage cartons when stored at 100 percent relative humidity at 26 °C. A glass petri dish, 60 mm in diameter and 13 mm high, containing 10 ml of distilled water was placed in the paper carton to absorb evolved chemicals. The carton was stored in a desiccator jar containing 25 ml of distilled water for 1 to 3 days, one day being generally sufficient. This extraction procedure was used in testing for the presence of formaldehyde, formic acid, and ammonia. Formaldehyde-urea and formaldyhyde-melamine resins have been widely used as wet-strengthening agents in paper manufacture for over 20 years. The chemicals detected were probably formed by hydrolysis of these resins at high relative humidities.

3.1. Detection of Formaldehyde, Formic Acid, and Ammonia

a. Formaldehyde

Two ml of the water solution which had been stored in the paper carton were added to 5 ml of a 1 percent solution of chromotropic acid (4,5-dihydroxy, 2,7-naphthalene disulfonic acid[2]) in concentrated sulfuric acid. Chromotropic acid readily detects formaldehyde in concentrations of 1 ppm (15). Chromotropic acid gave a pink to dark purple color, a positive test for formaldehyde. The less sensitive resorcinol test gave a positive indication of formaldehyde from some cartons when the same water solution was stored successively in 3 cartons for a period of 3 days each. This test was made by adding 0.1 ml of 1 percent solution of resorcinol to 5 ml of the water solution and pouring the mixture carefully down the side of a test tube containing 5 ml of concentrated sulfuric acid to form two layers. A pink color formed at the junction of the two layers. The formaldehyde was also identified by microwave absorption analysis.

[2] Obtained from Matheson Coleman and Bell, Cat. No. P5425, East Rutherford, New Jersey.

b. Formic Acid

The water stored in the paper cartons had a *p*H range of 3.5 to 4.5 after storage for 3 days at 100 percent relative humidity at 26 °C. Titration with 0.001 *N* sodium hydroxide solution indicated that the water stored in the cartons was about 0.001 *N* with respect to formic acid for some storage cartons. The water stored in the cartons decolorized a light pink solution of potassium permanganate, indicating that formic acid was present. When 5 ml of the water solution was added to 5 ml of saturated mercuric chloride and warmed in hot tap water for 10 min, a precipitate formed, indicating reduction of the mercuric chloride. This test indicated the presence of formic acid. A precipitate of reduced silver formed when 2 ml of silver nitrate solution containing 10 g per liter were added to 10 ml of the water solution from the paper cartons and warmed 15 min in hot tap water. The reduced silver indicated the presence of formic acid which is capable of reducing the silver ion. This procedure detected 5 ppm of formic acid in a known solution. The formic acid is evidently formed by oxidation of the formaldehyde by the peroxide generated in the storage cartons and possibly by aerial oxidation of formaldehyde, catalyzed by the silver in the image. A water solution of formaldehyde was found to increase in acidity when stored over silver dust for 4 hr showing that formic acid was formed by the oxidation of formaldehyde.

c. Ammonia

About 10 ml of the water stored in the paper cartons were placed in a 50-ml beaker and made alkaline with sodium hydroxide. The beaker was covered with a watch glass having a strip of moistened red litmus paper attached to the underside and the beaker was warmed in hot tap water. After 30 to 60 min the litmus paper turned blue suggesting the presence of ammonia. A control test run on the distilled water was negative.

3.2. Tests of Old and New Storage Cartons

Some new storage cartons readily evolved formaldehyde when stored for 3 hr in the drawer of a metal laboratory desk. A strong indication of formaldehyde was obtained after a new carton was stored at 100 percent relative humidity at 3 °C for 1 day, indicating that a low temperature does not stop the evolution of formaldehyde if the relative humidity is high. Most of the old storage cartons tested evidenced formic acid evolution.

Storage cartons from one collection of blemish-free microfilms evolved no formaldehyde or only a very small amount. Cartons from a second collection where blemishes have not been found evolved an appreciable amount of formaldehyde, but this collection is located in an arid climate which would minimize the evolution of formaldehyde and the formation of formic acid. All the tests of paper storage cartons from collections where blemishes have been found, even collections that were ten years old, gave a strong indication of formaldehyde.

3.3. Reactions of Formaldehyde, Formic Acid, and Ammonia on Silver and Gelatin

During natural storage, blemishes generally form on the outside leader and edges of the microfilm roll, which are the areas most accessible to gaseous chemicals evolved by the storage carton. Formaldehyde will harden gelatin by reacting with the amino groups attached to the amino acids in the gelatin. Blemish formation was inhibited in a blemish forming microfilm after an exposure of 24 hr to the gaseous phase of a 2 percent solution of formaldehyde. This severe test may not be relevant to natural storage conditions but suggests that formaldehyde, alone, may inhibit blemish formation. Formaldehyde and formic acid neutralize the alkalinity of the amino groups making the gelatin more acidic.

Formic acid and chloride ion reacted with the image silver at high relative humidities to form silver chloride in the same manner as described in section 2.4 for the sodium chloride-acetic acid solution, making the high-density uniform image more resistant and the edges of the blemishes sharp, when the film was exposed to peroxide evolved by the storage cartons.

In section 2.2 it was noted that tap wash water having as much as 1 ppm of chlorine formed a sufficient amount of silver chloride in the microfilm to make it resistant to blemish formation. The formic acid from cartons stored at high relative humidities appears capable of reducing the silver chloride concentration to a level favorable for blemish formation. Formic acid readily reduced the silver ion in an aqueous solution of silver nitrate, forming a gray precipitate of silver. Solid silver chloride in a solution of formic acid turned slightly gray after standing in the dark for 7 days. A control without formic acid did not exhibit this effect. The gray color was attributed to reduced silver.

Experiments were performed to see whether or not residual silver chloride in the image silver of processed microfilm is susceptible to reduction by formic acid and peroxide. To incorporate silver chloride into clear (image-free) processed microfilm, the film was washed 20 min in distilled water, treated 10 min in a solution containing 5 g of silver nitrate per liter, treated 10 min in a second solution containing 5 g sodium chloride per liter, washed 20 min in distilled water and dried. When exposed to 24 cm^2 of paper treated with formic acid, samples of this microfilm developed a yellow color in the gelatin layer, indicating reduction of the silver chloride. The test was made at 86 percent relative humidity and 26 °C and in the same type of desiccator jar used for peroxide tests. The paper was prepared by treating Whatman No. 3MM filter paper in a 10 percent formic acid solution for 30 min drying it 3 hr at 26 °C and storing it at approximately −10 °C. Microfilm placed in a new storage carton for 12 days at 86 percent relative humidity and 26 °C showed evidence of reduction of silver chloride. Samples exposed to 6 cm^2 of the peroxide paper also evidenced such reduction. Thus residual silver chloride reduction in stored microfilm should decrease the blemish resistance.

It was found that the silver-chloride-ammonia complex was more easily reduced by formic acid and peroxide than silver chloride precipitated in the gelatin layer as described above. Tests were made on clear (image-free) processed microfilm treated 5 min in a solution containing 0.5 g of silver chloride dissolved in one liter of water containing 8 ml of concentrated ammonium hydroxide. The results indicated that ammonia evolved by storage cartons may make the silver chloride more sensitive to reduction by formic acid and peroxide.

The above data shows how microfilm resistant to blemish formation when stored may lose its resistance to peroxide in the presence of other chemicals evolved by the paper storage carton. Although both peroxide and formic acid reduce silver chloride, formic acid may be the principal reducer since blemishes have generally been found in microfilm stored in paper cartons which evolve relatively large amounts of formaldehyde and formic acid.

4. The Chemistry of the Formation of Blemishes in Processed Microfilm

4.1. Theory

Paper cartons in which microfilm is stored undergo degradation at high relative humidity and high temperature to form peroxide. The silver in the image serves as a catalyst to decompose the peroxide, forming oxygen which oxidizes the image silver to the silver ion. The chloride ion catalyzes the oxidation of silver by peroxide. The peroxide [11] and formic acid reduce the silver ion to yellow colloidal silver.

Processed microfilms exposed for 2 min to the gas phase of 20-percent hydrochloric acid formed spot blemishes when exposed to peroxide paper. The hydrochloric acid reacted with the image silver to form silver chloride [10]. Many white spots formed, a few with a sharp ring structure, but they were colorless because the gelatin was too acid for the formation of the yellow to red colloidal silver found in naturally occurring spots. Under these conditions only oxidation of the silver occurred but concomitant oxidation and reduction must occur to form yellow to red colloidal silver. When the samples with the white spots were given a printout exposure and treated in a developer solution the spots were still colorless. This indicated that the silver ion had not remained in the colorless area but had migrated to the edge of the spots.

The silver ion may be reduced in an aqueous solution to form colloidal silver [9]. The reduction of silver ion in the gelatin layer of processed film by peroxide forms yellow colloidal silver. A proprietary product containing 19 to 23 percent silver in the colloidal state in gelatin is known in the trade as "Solargentum" [13]. Processed microfilm having no silver image was washed in distilled water, treated in a dilute solution of silver nitrate or silver acetate and dried. When samples were exposed to peroxide at 86 percent relative humidity and 26 °C, the gelatin layer turned yellow. Reducing agents evolved by paper storage

cartons formed the same yellow color in the gelatin of other samples stored in the cartons for 10 days at 86 percent relative humidity and 26 °C.

There is another type of colloidal silver formed when ionic silver is reduced in the presence of an insoluble silver salt such as silver chloride. This type of colloidal silver appears to be silver dispersed in a silver halide and gives colors ranging from pink, red, yellow, brown to gray when formed in an aqueous solution but yellow or reddish when formed in the gelatin layer of microfilm. Carey Lea claimed that this colloid was a mixture of silver chloride and a subhalide of silver. Mees [5] has pointed out that it may be regarded as a mixture of silver in silver halide.

Tests showed that the blemishes contained ionic silver in addition to colloidal silver. The black specks in the centers of many spots appear to be reduced silver since they are readily dissolved by strong nitric acid. In section 2 it was noted that large spots, with light yellowing and even attack on the image silver, were obtained when the microfilm was fixed in a neutral fixer or a nonhardening fixer and washed in distilled water. In these processing procedures no chloride or bromide ions should be present to form silver halide and the yellow color would be attributed to the silver-gelatinate type of colloidal silver. However, when the microfilm was fixed in the nonhardening fix or the acid-hardening fix and washed in chlorine-free tap water the spots were sharper, more yellow, attended by no edge attack or even attack on the image silver, and required more peroxide for spot formation. The chloride ion introduced by the tap water formed silver chloride which led to the formation of the silver-silver chloride type of colloidal silver in spots and prevention of even attack on the image silver. The silver-silver chloride colloidal silver probably predominates in blemish formation.

4.2. Formation of Silver-Silver Halide Colloidal Silver in Solution and on Silver Strips

It was found possible to form the silver-silver chloride type of colloidal silver in water solution. Thirty percent hydrogen peroxide was added to a solution containing varying concentrations of sodium chloride in the presence of solid silver oxide. A small amount of silver oxide dissolved making the solution alkaline. Reduced gray silver accumulated in the bottom of the beaker, leaving the solution clear when no chloride ion was present. When chloride ion was added, a colloidal suspension formed, ranging in color from pink to yellow and sometimes a reddish precipitate formed along with the gray reduced silver. Treatment of the reaction mixture with nitric acid dissolved the reduced silver and left a yellow or reddish colloidal suspension and a reddish precipitate. The pink, yellow and reddish color in the colloidal suspension resembled the color of natural spots. The optimum condition for producing the colloidal silver was a 60-ml solution containing 0.05 g of sodium chloride and about 0.5 to 1 g of solid silver oxide. The hydrogen peroxide was added dropwise with stirring.

Equal mol concentrations of potassium bromide (0.102 g) and potassium iodide (0.142 g) equivalent to 0.05 g of sodium chloride were used in the above procedure to test for the formation of colloidal silver. The potassium bromide solution produced a light yellowish colloidal suspension with a trace of reddish color and some reddish precipitate. The potassium iodide solution gave no visual evidence of the formation of colloidal silver in the solution although a faint trace may have been present. A small amount of sodium chloride in the potassium iodide solution did produce a slightly yellowish colloidal solution indicating that colloidal silver will form in the presence of potassium iodide and the chloride ion.

The silver-silver chloride type of colloidal silver was also formed on silver strips. The silver strips were cleaned with nitric acid, washed in distilled water and immediately immersed in a 50-ml solution containing 0.05 g of sodium chloride, to which 30 percent hydrogen peroxide was added dropwise. A heavy reddish coating of colloidal silver formed on the silver strip showing that the silver on the strip was both oxidized and reduced by the peroxide. When no sodium chloride was added, the silver strip remained bright and served only as a catalyst to decompose the peroxide into water and oxygen. There was no precipitate of reduced silver. These results showed that the chloride ion played an important part in the oxidation of the silver by the peroxide.

5. Test for the Formation of Blemishes in Processed Microfilm With Peroxide Paper

5.1. Preparation of the Peroxide Paper

It was found that paper treated in a solution of hydrogen peroxide was a good source of gaseous peroxide for the formation of blemishes in processed microfilm. All of the types of blemishes described in NBS Handbook 96 [2] have been produced by exposing films to such paper. The paper used was Whatman No. 3MM filter paper which is used in chromatography. The paper was treated 30 min in a 5-percent solution of hydrogen peroxide at room temperature with occasional stirring, hung in a ventilating hood for 2 hr, dried for 24 hr in a desiccator over anhydrous calcium sulfate at 26 °C and stored in a sealed glass bottle in a refrigerator at − 10 °C.

5.2. Apparatus

The tests were made in a desiccator jar containing a saturated salt solution to control the relative humidity. The jar had an inside diameter of 160 mm at the ground flange and a volume of approximately 2300 ml. The air and salt solution were not stirred but the relative humidity value reported is that recorded in the literature for equilibrium conditions. The jar was covered with a flat glass plate about 0.6 cm thick and sealed with petroleum jelly. A porcelain plate perforated with small holes was located just above the saturated salt

solution. Saturated solutions of sodium chloride and potassium chloride were used to obtain relative humidities of about 76 and 86 percent, respectively, at 26 °C.

The test samples, about 6 cm in length, were fastened at each end with black photographic masking tape to a thin glass plate about 8 × 10 cm in size. Four or five samples could be mounted on a plate. The glass plate was then fastened at two opposite edges to the underside of the cover with a strip of the tape, so that the emulsion faced downward. A glass dish, 60 mm in diameter and 13 mm high, was centered in the middle of the porcelain plate to hold the peroxide paper. The mounted microfilm samples were about 8.5 cm from the peroxide paper. In testing microfilms for blemish formation the peroxide paper was added to the glass dish and allowed to react 24 hr at 26° ± 1 °C. Two cm^2 of peroxide paper was sufficient for some microfilms. If no blemishes formed, 2 cm^2 more of peroxide paper was added and the test was continued. Most of the blemish forming microfilms required 2 to 4 cm^2 of the peroxide paper.

6. Summary

Microfilms fixed in a neutral or nonhardening acid bath and washed in distilled water or chlorine-free tap water, formed blemishes when exposed to peroxide paper. Microfilms fixed in an acid hardening bath and washed in chlorine-free tap water, also formed blemishes when exposed to peroxide paper but no blemishes formed after washing in distilled water. The distilled water wash did not reduce the concentration of the residual thiosulfate in the microfilm sufficiently to permit blemish formation. The silver sulfide formed in microfilm during fixation affords some protection against oxidation of the image silver by peroxide but its concentration is not large enough to prevent oxidation of the silver after washing in chlorine-free tap water. Residual thiosulfate reacts with the image silver in processed microfilm to form additional silver sulfide, giving a greater resistance to peroxide attack. Tap wash water containing a chlorine concentration of 1 ppm formed a sufficient amount of silver chloride in the image silver to make microfilm resistant to blemish formation when exposed to peroxide paper. One microfilm required a 10-min wash after fixing in a nonhardening acid bath to inhibit blemish formation. The resistance to blemish formation by the silver chloride in the image silver can be removed by treating the processed microfilm in a 0.2 percent solution of ammonium hydroxide. The image silver showed an even yellowing after this treatment and exposure to peroxide paper. Some resistance to blemish formation was found when microfilms were washed 30 min in tap water containing a chlorine concentration of 0.3 ppm. A trace of silver chloride in the image silver promoted blemish formation. Thus the type of fixing bath, concentration of the chlorine in the wash water, and the washing time after fixation can be factors in the formation of blemishes in processed microfilm stored in paper cartons.

Formaldehyde-urea and formaldehyde-melamine type resins are incorporated in microfilm paper storage cartons as wet-strengthening agents. These resins hydrolyze at high relative humidity to give formaldehyde and ammonia. Formic acid may form by the oxidation of the formaldehyde by the peroxide evolved by the storage carton and aerial oxygen in the presence of silver in the image. Microfilm containing sufficient residual silver chloride to prevent blemish formation loses this resistance when exposed to formic acid evolved in storage cartons. It was found that formic acid was capable of reducing silver chloride and the silver chloride ammonia complex in the gelatin layer of microfilm. The silver chloride ammonia complex was more easily reduced than silver chloride, suggesting that ammonia evolved by storage cartons may sensitize the reduction of the silver chloride in the image silver. A correlation has been found between the incidence of blemishes and the brand of storage cartons. Heavy blemish formation was found on a collection of 35 mm step tablets stored with paper sheets for 4 years in a desk drawer in this laboratory. These films had been washed 30 to 45 min in running tap water. The paper sheets were found to evolve formaldehyde and formic acid after 4 years in storage. These results show that chemicals evolved by paper cartons during storage may react with the image silver to form blemishes.

Microfilms fixed in a bath containing iodide ion formed blemishes when exposed to peroxide paper. However, the microfilms showed good resistance to blemish formation after storage in some paper cartons at 86 percent relative humidity. The same microfilms fixed in a bath without iodide showed appreciable blemish formation. The residual silver iodide in the image made the film resistant to attack by chemicals evolved by the storage cartons. These results are consistent with the finding of a lower incidence of blemish formation in stored microfilm containing iodide.

The present theory is that peroxide oxidizes the silver in the image and also reduces the silver ion. The reduced silver may form colloidal silver of the silver-gelatinate type or combine with a silver halide, forming the silver-silver halide type of coloidal silver.

7. Appendix. Formulas for Developing and Fixing the Silver Image in Microfilm

7.1. Developer

Monomethyl *p*-aminophenol sulfate	2.0 g.
Sodium sulfite, anhydrous	90.0 g.
Hydroquinone	8.0 g.
Sodium carbonate, monohydrate	52.5 g.
Potassium bromide	5.0 g.
Water to make	1 liter.

The development time was 3 min.

7.2. Stop Baths

No. 1 for Neutral Fixing Bath:

Treated sample 1 min in each of two 2-liter lots of distilled water.

No. 2 for Nonhardening Acid Fixing Bath:

Sodium bisulfite	60.0 g.
Water to make	2 liters.

Treated sample 2 min.

No. 3 for Acid Hardening Fixing Bath:

Glacial acetic acid	30 ml.
Water to make	2 liters.

Treated sample 30 secs.

7.3. Fixing Baths

Neutral Fixing Bath:

Sodium thiosulfate ($Na_2S_2O_3 \cdot 5H_2O$)	245.0 g.
Water to make	1 liter.

Fixed sample 4 min.

Nonhardening Acid Fixing Bath:

Sodium thiosulfate ($Na_2S_2O_3 \cdot 5H_2O$)	240.0 g.
Sodium bisulfite	25.0 g.
Water to make	1 liter.

Fixed sample 5 min.

Acid Hardening Fixing Bath:

Sodium thiosulfate ($Na_2S_2O_3 \cdot 5H_2O$)	300.0 g.
Sodium sulfite	10.0 g.
Glacial acetic acid	10 ml.
Boric acid	5.0 g.
Potassium aluminum sulfate	10.0 g.
Water to make	1 liter.

Fixed sample 4 min.

7.4. Chemical Specifications

All of the solutions were made up with distilled water. The following chemicals were of reagent quality meeting ACS specifications: sodium sulfite, acetic acid, boric acid, potassium bromide, and potassium iodide. The monomethyl *p*-aminophenol sulfate, hydroquinone, sodium carbonate, sodium thiosulfate, and potassium aluminum sulfate conformed to the USA Standards Institute Specifications for Photographic Grade Chemicals. The sodium bisulfite was analytical reagent grade.

8. References

[1] R. W. Henn and D. G. Wiest, Microscopic spots in processed microfilm: their nature and prevention, Phot. Sci. Eng. **7**, 253 (1963).

[2] C. S. McCamy, Inspection of processed photographic record films for aging blemishes, National Bureau of Standards Handbook 96 (U.S. Government Printing Office, Washington, D.C., 1964).

[3] C. S. McCamy and C. I. Pope, Summary of current research on archival microfilm, National Bureau of Standards Technical Note 261 (U.S. Government Printing Office, Washington, D.C., 1965).

[4] C. S. McCamy and C. I. Pope, Current research on preservation of archival records on silver-gelatin type microfilm in roll form, J. Res. NBS **69A** (Phys. and Chem.) No. 5, 385 (1965).

[5] C. E. K. Mees, The Theory of the Photographic Process, p. 103, (The Macmillan Co., New York, N.Y., 1954).

[6] Charles N. Durfor and Edith Becker, Public Water Supplies of the 100 Largest Cities in the United States, 1962, U.S. Geological Survey Water-Supply Paper 1812 (U.S. Government Printing Office, Washington, D.C.).

[7] W. A. Taylor and F. R. McCrumb, Modern *p*H and Chlorine Control, p. 42 (W. A. Taylor & Co., Baltimore, Md. 1931).

[8] William J. Ryan, Water Treatment and Purification, p. 197 (McGraw-Hill Book Co., New York, N.Y., 1946).

[9] J. R. Partington, A Text-Book of Inorganic Chemistry, pp. 334 and 804 (The Macmillan and Co., Limited, London, 1933).

[10] J. W. Laist, Copper, Silver and Gold, Vol. **II**, Comprehensive Inorganic Chemistry, p. 155 (D. Van Nostrad Company, Inc., New York, N.Y. 1954).

[11] W. M. Latimer and J. H. Hildebrand, Reference Book of Inorganic Chemistry, p. 24 (The Macmillan Co., New York, N.Y. 1935).

[12] C. I. Pope, Formation of silver sulfide in the photographic image during fixation, J. Res. NBS **64C** (Engr. and Instr.) No. 1, 65 (1960).

[13] The Condensed Chemical Dictionary, 3d edition, p. 592 (Reinhold Publishing Corp., N.Y., 1942).

[14] R. W. Henn, D. G. Wiest, and B. D. Mack, Microscopic spots in processed microfilm: The effect of iodide, Photo. Sci. Eng. **9**, 167 (1965).

[15] Eugene Sawicki, T. R. Hauser, and Sylvester McPherson, Spectrophotometric determination of formaldehyde and formaldehyde-releasing compounds with chromotropic acid, 6-amino-1-naphthol-3-sulfonic acid (J acid), and 6-anilino-1-naphthol-3-sulphonic acid (phenyl J acid), Anal. Chem. **34**, 1460 (1962).

(Paper 72A3–499)

JOURNAL OF RESEARCH of the National Bureau of Standards—A. Physics and Chemistry
Vol. 72A, No. 3, May–June 1968

Absolute Isotopic Abundance Ratios of Common, Equal-Atom, and Radiogenic Lead Isotopic Standards

E. J. Catanzaro, T. J. Murphy, W. R. Shields, and E. L. Garner

Institute for Materials Research, National Bureau of Standards, Washington, D.C. 20234

(February 28, 1968)

Absolute values have been obtained for the isotopic abundance ratios of common, equal-atom, and radiogenic lead isotopic standards using solid-sample mass spectrometry. Samples of known $^{208}Pb/^{206}Pb$ ratio, prepared from nearly pure separated ^{206}Pb and ^{208}Pb solutions, were used to calibrate the mass spectrometers.

Key Words: Absolute ratios, abundance, isotopic standards, lead.

1. Introduction

The NBS is conducting a long-term program of absolute isotopic abundance ratio and physical atomic weight determinations, using solid-sample mass spectrometry. Previous elements studied include silver [1],[1] chlorine [2], copper [3], bromine [4], chromium [5], and magnesium [6]. The present work extends the study to lead.

The extreme isotopic variability of natural lead is well authenticated. It results from the fact that ^{206}Pb, ^{207}Pb, and ^{208}Pb are continually being formed by the decay of ^{238}U, ^{235}U, and ^{232}Th, respectively. ^{204}Pb is nonradiogenic and is used as a fiduciary mark for the separation of the "common" and "radiogenic" portions of natural lead samples. A full discussion of natural lead isotope abundance variations is given by Russell and Farquhar [7].

The purpose of the present study was to establish the absolute isotopic compositions of three lead standards which cover the usual range of natural isotopic values, so that all future lead isotope measurements could be put on an absolute scale. Previous measurements, by numerous laboratories throughout the world, could only be considered relative because there has been no systematic attempt to calibrate instruments and techniques.

In addition, the NBS standard samples, which are distributed for a relatively nominal fee (see appendix), are very high purity lead metal and may also be used as gravimetric standards.

A preliminary study, which was concerned only with the determination of the absolute isotopic compositions of three common lead samples used as references by geochemists, has already been published [8].

The mass spectrometers used in this study were calibrated for bias by the use of samples of known $^{208}Pb/^{206}Pb$ ratio prepared from nearly pure separated ^{206}Pb and ^{208}Pb solutions. The collector and recorder systems used in this laboratory have been designed so that any biases they might contribute are constant. The only "random" bias associated with the isotopic ratio measurements is due to the mass-dependent fractionation of the isotopes during ionization, and this bias is independent of the isotopic composition of the samples. Thus, for each instrumental system used in this study, a single experimentally determined correction factor is valid over the entire range of isotopic compositions measured.

The fact that each mass spectrometer used in this study requires only a single correction factor for source discrimination has been proven by numerous systems calibrations performed mainly with a series of uranium-isotope standards (see appendix), with $^{235}U/^{238}U$ ratios ranging from 1/20 to 20/1. A "systems" calibration, as opposed to a "point" calibration in which only one isotopic ratio standard is used, is always necessary for an instrument which is to be used on an element with more than one isotopic ratio. In this laboratory a uranium-isotope systems calibration is performed on each instrument as soon as it is completed, or modified, and before it is ever used in a research project. In addition, whenever feasible, a partial systems calibration is also performed with widely differing isotopic standards of the element under study. For example, partial systems calibrations have been performed with copper [3] and magnesium [6]. In the

[1] Figures in brackets indicate the literature references at the end of this paper.

present study the systems calibration was rechecked and verified by comparing the results for calibration mixes with $^{208}Pb/^{206}Pb = 1.0$ and $^{208}Pb/^{206}Pb = 2.1$. It is not practicable to prepare standards of more than two isotopes, because the propagation of isotopic composition uncertainty involved in mixing more than two isotope solutions would greatly decrease the accuracy of the calculated ratios.

2. Experimental Procedure

2.1. Mass Spectrometry

Isotopic measurements of the calibration mixes and standard samples were made with three different single-stage solid-sample mass spectrometers. Two instruments (#1 and #3), used by operator I, are identical in all aspects and the third (#2), used by operator II, differed only in that it has an in-line beam valve on the tube. All three instruments have a 12-in radius of curvature 68° analyzer tube and 60° sector magnet, and all three have Z-lenses in the source assembly [9]. Triple-filament sources were used; with rhenium-ribbon (1×30 mil) sample filaments and a platinum-ribbon (1×30 mil) ionizing filament [10].

The samples were prepared to a concentration of 25 mg of Pb per milliliter of 2 percent HNO_3, and were mounted on the sample filaments by mixing, on the filaments, one drop each of the sample solution (~ 250 μg Pb) and of a 10 percent NH_4OH solution. The precipitated $Pb(OH)_2$ was dried with a heat lamp and a 1.2 A current (5 min). The mass spectrometric analysis was begun when the tube pressure was $< 1 \times 10^{-7}$ torr. An accelerating voltage of 10 kV was used and no memory or background signals were ever noted. Source assemblies were dismantled and cleaned between the analyses of the different groups of samples with widely differing isotopic compositions. A detailed description of the mass spectrometric procedure is given by Catanzaro [8].

A small amount of isotopic fractionation generally occurs during an analysis; the $^{208}Pb/^{206}Pb$ ratio generally increases by about 0.03 percent during the data-taking period of an analysis (24 min). To minimize the effect of this fractionation, all analyses were made in an identical manner; data were always taken during the same time interval, and the total lead ion signal was always kept within strict limits (3 to 5×10^{-11} A).

2.2. Preparation of the Separated Lead Isotope Solutions

Approximately 2 g each of electromagnetically separated lead isotopes, ^{206}Pb and ^{208}Pb, in the form of lead nitrate, $Pb(NO_3)_2$, were obtained from the Isotopes Division, Oak Ridge National Laboratory of the Union Carbide Nuclear Company. The $^{206}Pb(NO_3)_2$ was designated series JV, sample 1186(z); and the $^{208}Pb(NO_3)_2$ was designated series MA, sample 1456(a). The certificate of analysis accompanying each sample indicated a high degree of chemical purity. These samples were further analyzed by the Spectrochemical Analysis Section at the National Bureau of Standards by quantitiative emission spectrography. The results of the analyses are shown in table 1. Since the lead concentrations of solutions of the lead isotopes were to be determined by a method based on the precipitation of lead chromate ($PbCrO_4$) only those elements forming relatively insoluble chromates would cause errors in the determinations. These were the elements for which quantitative values or limits of detection were established. It was estimated that the maximum possible contamination of the lead isotope samples would be 0.002 percent for the ^{206}Pb isotope and 0.004 percent for the ^{208}Pb isotope based on the sum of amounts of the detected elements and limits of detection for the others. These concentrations were too low to cause significant error in the lead determinations so it was not necessary to further purify the isotope samples.

TABLE 1. *Results of spectrochemical analysis of lead isotope samples*

Quantitative (with standards) determinations of concentrations			
Element	^{206}Pb	^{208}Pb	Estimated limits of detection
	ppm	*ppm*	*ppm*
Ag	< 1	15	< 0.1
Ba			1
Bi			1
Cu	< 1	< 1	< 0.1
Hg			< 10
Tl			5
Zn			1

NOTES: ..., not detected; <, less than.

Solutions of each separated lead isotope were prepared as follows: the lead isotope as lead nitrate (about 3.1 g) was dissolved in about 20 ml of water and 1 ml of ultrapure grade nitric acid was added to this solution. The resulting solution was filtered and the filtrate was transferred to a 100 ml volumetric flask whose neck had been cut off so that only about 1 cm remained. Enough water was added to bring the final volume to about 65 ml. The solution was thoroughly mixed by swirling for several minutes and the flask was sealed with a rubber serum septum. (The total weight of the flask, solution, and septum was kept below 100 g so that a semimicro balance could be used for weighings.)

The two solutions prepared in this manner were designated "Pb 206" solution and "Pb 208" solution, respectively.

2.3. Lead Concentration of the Separated Isotope Solutions

A search of the chemical literature has shown that there is a need for a high precision—high accuracy method for the determination of lead. A method has

been developed which is based on the precipitation of lead chromate with a small excess of potassium dichromate and spectrophotometric determination of the excess chromate. This method takes advantage of the precise analysis of NBS Standard Reference Material 139b, potassium dichromate, which has been shown to be 99.977 ± 0.003 percent [11].

The flasks containing the solutions of the separated isotopes and a tare flask were placed in the case of a semimicro balance and allowed to stand overnight to insure thermal equilibrium. The flasks and contents were then weighed on the balance to ± 0.02 mg. Samples were withdrawn from each flask by inserting a platinum needle attached to a glass hypodermic syringe through the rubber septum and withdrawing the desired amount of solution. A second needle which just punctured the septum served as a vent. The syringe and needle were then washed with distilled water and the washings were combined with the withdrawn sample. The weight of the sample withdrawn was determined from the weight of the flask before and after withdrawal of solution.

Four samples of from 7.8 to 8.4 g each were withdrawn from each solution by this method for the purpose of determining the lead concentrations of the "Pb 206" solution and the "Pb 208" solution. Each sample was treated as follows: two milliliters of perchloric acid was added and the solution was evaporated to dryness at low heat on a hot plate. The residue was dissolved in a small amount of water and the resulting solution was again evaporated to dryness at low heat on a hot plate. This procedure completely freed the salt from nitrate ion which was found to interfere with the method by forming a lead-potassium-nitrate complex [12] which caused low results. The repeated evaporation also freed the salt from excess perchloric acid.

A 100 to 400 μg excess of potassium dichromate, $K_2Cr_2O_7$, over the amount needed to stoichiometrically precipitate lead chromate, $PbCrO_4$, was accurately weighed on a microbalance. The potassium dichromate used was NBS Standard Reference Material 139b which has been shown to have an assay value of 99.977 ± 0.003 percent [11]. This weight was corrected for assay of the $K_2Cr_2O_7$ and for the bouyancy effect of air.

The potassium dichromate was transferred to a 100 ml beaker and dissolved in about 30 ml of water. This solution was titrated with dilute ammonium hydroxide (1 + 99) to convert dichromate ion, $Cr_2O_7^{--}$, to chromate ion, CrO_4^{--}. The end point of this titration was noted by comparing the color to the yellow color of a potassium chromate solution of the same concentration. A Teflon enclosed magnetic stirring bar was added and the solution was stirred magnetically.

The solution containing the isotopic lead sample was slowly added to the chromate solution and the beaker was thoroughly washed into this solution. The *p*H of this solution was adjusted to 2.5 with (1 + 9) NH_4OH and finally to between 4.5 and 6.5 with (1 + 99) NH_4OH. The *p*H was monitored with a *p*H meter using a glass-calomel electrode system. The precipitate and solution was allowed to stand for 1 hr and then filtered through fine filter paper. The filtrate was caught in a 100 ml volumetric flask. After the precipitate was washed with a small volume of water, the filtrate was diluted to exactly 100 ml. One pellet of ACS grade potassium hydroxide, about 0.2 g, was added to produce an alkaline solution. The chromate concentration was determined by measuring the transmittancy of the solution at 367 nm (mu) of the solution in a 2-cm cell and comparing to a reference curve.

The millimoles (m mol) of lead present in the solution are equivalent to the millimoles of chromate added less the millimoles of chromate found in the filtrate. (The solubility of $PbCrO_4$ under these conditions was found to be negligible.) Table 2 shows the results of these determinations.

TABLE 2. *Concentration of lead isotope solutions*

Soln	Sample No.	Wt soln	$K_2Cr_2O_7$ Equivalent	Conc. soln Pb/g soln
		g	*mmol*	*mmol*
Pb 206.....	A	7.99061	1.131165	0.1415618
	B	8.24170	1.166716	.1415625
	C	8.00613	1.133361	.1415617
	D	7.86875	1.113944	.1415655
			Average	[a] 0.1415629
Pb 208.....	A	8.42849	1.186636	0.1407887
	B	7.85653	1.106099	.1407872
	C	8.36411	1.177473	.1407768
	D	8.27248	1.164649	.1407860
			Average	0.1407847

[a] The standard error of the average is calculated to be 0.00000405 mmol Pb/g soln and the uncertainty of the value of concentration at the 95 percent confidence level is 0.0000081 mmol Pb/g soln.

This method for determining the concentration of lead solutions was tested on solutions containing known amounts of lead. Nine such solutions, in the approximate concentration of the separated isotope solutions, were prepared from high purity lead containing less than 0.001 percent total detected metallic impurities. Four samples containing from 0.139 to 0.153 mmol of Pb were withdrawn from each solution and the lead ion concentrations were determined as described.

Data resulting from the analysis of these nine preliminary lead solutions showed that (a) the concentrations of these solutions as mmol Pb/g soln agreed to within 0.02 percent of the concentrations calculated, (b) a slight positive bias of 0.01 percent was detected but this would have a negligible effect on ratios, (c) the method was independent of sample size or concentration over the range studied, and (d) the analysis of the nine solutions were of equal precision.

Pooling the results of the analyses of the separated isotope solutions as shown in table 2 with the results from the nine sets described above yields a value of 0.0000081 mmol Pb/g soln for the standard deviation of an individual determination (33 deg of freedom). The standard error of the average of four determina-

293-857 O - 68 - 3

tions is therefore $\frac{0.0000081}{2}$ or 0.00000405 mmol Pb/g soln. At the 95 percent confidence level this is equal to 2.04×0.00000405 or 0.000008 mmol Pb/g soln.

2.4. Isotopic Analysis of the Separated Isotope Solutions

The separated isotope solutions were analyzed four times each on two mass spectrometers (#2 and #3). The averaged results are given in table 3. In all of the analyses the amount of ^{204}Pb could only be estimated because the signal was very small and could not be separated from possible baseline fluctuations with any degree of certainty. The isotopic compositions reported by ORNL are: "Pb 206", < 0.01 atom percent ^{204}Pb, 99.8 ± 0.02 atom percent ^{206}Pb, 0.2 ± 0.02 atom percent ^{207}Pb, and < 0.03 atom percent ^{208}Pb; "Pb 208", < 0.05 atom percent ^{204}Pb, 0.19 ± 0.05 atom percent ^{206}Pb, 0.52 ± 0.05 atom percent ^{207}Pb, and 99.3 ± 0.05 atom percent ^{208}Pb. The ORNL limits quoted express the precision of the measurements. From known sources of systematic error, the absolute error is estimated by ORNL to be less than 1 percent.

TABLE 3. *Isotopic composition of separated lead isotopes used in calibration samples*

Separated isotope		Isotopic composition (atom percent)
"Pb 206"	^{204}Pb	0.0010
	^{206}Pb	99.7403 ± 0.0040 [a]
	^{207}Pb	0.2299
	^{208}Pb	.0288
"Pb 208"	^{204}Pb	0.0010
	^{206}Pb	.1930
	^{207}Pb	.5057
	^{208}Pb	99.3003 ± 0.0040

[a] The uncertainties are based on a minimum error of 0.00002 for the ratio determinations. The calculated 95 percent confidence limits are well below this value.

2.5. Preparation of the Calibration Samples

Six calibration samples were prepared by mixing weighed portions of the "Pb 206" solution and the "Pb 208" solution to approximate the compositions of the three reference materials. The target 208/206 ratios were 2.16, 1.00, and 0.014. Two calibration samples were prepared for each target. However, since the errors associated with the preparation of mixes 7 and 8 (208/206 = 0.014) were large, they were not used for calibration purposes. Each calibration sample was thoroughly mixed by stirring and evaporated to dryness. The resulting $Pb(NO_3)$ was taken into solution with sufficient 2 percent HNO_3 so that the lead concentration was 25 mg/ml. The compositions of these calibration samples are given in table 4.

TABLE 4. *Composition of lead calibration samples*

Sample	Isotope	Wt soln	Conc. soln Pb/g soln	Pb
		g	*m mol*	*m mol*
3	206	2.02622	0.1415629	0.2868376
	208	2.08562	.1407847	.2936234
4	206	1.94738	0.1415629	0.2756768
	208	1.97846	.1407847	.2785369
5	206	0.97453	0.1415629	0.1379573
	208	2.10062	.1407847	.2957352
6	206	0.93376	0.1415629	0.1321858
	208	2.04303	.1407847	.2876274
7	206	4.12812	0.1415629	0.5843886
	208	0.05691	.1407847	.0080121
8	206	4.19283	0.1415629	0.5935492
	208	0.06345	.1407847	.0089328

2.6. Isotopic Analyses of the Calibration Mixes and Standard Samples

Two complete sets of analyses of the calibration mixes and standard samples were made; one by operator I using instruments #1 and #3, and one by operator II using instrument #2. In the case of the common lead and equal atom standards, each set consisted of a total of eight analyses of the standard and four analyses each of the two appropriate calibration mixes (mixes 3 and 4 for the common lead, and mixes 5 and 6 for the equal atom lead), run in a simple alternating pattern. In the case of the radiogenic standard each set also consisted of a total of eight analyses of the standard and four analyses each of two calibration mixes (mixes 7 and 8). However, subsequent statistical evaluation of the data showed that both the chemical error in the preparation of these very low $^{208}Pb/^{206}Pb$ mixes and the error in the measurements (minimum error on a ratio = 0.00002) of these extreme ratios were too large, so that these mixes were essentially useless for calibration purposes. The principal source of the chemistry portion of the error was in the weighing and transferring of the small amounts of "Pb 208" solution (~ 60 mg). The results for these calibration mixes were therefore discarded and the final bias correction factor was calculated only on the basis of the four calibration mixes which had approximately the same $^{208}Pb/^{206}Pb$ values of either the common lead or equal atom standards.

In each standard sample analysis eight values each were obtained for the $^{204}Pb/^{206}Pb$, $^{207}Pb/^{206}Pb$, and $^{208}Pb/^{206}Pb$ ratios in the order: four values of $^{208}Pb/^{206}Pb$, four values of $^{207}Pb/^{206}Pb$, eight values of $^{204}Pb/^{206}Pb$, four values of $^{207}Pb/^{206}Pb$, and four values of $^{208}Pb/^{206}Pb$. This pattern was followed so that the data was symmetrical to any fractionation effect. In the analyses of the calibration mixes, twenty-four measurements of the $^{208}Pb/^{206}Pb$ ratio were taken over the normal data-taking time interval of a standard sample analysis.

In all analyses, base-line readings were taken immediately before and after the data. The peak-top data were taken by step-wise changes in the magnet current and each peak-top was monitored for 30 sec.

3. Results and Discussion

Table 5 summarizes the results for the four calibration mixes. There is no statistically significant difference between any of the values. The seemingly large difference between operator II's values for mixes 5 and 6 and mixes 3 and 4 is probably the result of either an operator bias in base-line readings or an attenuator error.

Table 6 gives the observed and corrected ratios for the two sets of data. $^{207}Pb/^{206}Pb$ is corrected by 1/2 of the measured bias, and $^{204}Pb/^{206}Pb$ is corrected by the inverse of the measured bias. Table 7 gives the

TABLE 5. *Determination of mass spectrometric bias*

Calibration sample No.	Isotopic ratio, $^{208}Pb/^{206}Pb$			Correction factor	
	Calculated	Operator I	Operator II	Operator I	Operator II
3	1.017415	1.01677	1.01685	1.000634	1.000556
4	1.004243	1.00378	1.00379	1.000461	1.000451
5	2.125686	2.12462	2.12593	1.000502	0.999885
6	2.117538	2.15718	2.15798	1.000166	.999795
Mean values of correction factors				1.000441	1.000172

TABLE 6. *Observed and corrected isotopic ratios for the standard samples*

Sample	Operator	Observed ratios			Corrected ratios		
		$^{204}Pb/^{206}Pb$	$^{207}Pb/^{206}Pb$	$^{208}Pb/^{206}Pb$	$^{204}Pb/^{206}Pb$	$^{207}Pb/^{206}Pb$	$^{208}Pb/^{206}Pb$
Common SRM 981	I	0.059067	0.91437	2.1669	0.059041	0.91457	2.1678
	II	.059053	.91465	2.1680	.059043	.91472	2.1684
Equal-Atom SRM 982	I	0.027223	0.46679	0.99964	0.027211	0.46689	1.00009
	II	.027232	.46721	1.00007	.027227	.46725	1.00024
Radiogenic SRM 983	I	0.0003723	0.071178	0.013611	0.0003721	0.071194	0.013617
	II	.0003693	.071202	.013619	.0003692	.071208	.013621

TABLE 7. *Absolute isotopic ratios for the three standard samples*

	$^{204}Pb/^{206}Pb$	$^{207}Pb/^{206}Pb$	$^{208}Pb/^{206}Pb$
Common Lead (SRM 981)	0.059042	0.91464	2.1681
Overall limit of error [a]	±0.000037	±0.00033	±0.0008
Uncertainty Components:			
95% confidence limits on ratio determination (minimum=0.00002)	±0.000020	±0.00007	±0.0002
Bounds due to possible systematic error in chemical analyses	±0.000005	±0.00007	±0.0002
Bounds due to possible systematic error in correction factor (including errors in separated isotopes)	±0.000012	±0.00019	±0.0004
Equal-Atom Lead (SRM 982)	0.027219	0.46707	1.00016
Overall limit of error	±0.000027	±0.00020	±0.00036
Uncertainty Components:			
95% confidence limits on ratio determination (minimum=0.00002)	±0.000020	±0.00006	±0.00007
Bounds due to possible systematic error in chemical analyses	±0.000002	±0.00004	±0.00008
Bounds due to possible systematic error in correction factor (including errors in separated isotopes)	±0.000005	±0.00010	±0.00021
Radiogenic Lead (SRM 983)	0.000371	0.071201	0.013619
Overall limit of error	±0.000020	±0.000040	±0.000024
Uncertainty Components:			
95% confidence limits on ratio determination (minimum=0.00002)	±0.000020	±0.000020	±0.000020
Bounds due to possible systematic error in chemical analyses	±0.000000	±0.000006	±0.000001
Bounds due to possible systematic error in correction factor (including errors in separated isotopes)	±0.000000	±0.000014	±0.000003

[a] The overall limit of error is the sum of the 95 percent confidence limits for the ratio determinations and the terms covering effects of known sources of possible systematic error.

293-857 O - 68 - 4

TABLE 8. *Atom percents and atomic weights for the three standard samples*

	Overall limit of error [a]	Uncertainty components		
		Mass spectrometric analytical error	Possible systematic error in chemical analysis	Possible systematic error in composition of separated isotopes
Common Lead (SRM 981)				
Atomic weight..... 207.2152...	±0.00015	±0.00004	±0.00003	±0.00008
Atom percent:				
^{204}Pb..... 1.4245...	±0.0012	±0.0005	±0.0002	±0.0005
^{206}Pb..... 24.1447...	±0.0057	±0.0014	±0.0012	±0.0031
^{207}Pb..... 22.0827...	±0.0027	±0.0019	±0.0002	±0.0006
^{208}Pb..... 52.3481...	±0.0086	±0.0028	±0.0016	±0.0042
Equal-Atom Lead (SRM 982)				
Atomic weight..... 206.9429...	±0.00014	±0.00003	±0.00003	±0.00008
Atom percent:				
^{204}Pb..... 1.0912 ..	±0.0012	±0.0008	±0.0001	±0.0003
^{206}Pb..... 40.0890...	±0.0072	±0.0015	±0.0016	±0.0041
^{207}Pb..... 18.7244...	±0.0023	±0.0022	±0.0000	±0.0001
^{208}Pb..... 40.0954...	±0.0077	±0.0019	±0.0016	±0.0042
Radiogenic Lead (SRM 983)				
Atomic weight..... 206.0646...	±0.00009	±0.00006	±0.00001	±0.00002
Atom percent:				
^{204}Pb..... 0.0342...	±0.0020	±0.0020	±0.0000	±0.0000
^{206}Pb..... 92.1497...	±0.0041	±0.0029	±0.0003	±0.0009
^{207}Pb..... 6.5611...	±0.0025	±0.0017	±0.0002	±0.0006
^{208}Pb..... 1.2550...	±0.0022	±0.0018	±0.0001	±0.0003
Nuclidic Masses: 203.973044, 205.974468, 206.975903, 207.976650				

[a] The overall limit of error is the sum of the 95 percent confidence limits for the ratio determinations and the terms covering effects of known sources of possible systematic error.

final absolute values for all of the ratios along with the overall limits of error and uncertainty components. The precision was essentially the same for both sets of data, so the final values are straight averages of the two sets. Because of instrumental uncertainties, such as dead zone and recorder nonlinearity, it is assumed that no ratio can be measured to better than 0.00002; so this figure is used as an error value whenever the statistically determined 95 percent confidence limit is smaller than 0.00002.

Table 8 gives the atomic percents for each of the isotopes in each standard sample, and the atomic weights ($^{12}C = 12$) of each standard. Nuclidic masses were taken from Mattauch et al. [13].

We are indebted to Mrs. Martha Darr for the quantitative spectrochemical analyses of the lead isotope samples and to Hsien H. Ku for the statistical analysis of the experimental data.

4. Appendix

A catalog listing all of the NBS Standard Reference Materials, including Isotopic Standards, may be obtained from the Superintendent of Documents, U.S. Government Printing Office, Washington, D.C. 20402. The serial number of the catalog is: NBS Miscellaneous Publication 260. The price is 45 cents.

Aliquots of the lead isotope standards described in this paper may be purchased from the NBS in the following manner. Orders should be addressed to the Office of Standard Reference Materials, National Bureau of Standards, Washington, D.C. 20234. The order should stipulate: 1 g each of NBS SRM Nos. 981, 982, and 983 (lead isotope reference standards). The price is $100 per set and they are only sold as a set.

The isotopic compositions of the uranium-isotope standards are given in the table below. These materials are sold individually in 1-g units of U_3O_8. Prices range from $37.50/unit for U005 to $54.50/unit for U930.

NBS best estimate from pooled data of isotopic composition of uranium standards (atom %)

SRM No.	U234	U235	U236	U238	235/238
U005	0.0022	0.4896	0.0047	99.5035	0.004920
U010	.0054	1.0038	.0068	98.9840	.010141
U015	.0085	1.5322	.0164	98.4429	.015564
U020	.0125	2.0383	.0165	97.9327	.020813
U030	.0190	3.0459	.0204	96.9147	.031429
U050	.0279	5.0089	.0480	94.9152	.05277

NBS certified values (atom %)

U100	0.0676	10.190	0.0379	89.704	0.11360
U150	.0993	15.307	.0660	84.528	.18109
U200	.1246	20.013	.2116	79.651	.25126
U350	.2498	35.190	.1673	64.393	.5465
U500	.5181	49.696	.0755	49.711	.9997
U750	.5923	75.357	.2499	23.801	3.166
U800	.6563	80.279	.2445	18.820	4.266
U850	.6437	85.137	.3704	13.848	6.148
U900	.7777	90.196	.3327	8.693	10.375
U930	1.0812	93.336	.2027	5.380	17.349

5. References

[1] W. R. Shields, E. L. Garner, and V. H. Dibeler, J. Res. NBS **66A** (Phys. and Chem.), No. 1, 1 (1962).

[2] W. R. Shields, T. J. Murphy, E. L. Garner, and V. H. Dibeler, J. Am. Chem. Soc. **84,** 1519 (1962).

[3] W. R. Shields, T. J. Murphy, and E. L. Garner, J. Res. NBS **68A** (Phys. and Chem.), No. 6, 589 (1964).

[4] E. J. Catanzaro, T. J. Murphy, E. L. Garner, and W. R. Shields, J. Res. NBS **68A** (Phys. and Chem.), No. 6, 593 (1964).

[5] W. R. Shields, T. J. Murphy, E. J. Catanzaro, and E. L. Garner, J. Res. NBS **70A** (Phys. and Chem.), No. 2, 193 (1966).

[6] E. J. Catanzaro, T. J. Murphy, E. L. Garner, and W. R. Shields, J. Res. NBS **70A** (Phys. and Chem.), No. 6, 453 (1966).

[7] R. D. Russell and R. M. Farquhar, Lead Isotopes in Geology (Interscience, New York, 1960).

[8] E. J. Catanzaro, Earth and Plan. Sci. Letters **3,** No. 4, 343, (1968).

[9] W. R. Shields, editor, NBS Tech. Note 426 (1967).

[10] E. J. Catanzaro, J. Geophys. Res. **72,** No. 4, 1325 (1967).

[11] G. Marienko and J. K. Taylor, J. Res. NBS **67A** (Phys. and Chem.), No. 5, 453 (1963).

[12] B. K. N. Murthy, Pro. of Indian Acad. Sci. **31A,** 160 (1950).

[13] J. H. E. Mattauch, W. Thiele, and A. H. Wapstra, Nuclear Physics **67,** 1 (1965).

(Paper 72A3–500)

JOURNAL OF RESEARCH of the National Bureau of Standards—A. Physics and Chemistry
Vol. 72A, No. 3, May–June 1968

Role of Nickel in Al-10 Percent Si Composites Containing Nickel-Coated Sapphire Whiskers

H. Yakowitz, W. D. Jenkins, and H. Hahn*

Institute for Materials Research, National Bureau of Standards, Washington, D.C. 20234

(January 29, 1968)

The role of nickel in regard to whisker-matrix bonding in a composite of nickel-coated sapphire whiskers inserted into a matrix of aluminum-10 percent silicon alloy by means of liquid phase hot-pressing was investigated. The study was carried out with the aid of optical and electron microscopy, electron probe microanalysis, and microhardness measurements. Results show that most of the nickel is distributed within the matrix alloy.

Some of the nickel apparently interacts with the matrix and forms $NiAl_3$. The presence of $NiAl_3$ in this form increases the average hardness of the composite but apparently does not contribute significantly to strengthening of the alloy. Occasionally, clusters or clumps of nickel-rich material which also contains aluminum are found at or very near whisker-matrix interfaces. It is concluded that if any bonding of the nickel to the sapphire occurred, it was in these regions. Finally, a heat treatment to improve nickel to sapphire bonding and hence bonding of the entire composite is suggested.

Key Words: Al-10 percent Si alloy, electron probe microanalyzer, fiber composites, matrix-whisker bonding, Ni coated sapphire whiskers, optical metallography, sapphire whiskers.

1. Introduction

The availability of sapphire (α-Al_2O_3) fibers (whiskers) in the form of single crystals having very high strength has created extensive interest in the incorporation of whiskers in metallic matrices. It is hoped that such composites will combine the desirable properties of ductile metals with those of the ultrahigh-strength whiskers which would be oriented so as to provide reinforcement in the direction of the applied stresses. In one study [1],[1] 15 volume percent of 1 to 30 μm diam sapphire whiskers added to an aluminum-10 percent silicon matrix by liquid phase hot-pressing at 580 °C resulted in some cases in an increase of 60 percent in tensile strength coupled with a 50 percent increase in elastic modulus. The beneficial effects were still present up to 800 °F (426 °C); some specimens were stronger than any wrought commercial aluminum alloy at this temperature. However, strengthening from sample to sample occurred with less than satisfactory consistency. It was thought that this lack of consistency might be due to poor bonding of the whisker to the matrix.

In an effort to improve this bond between the matrix and the sapphire the specimens were prepared using nickel-coated fibers [1]. Nickel was chosen because it could be deposited with relative ease by the thermal decomposition of nickel tetracarbonyl, $Ni(CO)_4$. Hence, a matte of nickel-coated whiskers could be prepared; the matte could then be inserted into the matrix by liquid phase hot-pressing. Apparently, an NiO-Al_2O_3 spinel forms which serves to bond the Ni to Al_2O_3. In the absence of this spinel, adhesion of Ni to Al_2O_3 may be poor or not occur at all [2, 3]. The presence of the spinel is taken to indicate the probability of good Ni-to-fiber adhesion. In addition, bonding of the fiber matte to the matrix by diffusion during liquid phase hot-pressing is expected. Hence, better bonding of the nickel-coated whiskers to the matrix was expected as contrasted to uncoated whiskers.

Detailed studies concerning the adherence of Ni and Ni-base alloys to sapphire have been carried out [4, 5]. The contact angle between Ni and sapphire is 100°-a higher value than that for Al and sapphire. Adhesion of Ni to sapphire was studied for coatings applied under a pressure of 4×10^{-6} torr. The apparent shear strength at room temperature was high for pure Ni being about 18,000 psi (124.1 MN/m^2). This result is qualitative since the testing method did not ensure true shearing load [5]. Nevertheless, the beneficial effect of the Ni coating was clearly demonstrated.

*Melpar, Inc., Falls Church, Va. 22046.

[1] Figures in brackets indicate the literature references at the end of this paper.

Fracture tests usually showed that at least part of the failure was through the sapphire. In a few cases, fracture was entirely along the interface between the Ni and the sapphire [5]. Thus, good Ni to sapphire bonding should indeed offer improved composite strength.

However, we do not wish to imply that whisker-matrix adhesion is the limiting strength factor in the system. Other contributory factors include: (1) whisker orientation, length and aspect ratio, (2) matrix shear strength and shear modulus, (3) composite failure mode and (4) matrix hardening during composite loading. In the tests of strength which were conducted, each of the above factors was nearly the same. Hence, we believe that most significant differences observed were due to whisker-matrix adhesion effects.

Although some of the specimens containing nickel were stronger than those in which nickel was absent, the strengthening effect was not reproducible in all cases. The degree of strengthening was about the same for both coated and uncoated whiskers when (apparently) satisfactory bonding of the whiskers to the matrix occurred. Evidence of this was that tensile tests on both types of specimens gave similar results [1]. The present report concerns a further investigation into the distribution of the nickel in the composite.

2. Tests of the Composite Specimens

2.1. Optical Results

Metallographic examination of the as-pressed material was carried out. Typical microstructures are shown in figures 1 and 2 for Ni-coated and uncoated whiskers respectively. A great number of broken whiskers are seen; these are more or less randomly oriented. The chief difference is that specimens containing the Ni-coated whiskers exhibit an extra constituent which appears as pale blue dots under white light after etching in Keller's reagent; the color is enhanced in polarized light (fig. 1). No such constituent appeared in composites formed with uncoated whiskers (fig. 2).

In the study of Al-Ni alloys, the intermetallic compound $NiAl_3$ has been reported to appear blue after etching [6]. The presence of a dispersed "blue dot" constituent led to the suspicion that the Ni coating had been lost from the whiskers during processing.

In this regard, a pertinent question concerns the diffusivity of nickel in molten aluminum-silicon alloy at the pressure of 2000 psi used for liquid phase hot-pressing [1]. Unfortunately, there are very few data on diffusion in liquid metals other than for the alkali group. However, an approximate value of the diffusion coefficient of Ni in liquid Al, called $D_{Ni,\,Al}$, has been suggested as being 10^{-5} to 10^{-6} cm^2/sec [7]. The effect of 2000 psi (13.79 MN/m^2) pressure would be to reduce this value, but only by a factor of about two at most [8]. Therefore, we shall take $D_{Ni,\,Al}$ as being 10^{-6} cm^2/sec for the liquid phase hot-pressing step. For comparison, we note that the diffusion coefficient of Ni in solid Al has been reported as 10^{-11} cm^2/sec at 580 °C [9].

In order to determine the random walk distance, X for the nickel during liquid phase hot-pressing the relation is:

$$X = (Dt)^{1/2} \tag{1}$$

where t is the time at temperature. The value of X is 50 μm for t of 25 sec. The average distance between whiskers is only 50 to 100 μm as determined by optical metallography (see fig. 1 for example). Thus, diffusion of Ni would have occurred throughout the matrix in something less than a minute during liquid phase hot-pressing. The molten aluminum-silicon matrix would have been saturated with nickel and, upon cooling, $NiAl_3$ would have precipitated. This is precisely what Castleman and Seigle observed in aluminum melted in the presence of nickel which was examined metallographically after cooling [10]. Complete loss of Ni from sapphire whiskers in a molten aluminum matrix was observed by Mehan et al. [11]. In their study the presence of $NiAl_3$ in the resulting solid samples was confirmed by x-ray diffraction methods.

Reference to the Ni-Al constitution diagram shows that the solubility of Ni in solid Al is very low (much lower than in liquid aluminum) [12]. Furthermore, formation of the phase Ni_2Al_3 is inhibited by the application of pressure and the pressure induced decrease in the diffusion coefficient is the rate controlling factor in the growth kinetics of Ni_2Al_3 [6]. Therefore, we conclude that the "blue dots" are $NiAl_3$ and that the matrix alloy contains some Ni in solid solution. No great amount of Ni_2Al_3 or other phases richer in nickel would be expected.

2.2. Electron Probe Microanalysis

Electron probe microanalysis was performed to determine the actual nickel distribution within the coated whisker composite. In addition, specimens of composites containing uncoated whiskers and a control specimen of Al-10 percent Si without whiskers were examined. Composites containing uncoated whiskers contained no nickel; a search was made with the microprobe to make certain of this. However, the silicon was found to be inhomogeneously distributed within the specimen; the same was true for the matrix alloy containing no whiskers. Such an inhomogeneous silicon distribution in the matrix would not have helped to improve whisker bonding and may have had an injurious effect.

Scanning photographs of a specimen of a composite containing nickel coated whiskers were prepared [13]. The presence of clumps of nickel concentrates near the edges of whiskers as well as the presence of nickel dispersed within the matrix was noted. The presence of nickel away from the blue dots was confirmed by step scanning the spectrometer through the Ni-Kα x-ray peak with a finely focused static

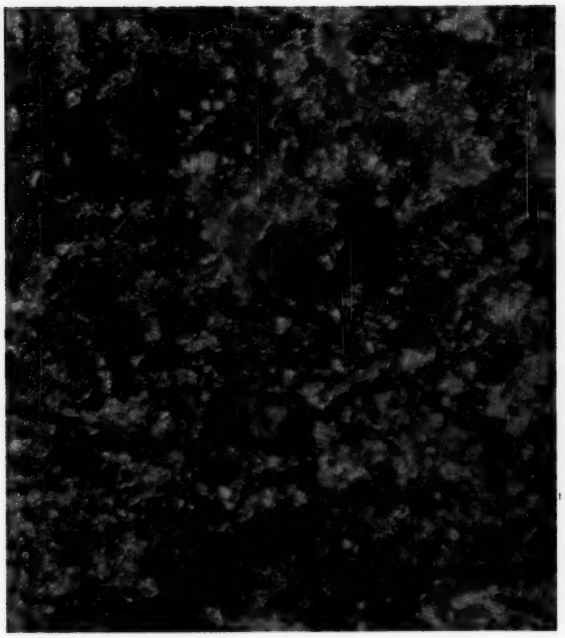

FIGURE 1. *Photomicrograph taken in polarized light of composite containing 15 v/o Ni–coated sapphire whiskers in the as–pressed condition.*

Note the blue dots which are probably $NiAl_3$ (A–1). Note also the broken whiskers which appear yellow to white (A–2). Larger whiskers are blue and orange (A–3). ×1000.

FIGURE 2. *Photomicrograph taken in polarized light of composite containing 15 v/o uncoated sapphire whiskers in the as–pressed condition.*

Note the complete absence of the blue dots. Again many broken whiskers are present. ×1000.

FIGURE 3. *Composite map of scanning microprobe photographs of composite containing 15 vol. percent Ni coated sapphire whiskers in the as–pressed condition.*

The yellow–green areas are the whiskers as photographed by means of cathodoluminescence. The red represents the Ni distribution. The pale blue represents the Si distribution. Note the nickel clumps (solid red blobs) at or very near whisker edges. The remainder of the Ni is distributed throughout the matrix without regard for the presence of Si clumps. Color–addition methods were used to combine separate cathodoluminescence (whiskers), Ni-K x–ray distribution, and Si-K x–ray distribution photographs of the same area. ×1125.

FIGURE 4. *Electron micrograph of typical whisker from the same sample as shown in figure 3.*
Note the heavily etched material (A–1) which is probably high in Ni. Note points of coherency of this material with whisker (A–2).

probe placed in the matrix as far away as possible from the blue dots. Nickel count rates were 15 percent above background in these regions.

In order to show the distributions observed, a composite map in color was prepared using the data from the scanning photographs. The result is shown in figure 3. Most of the Ni coating has been lost from the whisker and is dispersed in the matrix. The regions of Ni concentration at or near whisker surfaces were investigated further in an effort to determine what role, if any, such regions play in the bonding of the sapphire to the nickel. It has been postulated that the wetting of sapphire by nickel is caused by the formation of $NiO \cdot Al_2O_3$ spinel although the complete mechanism is not yet fully apparent [2, 3]. Therefore, a microprobe search of the Ni concentrate regions for Ni and oxygen in combination was performed using x-ray scans at magnifications of 2350 × and 4700 ×. The oxygen distribution indicates that the high nickel regions are not spinel but that there are portions of these regions which appear to contain oxygen. In addition, the high nickel regions also contain aluminum but virtually no silicon. Hence, the results of the search for spinel were inconclusive.

2.3. Electron Metallography

The electron microscope was used to search for evidence of spinel formation at the whisker-matrix interface. Several replicas were taken from metallographically polished and etched surfaces of specimens containing Ni-coated whiskers. A typical electron micrograph is shown as figure 4. We believe the heavily etched region to be the material richer in Ni since similar roughening occurs between Ni-base alloys and sapphire where definite reactions have indeed been confirmed [5, 14]. This roughened material tends to blend into the whisker at several spots. There is no evidence for the formation of a discrete phase at the whisker-matrix interface at magnifications up to 20,000 ×. As control samples, replicas were taken from specimens containing no whiskers and from specimens containing uncoated sapphire whiskers respectively. In the case of no whiskers the electron microscope revealed an almost textureless surface punctuated by large masses of high Si material. For the uncoated whisker case, the surface between whiskers was also free of texture.

It seems reasonable that the areas where the Ni rich material blends directly with the whisker would be the areas where the matrix and whisker are most adherent to one another. Nevertheless, like Ritter and Burton [3], we were unable to find evidence of the presence of a region which might be $NiO \cdot Al_2O_3$ even in these areas. If any spinel is present it is contained in a band which is not visible at 20,000 ×. If the spots where Ni and whiskers blend are responsible for improvement in bonding then the whiskers are bound into the matrix at more or less random points along the interface. Such randomness would aid in explaining why an unacceptably large percentage of composites were still not strengthened even after the change to Ni-coated whiskers was made.

2.4. Hardness Testing Results

If the blue dots are indeed dispersed $NiAl_3$, the average hardness of specimens containing such a hard, brittle intermetallic phase would be expected to be greater than that of specimens prepared without nickel coated whiskers.

Hardness measurements were made in typical specimens containing both Ni coated fibers and uncoated fibers. The Knoop indenter with a 20 × objective and 200 g load was used; the results were converted to Rockwell *B* values. While there was considerable scatter of the data, the average hardness was greater for composites containing Ni-coated fibers than for composites containing uncoated fibers. Typical values were R_B of 65 for the Ni-coated fiber composites and R_B of 40 for uncoated fiber composites. The Al-Si base alloy without fibers was too soft to give a meaningful Rockwell *B* value. Thus, these results are certainly not at variance with the conclusion that the blue dots are dispersed $NiAl_3$.

3. Conclusions

Considerable diffusion of nickel occurred in the composites containing nickel-coated whiskers during the liquid phase hot-pressing step. This resulted in the formation of a blue dot phase dispersed within the alloy; evidence indicates strongly that this phase is $NiAl_3$. Electron probe microanalysis and hardness tests are not at variance with this conclusion.

Concerning the bonding of the nickel to the sapphire whiskers, the evidence is not conclusive. However, the electron probe microanalyzer results indicate that nickel-rich clumps often appear at whisker surfaces. It is not unreasonable to conclude that whatever the mechanism of bonding the whisker to the nickel, it occurs in these regions.

Tensile tests of strengthened coated and uncoated fiber composites gave approximately the same results since the fibers are the same and they are equivalently combined into the matrix with or without the aid of nickel. The $NiAl_3$ formed in the coated fiber composites increased the hardness of the material but the (brittle nature of) $NiAl_3$ was apparently ineffective in improving the tensile strength when the $NiAl_3$ is in the randomly dispersed small spherules.

The results indicate that better bonding of the nickel to the sapphire might further improve the percentage of strengthened samples. There is definite evidence that nickel will bond to sapphire by diffusion in the presence of oxygen [2]. Possibly heating the nickel-whisker matte at 1350 to 1400 °C for an appropriate time in vacuum of about 0.1 to 1 torr (prior to liquid-hot-pressing) would offer improvement.

We thank D. B. Ballard for the electron microscope studies and K. F. J. Heinrich for aid and advice in preparing the scanning microprobe pictures.

4. References

[1] H. Hahn, A. P. Divecha, P. Lare, and B. Dennison, Melpar Rept. 5192, 64 pp. (1966) [unpublished].
[2] D. B. Wittry, Advances in X-ray Analysis **3**, 197 (1960).
[3] J. E. Ritter, Jr. and M. S. Burton, Trans. AIME **239**, 21 (1967).
[4] W. H. Sutton, Investigation of Bonding in Oxide-Fiber (Whisker) Reinforced Metals, Final Report, Contract No. DA 36-034-ORD-3768 (Z), Technical Report AMRA CR 63-01/8 (June 30, 1964), DMIC No. 58778.
[5] W. H. Sutton and E. Feingold, Investigation of Bonding in Oxide-Fiber (Whisker) Reinforced Metals, Final Report AMRA CR 65-01/4 (July 1, 1964-July 31, 1965), Contract No. DA 19-066-AMC-184 (X), DMIC No. 64060.
[6] W. L. Fink and L. A. Willey, Trans. AIME **111**, 293 (1934).
[7] J. R. Manning, private communication (1967).
[8] L. S. Castleman, Acta Met. **8**, 137 (1960).
[9] K. Hirano, R. P. Agarwala, and M. Cohen, Acta Met. **10**, 857 (1962).
[10] L. S. Castleman and L. L. Seigle, Trans. AIME **212**, 589 (1958).
[11] R. L. Mehan, C. A. Bruch, and E. Feingold, Rep't. AFML-TR-66-337, 167 pp. (1966) [unpublished].
[12] M. Hansen, Constitution of Binary Alloys, p. 118, 2d ed. (McGraw-Hill Book Co., New York, N.Y. (1958)).
[13] For a recent review of microprobe scanning techniques see, K. F. J. Heinrich NBS Tech. Note 278, 39 pp. (1967).
[14] Preliminary information reported by General Electric Company under Army Contract DA-19-066-AMC-330 (X).

(Paper 72A3-501)

JOURNAL OF RESEARCH of the National Bureau of Standards—A. Physics and Chemistry
Vol. 72A, No. 3, May–June 1968

Publications of the National Bureau of Standards*

Selected Abstracts

A review of studies made on the decade fluctuations in the earth's rate of rotation, W. R. Davey, *Tech. Note 358 (Oct. 16, 1967), 20 cents.*
Studies of variations in the length of the day (l.o.d.) on the order of a few milliseconds over the period of a few decades are briefly reviewed. In this connection, studies on the dynamo theory of geomagnetism, the westward drift of the magnetic field, and electromagnetic core-mantle coupling preface the theory of the decade fluctuations in the l.o.d.

Key Words: Core-mantle coupling, decade fluctuations, dynamo theory, earth's core, geomagnetism, rotation of the earth, westward drift.

Activation analysis: Cockcroft-Walton generator, nuclear reactor, Linac, July 1966 through June 1967, Ed. J. R. DeVoe, *Tech. Note 428 (Nov. 1967), 55 cents.*
This is the first separate (not combined with that of Radiochemical Analysis) summary of progress for the Activation Analysis Section of the Analytical Chemistry Division of the National Bureau of Standards.
Pertinent information on the irradiation facilities of the nuclear reactor, Linac, and Cockcroft-Walton generator are described. The initial installation of pneumatic transfer tubes is completed. Of great significance is the completion of a clean room that is used for pre-irradiation chemical separation for high sensitivity activation analysis.
A dual-sample biaxial rotating 14-MeV neutron-irradiation assembly has been tested. This assembly is part of a system that is controlled by a relay type of programmer to automate those irradiation steps that adversely affect precision of the analysis. This system was used to improve greatly the precision of analysis for oxygen and fluorine. As a result of improved precision with the 14-MeV neutron irradiation, a study of systematic errors is now possible. Efforts to establish a reproducible correction factor for neutron and gamma-ray absorption between different matrices within the sample have shown considerable promise.
Standard Reference Material (SRM) steel chip Nos. 3b, 3c, and 30f have been analyzed for vanadium. Preliminary analyses of high purity platinum (a potential SRM) showed silver, copper, gold, palladium, and iridium at the ppm level. Future biological SRM's (tree leaves, and beef liver) were tested for homogeneity and found satisfactory.
A variety of service analyses were performed. In particular, very pure aluminum was found to contain fractions of a ppm of chromium and scandium.
Additional efforts are being made to monitor reactor neutron fluxes. Additional nuclear instrumentation is being assembled to improve the versatility of the analysis technique.
Performance of the bremsstrahlung target, used with the linear electron accelerator, has been evaluated. Photon intensity distribution and stability was found to be within usable range. Analyses using the (γ, n) or (γ, p) reactions have been developed for magnesium in steels, and carbon in sodium metal.

Key Words: NBS reactor, NBS Linac, Cockcroft-Walton generator, digital computers, activation analysis, Standard Reference materials, photoneutron reactions, flux monitors, vanadium in irons and steels; homogeneity testing, biological, botanical samples, carbon in sodium, self absorption corrections, high precision 14 MeV neutron activation, instrumentation, flux monitors.

Calculation of the properties of vacancies and interstitials. Proceedings of a conference May 1–5, 1966, Ed. A. D. Franklin, *Misc. Publ. 287 (Nov. 17, 1967), $2.50.*
This is the Proceedings of a Conference on the Calculation of the Properties of Vacancies and Interstitials, Skyland, Virginia, USA, held on May 1–5, 1966. The Conference dealt with the theory and techniques of calculation of the properties of point defects in metallic and nonmetallic crystals. The contributed and invited papers divided about evenly among three major topics: (1) static-lattice calculations of the energies and configurations of simple vacancies and interstitials in, mainly, metals and ionic crystals; (2) electronic states at and near point defects in metals, rare gas solids, and insulators (*f*-centers, electron traps); and (3) vibrational states at point defects. The report of a panel discussion on each topic is also included. The emphasis is on the theory of the properties of isolated, simple defects rather than on the statistical properties of defect assemblies. The Conference attempted to examine the point defect theory and calculations critically, from the standpoint of general theory, rather than simply compare results with experiment.

Key Words: Calculations, electronic states, energies of formation, energies of motion, interstitials, point defects, theory, vacancies, vibrational states.

Disclosures on: Autosort—an automatic collating and sorting machine, optical heterodyne refractometer, liquid metering pump, stable wideband relaxation oscillator using three inverting amplifiers, and seat belt webbing abrasion resistance testing machine, Ed. D. Robbins and A. J. Englert, *Tech. Note 437 (Nov. 1967), 25 cents.*
This booklet presents descriptions and drawings of five devices that embody interesting and unusal solutions to problems frequently encountered in their respective fields. The devices are: Autosort—An Automatic Collating and Sorting Machine; Optical Heterodyne Refractometer; Liquid Metering Pump; Stable Wideband Relaxation Oscillator Using Three Inverting Amplifiers; Seat Belt Webbing Abrasion Resistance Testing Machine.

Key Words: Automatic document distribution, programmed document distribution, rotatable document bin array, optical refractive index, laser beam phase shift, laser heterodyning, flexible tubing pump, liquid metering pump, relaxation oscillator, inverting amplifiers, seat belt webbing abrasion, abrasion resistance testing.

Evaluation of information systems: A selected bibliography with informative abstracts, M. M. Henderson, *Tech. Note 297 (Dec. 1967), $1.00.*
A survey of the literature on evaluation of information systems has been conducted by the Technical Information Exchange, Center for Computer Sciences and Technology, National Bureau of Standards. During the early stages of the survey, the literature was divided among descriptions of programs which compared the performance of two or more information systems, accounts of programs which studied the performance of one system, papers and reports which discussed the problems of evaluation programs, and documents which proposed new techniques for evaluation of systems. From the total literature collected, those references which were judged to be most directly concerned with the subject of evaluation of information systems were selected and abstracted. The abstracts are designed to give a summary of the content of the corresponding paper; the author's own wording was used extensively, in order to avoid misinterpretation. All of the references collected are listed,

in alphabetic order of authors names, in the appendix to the main body of this publication.

Key Words: Evaluation, performance, testing of information systems, effectiveness, relevance.

Low temperature mechanical properties of copper and selected copper alloys. A compilation from the literature, R. P. Reed and R. P. Mikesell, *Mono. 101 (Dec. 1, 1967), $2.75.*
In the past 60 years considerable data has accumulated concerning the mechanical properties of copper and its alloys. It was felt that there was a great need to adequately document these results in one publication. Therefore a unique type of compilation is presented. The compilation is divided into four parts. The first section is intended for quick reference use for those who are interested in average values. The second section includes data from most of the investigators who have published results on the mechanical properties of copper and its alloys. The third section is composed of tables classifying the investigations which were not included in section two. These usually involve investigations in which data were obtained only at one temperature, such as room temperature. The fourth section lists, in alphabetical order, all references used.

Key Words: Compilation, copper, copper alloys, low temperature, mechanical properties.

Radiochemical analysis nuclear instrumentation, radiation techniques, nuclear chemistry radioisotope techniques July 1966 through June 1967, Ed. J. R. DeVoe, *Tech. Note 421 (Nov. 1967), 50 cents.*
This is the fourth summary of progress of the Radiochemical Analysis Section of the Analytical Chemistry Division at the National Bureau of Standards.
The section's effort comprises four major areas: Mössbauer spectroscopy, nuclear chemistry, nuclear instrumentation, and the application of statistics in nuclear and analytical chemistry.
A new design of transducer which is more compact than the previous design has been made so that low temperature experiments can be more easily performed. A method of simultaneously measuring two spectra with a single transducer has been devised. A single line nickel-61 source has been made and the magnetic moment of the excited 5/2 state has been measured with this source. Efforts have continued on the interpretation of the spectral parameters and their relation to structure analysis. Studies are continuing on the production of a standard for chemical shift of tin compounds. Equipment is in the final state of assembly and initial testing for measuring cross sections of reactions such as $(\gamma, {}^3He)$ or $(\gamma, {}^4He)$ by mass spectrometry of the reaction products.
The precision of an analytical method must be carefully used when expressing a detection limit. In addition, care must be taken to be definitive about the meaning of a limit of detection. A suggested procedure for uniformity in reporting these often used terms is presented in this report.
The practical operation of Ge(Li) and Si(Li) detectors has been evaluated. It is found that careful control of the preamplifier noise and response is required for optimum performance.
A study of the precision and accuracy of gamma-ray excited x-ray fluorescence was made. Using as a basis the analysis of certified Standard Reference Materials, an improvement of a factor of two in precision was measured. The major advantage concluded from this work is that if rapid analysis requiring portability is desired, the radioisotopic source approach is useful.

Key Words: NBS Linac, computers, standard reference materials, photoneutron reaction, cross sections, flux monitors, nickel-61, Mössbauer spectroscopy, tin standard for chemical shift, PARLORS program for Mössbauer spectra, Mössbauer instrumentation, detection limits for analysis, solid state detectors.

High-precision coulometric iodimetry, G. Marinenko and J. K. Taylor, *Anal. Chem.* **39,** *No. 13, 1568–1571 (Nov. 1967).*
On the basis of measurement of the potential of the working platinum anode as a function of current density and concentration of KI in solution, conditions were established for 100.0000% efficient generation of iodine. NBS Standard Reference Material arsenious oxide was analyzed utilizing optimum conditions for generation of iodine and for the stoichiometric reaction of arsenious acid with iodine. The precision of the method for titration of 0.5-g samples of As_2O_3 is about 0.003%. Analysis of data for the assay of samples ranging in size from 100 mg to 1 g indicates no bias in the method. Coulometric assay of SRM 83c is $99.986 \pm 0.003\%$, which is in close agreement with the titrimetric comparison of 83c to iodine, purified by sublimation. This fact serves as additional evidence of the accuracy of the developed method.

Key Words: Constant-current coulometry, high-precision analysis, iodimetry, arsenious oxide, current efficiency.

Light scattering phenomena near the critical point, D. McIntyre and A. M. Wims (*Proc. 2d Interdisciplinary Conf. Electromagnetic Scattering ICES–11, University of Massachusetts, Amherst, Mass., June 28–30, 1965*), *Book, Electromagnetic Scattering, Ed. R. L. Rowell and R. Stein, pp. 457–484 (Gordon and Breach, Inc., New York, N.Y., 1967).*
The scattering from liquids and liquid mixtures near their critical points has been extensively studied in recent years. The existing experimental data are discussed with respect to their usefulness and limitations in sorting out the various statistical mechanical descriptions of critical phenomena. Scattering measurements on polystyrenecyclohexane, cyclohexane-aniline, perfluoroheptane-isooctane, nitroethane-3-methylpentane are reported and discussed.

Key Words: Critical opalescence, light scattering, critical mixtures, binary mixtures, coexistence curves, phase separations.

NMR studies of inorganic fluorides. III. Si_3F_8, R. B. Johannesen, *J. Chem. Phys.* **47,** *No. 3, 955–960 (Aug. 1, 1967).*
A high-resolution n.m.r. study of octafluorotrisilane, Si_3F_8, is reported. The chemical shifts of ^{19}F and ^{29}Si, relative to SiF_4 as a reference, are given. Coupling constants, including in every case the relative sign, are given for isotopic species containing not more than one ^{29}Si atom. The results are compared with the corresponding values for SiF_4 and Si_2F_6.

Key Words: Nuclear magnetic resonance, fluorine, silicon, fluorosilanes, octafluorotrisilane, chemical shift, spin coupling constants, double resonance.

Periodic acid, a novel oxidant of polycyclic aromatic hydrocarbons, A. J. Fatiadi, *Chem. Communications* **21,** *1087–1088 (1967).*
Certain polycyclic, aromatic hydrocarbons can be oxidized in good yield to quinones with paraperiodic acid in aprotic solvents containing a small proportion of water. No reaction was observed when oxidation was attempted with sodium periodate, instead of periodic acid. A possible reaction path for the oxidation has been suggested.

Key Words: Polycyclic aromatic hydrocarbons, paraperiodic acid, sodium periodate, aprotic solvent, reaction mechanism.

Phenylhydrazono-phenylazo tautomerism. Part II. Structures of 2-oxo-1,3-bis(phenylhydrazono) compounds and related compounds. A. J. Fatiadi and H. S. Isbell, *Carbohydr. Res.* **5,** *302–319 (1967).*
The structures of *xylo*-4,5,6-trihydroxy-2-oxo-1,3-bis(phenylhydrazono)cyclohexane (*1*), 2-oxo-1,3-bis(phenylhydrazono)cyclohexane (*2*), 2-oxo-1,3-bis(phenylhydrazono)cyclopentane (*3*), 3-oxo-2,4-bis(phenylhydrazono)cyclonexanecarboxylic acid (*4*), 2-oxo-1,3-bis(phenylhydrazono)indane (*5*), and 2-oxo-1,3-bis(phenylhydrazono)propane (*6*) were studied by comparison of their n.m.r., u.v., visible and i.r. spectra with the spectra of reference compounds of known structures. The results show the compounds exist in two forms. The red forms have an enolic (chelated) phenylhydrazono–phenylazo structure. A similarity of the compounds to the dipheynlformazans is noted and substantiated by a comparison of absorption spectra. Compound *2* crystallizes from aqueous ethyl alcohol in the form of a yellow hydrate shown to have a phenylhydrazono structure. On dehydration, the yellow hydrate yields the red enolic form. The structures of the 1,2,3-tris(phenyldrazono) derivations of cyclohexane, cyclopentane and cyclohexanecarboxylic acid were also studied.

Key Words: Diphenylformazans, infrared spectra, enolic phenylhydrazono–phenylazo structure, molecular structure, nuclear magnetic resonance, oxo-bis(phenylhydrazono) compounds, phenylhydrazono–phenylazo tautomerism, phenylosazones, tautomerism, ultraviolet spectra.

Curve-fitting techniques and applications to thermodynamics, J. G. Hust and R. D. McCarty, *Cryogenics* **7,** *No. 4, 200–206 (Aug. 1967).*
The general problem of least squares fitting is considered. For completeness, derivations of well-known relations are included along with the developments of new techniques for imposing constraints on the unknown parameters, and of fitting data for several different properties simultaneously for both linear and non-linear equations. Several thermodynamic applications are included to illustrate the techniques developed.

Key Words: Curve fitting, least squares, thermodynamics, constraints, weighting, non-linear.

Application of computers to quantitative analysis of microstructures, G. A. Moore, *Book, Proc. 2d Intern. Congress for Stereology, Chicago, Ill., Apr. 8–13, 1967, Ed. H. Elias, pp. 281–284 (Springer-Verlag, New York, N.Y., 1967).*
Stereological projections from any micrograph require evaluation of particle size and shape, thus observation on a dense raster limited only by the resolution of the microscope and observing system. The required large number of observations dictate automatic scanning and computer processing of the image. Results are limited by statistical inefficiency and precision of observation. Using high precision scanning equipment, the inaccuracies of measurement remain comparable to the limits imposed by statistics. Presently attainable precision is, however, an order of magnitude better than can normally be obtained by manual methods.
The presence or absence of a specific phase can be represented by a two-dimensional binary array which can be rapidly processed to yield the required measurements. Logical modification by the computer is frequently necessary to substitute for some of the logical discriminations normally made by the human analyst and to facilitate the desired measurements. Logical processes can reveal stereological relationships, construct morphological models, and dissect and describe the individual particles.

Key Words: Automatic scanning (of micrographs), computer processing (of micrographs), logical modification of pictures, precision scanning (of micrographs), quantitative microscopy, stereological analysis.

The metric system in illuminating engineering, L. E. Barbrow, *Illum. Engr.* **LXII,** *No. 11, 638–640 (Nov. 1967).*
The most commonly used unit of illumination in the USA is the footcandle. There are two commonly used units of luminance, the footlambert and the candela per square inch. The growing international adoption of SI units makes it advisable for illuminating engineers to introduce the use of these units in their publications in the immediate future and to understand the implications of the use of the SI units. The SI unit of illumination is the lux (one lumen per square meter). The SI unit of luminance is one candela per square meter (sometimes named the nit). One of the basic principles and advantages of SI is that there can be only one unit for each quantity; thus there cannot be an SI unit similar to footlambert which is expressed in terms of lumens per unit area. Council of the Illuminating Engineering Society has been officially requested to (1) approve the policy of having SI units given primary use in its publications, and (2) promote the deprecation of "lumens per unit area" as a unit of luminance and sponsor its use solely as a unit of luminous exitance (formerly emittance).

Key Words: Exitance, illumination, luminance, lux, metric units, nit, SI units in illuminating engineering.

Born-model calculation of point-defect formation energies in alkaline-earth fluorides, A. D. Franklin (*Proc. 2d Meeting Point Defects in Non-metallic Solids, Univ. of Sussex, Brighton, England, Sept. 26–28, 1966*) *Proc. British Ceram. Soc.* **9,** *15–24 (July 1967).*
A Born-model calculation of the lattice energy required to form anion and cation vacancies and interstitials has been performed for SrF_2 and BaF_2, following techniques used earlier for CaF_2. Anion Frenkel pairs are the favored intrinsic defects for SrF_2 and BaF_2 as well as for CaF_2, the formation energy decreasing somewhat from CaF_2 to BaF_2. In the presence of substitutional trivalent cation impurities, the tendency to form anion interstitials as the charge-compensating defect should be strongest in BaF_2, least in CaF_2, with SrF_2 again intermediate.

Key Words: Alkaline earth fluorides, Born model, energies of formation, ionic crystals, point defects.

Negative dispersion and brillouin scattering, R. D. Mountain and T. A. Litovitz, *J. Acoust. Soc. Am.* **42,** *No. 2, 516–517 (Aug. 1967).*
The fluctuations in density observed in Brillouin scattering may be represented as temporally absorbed waves. Negative dispersion occurs for these waves although it may be masked by positive dispersion due to relaxation processes. Numerical estimates of velocity and of negative dispersion are made for CCl_4 at 20 °C. The importance of measuring both the position and the width of the Brillouin peaks in order to obtain the elastic modulus of the liquid is stressed.

Key Words: Brillouin scattering, elastic modulus, liquid, negative dispersion relaxation of viscosity, Temporal absorption.

Response of pneumatic pressure-measurement systems to a step input in the free molecule, transition, and continuum flow regimes, J. Hord, *ISA Trans.* **6,** *No. 3, 252–260 (July 1967).*
A simplified analysis of the response of pressure-sensing devices and their interconnecting tubing is presented. The results are conveniently presented in the form of time equations, with the fractional change in the applied step (usually 63.2%) as the variable. A single algebraic equation adequately predicts (within about ±20%) the response of simple pressure-measuring systems in the free molecule, transition and continuum flow regimes. Two very simple algebraic equations (for free molecule and continuum flow) may be used to predict time response throughout the flow regimes if a maximum error of about 2:1 (predicted time constants are 2 times too large) is tolerated in the mid-transition range. The criterion is given for extension of these formulae into the transition flow range. The formulae are limited to relatively small pressure steps in the viscous flow region (Poiseuille flow) and are not restricted for free molecule flow. All of the formulae developed are suitable for field engineering applications. The existing literature is synthesized by comparison with the analysis. The relative importance of the numerous variables encountered in this type of analysis is discussed.

Key Words: Response of pneumatic pressure-measurement systems in the free molecule, transition, and continuum flow regimes, response of pneumatic pressure-sensing tubulation, response of pneumatic transmission lines, time constants of pneumatic pressure lines, time lag and delay in pneumatic pressure-sensing lines, time response of pneumatic pressure-sensing systems to step inputs.

Rotational excitation of diatomic molecules by slow electrons; application to H_2, N. F. Lane and S. Geltman, *Phys. Rev.* **160,** *No. 1, 53–67 (Aug. 1967).*
The theory of electron scattering from a rigid rotator is applied to the case of low-energy scattering of electrons from hydrogen molecules in ground electronic and vibrational states. The coupled equations are solved numerically and the resulting S-matrix used to calculate elastic, rotational excitation, and rotational de-excitation cross sections. The electron-molecule interaction potential is based on the approximate charge distribution of H_2 and includes the effects of polarization, which are shown to be important. Cross sections are given for several rotational states, and it is pointed out that, while the elastic and inelastic cross sections are found to depend on the initial rotational angular momentum j of the molecule, their variation in j is such that the total cross section remains independent of j. The effects of "back-coupling" and coupling with higher rotational states are illustrated by comparing the results of the close-coupling calculation with those of the Born and distorted-wave methods; the distorted wave and close-coupling results for rotational excitation are found to agree within 20 percent for all energies.

Key Words: Electron scattering, rotational excitation, rigid rotator, diatomic molecules, H_2.

Stretch scheme, a shell-model description of deformed nuclei, M. Danos and V. Gillet, *Phys. Rev.* **161,** *No. 4, 1034–1044 (Sept. 20, 1967).*

A good angular momentum wave function containing the maximum possible intrinsic angular momenta leads to a microscopic description of the nuclear rotational spectra in terms of spherical shell model states. The rotational excitation energies arise from the residual two-body force. In the actual model calculations the only approximation was a partial violation of the exclusion principle. The computed departures from the $I(I+1)$ law are consistent with the experiment. Reasons are given for the preference of positive over negative intrinsic deformations.

Key Words: Nuclear rotation, nuclear structure, nuclear shell model, deformed nuclei, nuclear spectra, nuclear moments of inertia.

Superposition of configurations and atomic oscillator strengths—carbon I and II, A. W. Weiss, *Phys. Rev.* **162,** *No. 1, 71–80 (Oct. 5, 1967).*
Variational wavefunctions are computed for the ground state and a number of excited states of carbon I and II by the method of superposition of configurations. To accelerate convergence, the virtual orbitals are obtained from a psuedo-natural orbital transformation on a single electron-pair, out of all those possible within a given quantum shell. Expansions of up to 50 configurations are generated and used to study the effects of correlation on the oscillator strengths. The method appears to be fairly successful in correcting for most of the correlation error in both the energy and "correlation sensitive" oscillator strengths. Term values are substantially improved over the Hartree-Fock, and generally, although not always, *f*-values appear to be obtainable with an accuracy of about 25 percent.

Key Words: Superposition of configurations, oscillator strengths, atomic energy levels, wavefunctions.

Diminishing discoloration in methacrylate accelerator systems, R. L. Bowen and H. Argentar, *J. Am. Dental Assoc.* **75,** *No. 4, 918–923 (Oct. 1967).*
A method was devised for accentuating the formation of discoloration products that may form during the free radical polymerization of methacrylates at room temperature. Various accelerators and stabilizers were compared on an equimolar basis. The selection of the materials was based on literature information regarding current theories of free radical polymerization and the absorption of visible light by organic compounds. The use of the sterically hindered phenol, butylated hydroxytoluene, did not produce discoloration whereas, the use of hydroquinone or the monomethylether of hydroquinone had a darkening effect. A compound (N,N-dimethyl-3,5-dimethylaniline) was synthesized which was an effective accelerator and which produced less discoloration than did N,N-dimethyl-*p*-toluidene.

Key Words: Color formation, discoloration, methacrylate, polymerization *N,N*-dimethyl-3,5-dimethylaniline, accelerators.

Gas-phase photolysis of ethyl iodide at 2537 and 2288 Å. Reactions of hot ethyl radicals with added hydrocarbons, R. E. Rebbert and P. Ausloos, *J. Chem. Phys.* **47,** *No. 8, 2849–2855 (Oct. 15, 1967).*
The photolysis of C_2H_5I and C_2D_5I have been investigated at 2537 Å and 2288 Å in the presence of thermal alkyl radical scavengers such as O_2 and I_2. The ethane (quantum yields at 2537 Å: $\phi C_2H_6 = 0.82 \times 10^{-3}$, $\phi C_2D_6 = 0.29 \times 10^{-3}$) formed in such mixtures can be entirely ascribed to abstraction of a H (or D) atom by a "hot" ethyl radical formed in the primary dissociation of ethyl iodide. When C_2D_5I or C_2H_5I is photolyzed in the presence of a cyclo-C_6H_{12}-cyclo-C_6D_{12}-O_2 mixture (1:1:0.1), or of a cyclohexane-1,1,2,2,3,3-d_6-O_2 mixture, the relative probability for abstraction of an H atom versus that for abstraction of a D atom (π_H/π_D) is equal to 1.5 ± 0.1. Added gases do reduce the probability of the abstraction process. The relative quenching probability of the "hot" C_2D_5* radical by different additives is as follows: He—0.50; Na—0.62; N_2—1.00; and CO_2—1.51.
When C_2H_5I is photolyzed at 2537 Å in the presence of $CD_3CH_2CD_3$, $CH_3CD_2CH_3$ or $CD_3CH_2CH_2CD_3$ the relative probability per atom for the abstraction of a primary compared to a secondary H-atom in a hydrocarbon molecule by a hot ethyl radical is 1:4.5. Moreover, the quantum yield for ethane formation at 2537 Å per secondary hydrogen atom for a series of cycloalkanes and normal alkanes is $0.32 \pm 0.07 \times 10^{-3}$

Key Words: Photolysis, "hot" radicals, ethyl iodide, deactivation, alkyl radicals, hydrogen abstraction.

Matrix-isolation study of the reaction of carbon atoms with HCl. The infrared spectrum of the free radical HCCl, M. E. Jacox and D. E. Milligan, *J. Chem. Phys.* **47,** *No. 5, 1626–1633 (Sept. 1, 1967).*
The infrared spectrum of samples of cyanogen azide plus hydrogen chloride isolated in an argon or a nitrogen matrix at 14 °K and subjected to photolyzing radiation under conditions previously shown to lead to the production of carbon atoms includes features at 815 and 1201 cm^{-1} which may be assigned to the free radical HCCl. ^{13}C- and D-substitution experiments are consistent with this identification. A band system extending between about 7500 and 5600 Å corresponds to the band system previously reported for HCCl in the gas phase. These observations confirm the production of HCCl in the present experiments and indicate that the lower state of the transition observed for HCCl in the gas phase studies is the ground state. The force constants and thermodynamic properties of HCCl have been estimated. Evidence is presented for the reaction of NCN, a photolytic intermediate in the production of carbon atoms from cyanogen azide, with HCl to produce an incompletely characterized species, probably either monochlorocyanamide or monochlorocarbodiimide. HCCl reacts with HCl with little or no activation energy, leading to the stabilization of CH_2Cl_2.

Key Words: C atom reactions, cyanogen azide, electronic spectrum, force constants, HCCl free radical, HCl reaction, infrared spectrum, matrix isolation, monochlorocarbodiimide, monochlorocyanamide, NCN reactions, photolysis, thermodynamic properties.

Observing the effect of a change in mass on deBroglie wavelength: the 600-Å bands of $^3He_2$, A. L. Smith, *J. Chem. Phys.* **47,** *No. 4, 1561–1562 (Aug. 15, 1967).*
The band-like continuum emitted in the radiative deexcitation of singlet metastable ^3He by ^3He has been observed. This spectrum and the corresponding continuum in ^4He are interpreted as reflecting the structure of a standing deBroglie wave over an attractive potential well. The ^3He continuum contains one less maximum than does the ^4He continuum in the range $602 \text{ Å} < \lambda < 666 \text{ Å}$; i.e., for two particles of different mass moving with the same energy over the same attractive well, the lighter particle has the longer deBroglie wavelength. The shifts in peak positions are accounted for quantitatively by calculating the continuum-continuum band strengths of the $A\,^1\Sigma_u^+ \rightarrow X\,^1\Sigma_g^+$ transition of He_2 for both isotopes.

KeyWords: Continuum emission, diatomic molecule, He_2, helium isotopes, ultraviolet spectra, radiative deexcitation, quantum mechanics, deBroglie wavelength, band strengths.

Thermal titration of platinum black and the initial heat of adsorption for hydrogen, E. S. J. Tomezsko and G. T. Furukawa, *J. Catalysis* **8,** *No. 4, 386–388 (Aug. 1967).*
The heat of adsorption of hydrogen on platinum black was investigated by means of an automatically controlled adiabatic calorimeter. When the platinum black was carefully freed of adsorbed oxygen, no rapid decrease was observed in the heats of adsorption with increasing coverage of hydrogen. The heat of adsorption of hydrogen on clean platinum surface was found to be 17.5 (73.2 kj/mole) kcal/mole of hydrogen, with an estimated uncertainty of ± 0.2 kcal/mole (± 0.8 kj/mole).

Key Words: Adsorption of hydrogen on platinum black, heat of adsorption of hydrogen, platinum black, thermal titration.

Volume changes accompanying collagen denaturation, R. G. Christensen and J. M. Cassel, *Biopolymers* **5,** *685–689 (1967).*
A dilatometric technique is employed to measure the volume changes occurring on denaturation of collagen solutions and tendons. Partial specific volumes of tropocollagen are calculated to be 0.686 ml/g in water and 0.689 ml/g in 0.1M citrate buffer. From data on non-aqueous solutions, it is estimated that most of the volume change arises from changes in polymer configuration rather than from changes in solvation.

Key Words: Partial specific volume, collagen, dilatometry, denaturation, solvation, hydration.

Improving pressure and vacuum measurement standards, E. C. Lloyd, *Instr. Control Systems* **40,** *No. 9, 105–109 (Sept. 1967).*
Results of NBS developments are outlined in a number of projects relating to standards for improved measurement of pressures throughout the range from vacuum to very-high pressures. In the vacuum range this includes techniques for generation of stable reference pressures, and improved absolute instruments for force per unit area measurement down to 10^{-9} torr. In the range from a few millibars to hundreds of kilobars the use of fixed points, and the performance of improved piston gages and interpolation instruments, are described. Problems presently limiting accuracy of calibration and NBS investigations of possible solutions are mentioned. Two new "accuracy charts" are presented showing present and possible future NBS capabilities.

Key Words: Standards, calibration, measurement, pressure, vacuum, accuracy.

Configuration of isolated polymer molecules adsorbed on solid surfaces studied by Monte-Carlo computer simulation, F. L. McCrackin, *J. Chem. Phys.* **47,** *No. 6, 1980–1986 (Sept. 15, 1967).*
The configurations of adsorbed polymer molecules with excluded volume were simulated on a four-choice simple cubic lattice using a computer. The average values of the fraction of segments on the surface, loops off the surface, normal distance of the end of the molecule from the surface, root-mean-square of the normal distance, maximum normal distance from the surface, and root-mean-square end-to-end distance were calculated for various lengths of the molecules and attractive energies to the surface. When these averages over the configurations are compared with previous results which had neglected the excluded volume effect and important differences are found.

Key Words: Adsorption, configurations, four-choice cubic lattice, Monte Carlo, polymers.

Ears on the line profile of decay transitions in a gas laser, W. G. Schweitzer, Jr., M. M. Birky, and J. A. White, *J. Opt. Soc. Am.* **57,** *No. 10, 1226–1230 (Oct. 1967).*
In a gas laser a spectrum line whose upper state is the lower state of the laser transition may contain a structure due to the laser action. We have observed this structure, which we refer to as *ears*, on the 6096 Å Neon line emitted spontaneously in a 1.15 μm He-Ne laser. The width of the *ear* was measured interferometrically and compared with the width predicted from the phenomenological width ν_{ab}/π in the laser transition.

Key Words: Laser, line profile, lifetime, neon.

Entropy and susceptibility of a pure dipole-dipole substance, J. R. Peverley and P. H. E. Meijer, *Phys. Stat. Sol.* **23,** *No. 1, 353–360 (1967).*
Recalculation of the lattice sums for a pure dipole-dipole interaction show that the Curie-Weiss constant, for fields perpendicular to the *C*-axis is equal to 0.273 millidegrees for cerous magnesium nitrate. A *g* value of 1.82 was used. The temperature dependence of the entropy was determined and is compared with the experimental values of Hudson and Kaeser.
All lattice sums have been determined as a function of slight changes in the lattice constants. The *z*-component of the dipolar lattice sum is determined by means of a new procedure to improve the slow convergence of this series.

Key Words: Cerous magnesium nitrate, Curei-Weiss constant, dipole-dipole interaction (pure), entropy, lattice sums, magnetic susceptibility, transition temperature.

Inelastic scattering of kilovolt electrons by solids and liquids: determination of energy losses, cross sections, and correlations with optical data, C. J. Powell, *Health Phys.* **13,** *No. 12, 1265 (1967).*
Some recent measurements of the inelastic scattering of kilovolt electrons by solids and liquids are described. The determination of energy losses and cross sections is discussed as well as factors influencing the accuracy of measurement. The degree of correlation between optical and electron energy loss experiments also is described.

Key Words: Characteristic energy losses, comparison with optical data, cross sections, inelastic scattering, kilovolt electrons, liquids, solids.

N_2O bond dissociation energy by photon impact, V. H. Dibeler, *J. Chem. Phys.* **47,** *No. 6, 2191–2192 (Sept. 15, 1967).*
A brief report is made of the dissociative ionization of N_2O to give the N_2^+ ion from ordinary and from ^{15}N-labeled material. The latter is employed to avoid the effects of nitrogen impurity. The resulting experimental value of $D(N_2\text{-}O) = 39.0$ kcal mol^{-1} is in good agreement with the value calculated from heats of formation.

Key Words: Photoionization, bond-dissociation energy, N_2O, N_2^+.

Nuclear magnetic resonance in sodium thallide, L. H. Bennett, *Acta. Met.* **14,** *No. 8, 997–999 (1966).*
The nuclear magnetic resonance signal for $Tl^{203, 205}$ is observed in sodium thallide alloys. It is determined that the previously reported negative Knight shift value of one percent for NaTl was essentially correct, and the more recently reported negative value of one-half percent was in fact for $NaTl_2$. A crystal structure is proposed for $NaTl_2$.

Key Words: Nuclear magnetic resonance, sodium, thallium, alloys, intermetallic, compounds, x-ray diffraction, Knight shift.

Mass-spectrometric study of photoionization. VI. O_2, CO_2, COS, and CS_2, V. H. Dibeler and J. A. Walker, *J. Opt. Soc. Am.* **57,** *No. 8, 1007–1012 (Aug. 1967).*
Photoionization efficiency curves are obtained for the molecule and fragment ions of the subject molecules in the wavelength region extending from onset of ionization to 600 Å. The initial onset of O_2^+ is observed at 12.072 eV. Autoionization in the continuum is correlated with various progressions of Rydberg series. Curves for both O^+ and O^- ions formed by the ion-pair process from O_2 are obtained and 1.48 eV is derived for the electron affinity of oxygen atoms. The shape of the CO_2^+ curve including structure ascribed to autoionization is discussed. The unresolved $^2\Pi_g$ doublet threshold is observed at 13.77 eV with the first vibrational level at 13.93 eV. The onset of the O^+ fragment ion indicates about 0.04 eV excess energy in the dissociation process. It is suggested that dissociative ionization occurs from the autoionizing Rydberg level just above the calculated threshold value. Partially resolved doublet components of COS^+ are observed at 11.18 and 11.22 eV, respectively. Intense autoionization is observed. Various thermochemical values are calculated from the fragment ion thresholds. The doublet components of the ion ground state of CS_2^+ are observed at 10.059 and 10.12 eV, respectively. Intense autoionization is observed at wavelengths which are in excellent agreement with known Rydberg levels for the molecule. Although the S^+ ion is formed with excess energy, the CS^+ ion gives a value of 11.71 eV for the ionization energy of the CS radical. This is in agreement with, but more precise than, a directly measured electron impact value.

Key Words: Photoionization, autoionization, Rydberg series, electronic, excited states, ionization thresholds, mass spectrometry, vacuum ultraviolet, heats of formation, ions, radicals, O_2, CO_2, COS, CS_2.

Nuclear quadrupole resonance thermometry, D. B. Utton, *Metrologia* **3,** *No. 4, 98–105 (Oct. 1967).*
The nuclear quadrupole resonance frequency of ^{35}Cl in $KClO_3$ has been studied in the temperature range 12 °K–297 °K. The combined uncertainties in the frequency and temperature measurements correspond to ±.001 °K in the range 50 °K–297 °K, deteriorating to ±.004 °K at 30 °K and ±.010 °K at 20 °K. Both the nuclear resonance spectrometer and the temperature control apparatus are described. The experimental data are fitted to a theoretical expression in the temperature range 12 °K–90 °K; at higher temperatures the data are fitted to empirical polynomials.

Key Words: Nuclear quadrupole resonance thermometry 12 °K–297 °K, potassium chlorate, instrumentation.

Nuclear magnetic resonance in zintl intermediate phases LiCd and LiZn, L. H. Bennett, *Phys. Rev.* **150,** *No. 2, 418–420 (Oct. 1966).*

The nuclear magnetic resonances have been observed for Li^7 and Cd^{113} in LiCd and for Li^7 and Zn^{67} in LiZn. The Knight shift for $LiCd^{113}$ is 0.39% for $LiZn^{67}$ 0.20%, for LiCd or LiZn less than 0.01%. An energy band scheme is proposed.

Key Words: Zintl phase, LiCd, LiZn, B–32 structure, nuclear magnetic resonance, Knight shifts, linewidths.

Stochastic theory of multistate relaxation processes, I. Oppenhein, K. E. Shuler, and G. H. Weiss, *Adv. Mol. Relaxation Processes* **1,** *No. 1, 13–68 (Nov. 1967).*
The stochastic theory of multistate relaxation processes is discussed with special reference to Markov Processes, the derivation and properties of the Master Equation, the derivation and properties of the Fokker-Planck Equation and First Passage Time problems. The theory developed is then applied to a number of examples.

Key Words: Stochastic processes, relaxation processes, Markov processes, Fokker-Planck equation, master equation, first passage times.

SU(3), meson-baryon scattering, and asymptotic limits, S. Meshkov and G. B. Yodh, *Phys. Rev. Letters* **19,** *No. 10, 603–608 (Sept. 4, 1967).*
The meson-baryon total cross sections and elastic scattering data in the forward direction are fitted using SU(3) invariant t-channel amplitudes. The analysis implies: (1) $0 \leq \sigma_{\text{Tot}}(s \to \infty) \leq 10$ mb, and; (2) $-0.11 \leq \text{Real } T(s,t=0)/\text{Im } T(s,t=0) \leq 0$ as $s \to \infty$.

Key Words: Scattering, mesons, asymptotic, SU(3), baryons, reaction.

Transitions in vapor-deposited alumina from 300 to 1200 °C, A. L. Dragoo and J. J. Diamond, *J. Am. Ceram. Soc.* **50,** *No. 11, 568–574 (Nov. 1967).*
The transition of amorphous alumina to α-alumina was studied by x-ray diffraction, electron diffraction, DTA, TGA, and microscopic observation. The amorphous alumina was prepared by evaporation of molten alumina *in vacuo* and its deposition on the glass envelope of the vacuum chamber. Two transition paths were observed after the amorphous alumina passed through an initial crystallization region (between 570 and 670 °C at 16 hours). The principal sequence was γ-, to δ- to α-alumina. A minor amount of θ-alumina developed from the initial crystallization and persisted throughout the duration of the former sequence as a parallel path. Some conversion of δ- to θ-alumina was detected above 900 °C. DTA produced an unexplained exothermic peak at 320 °C and a second exothermic peak at 860 °C which corresponded to formation of metastable aluminas.

Key Words: Alumina, alpha alumina, amorphous alumina, delta alumina, gamma alumina, intermediate aluminas, metastable aluminas, phase transitions, theta alumina.

Selected tables of atomic spectra. Atomic energy levels and multiplet tables Si I, C. E. Moore, *NSRDS–NBS* **3,** *Sect. 2 (Nov. 30, 1967), 20 cents.*
The present publication is the second Section of a series being prepared in response to the increasing demand for a current revision of two sets of tables containing data on atomic spectra as derived from analyses of optical spectra.
Both the atomic energy levels and the multiplet table are included in the same publication, as parts A and B, respectively. The Sections are being prepared at irregular intervals for these spectra whose analyses are essentially complete. A flexible paging system permits the arrangement of the various Sections by atomic number regardless of the order in which the spectra are published in this series. Section 1 included three spectra of silicon, Z = 14: Si II, Si III, Si IV. The present Section contains similar data for Si I. The form of presentation is described in detail in the text to Section 1, and need not be repeated here.

Key Words: Atomic energy levels; atomic spectra SiI; multiplet table; silicon, first spectrum; spectrum, SiI; wavelengths, SiI.

Tables of bimolecular gas reactions, A. F. Trotman-Dickenson and G. S. Milne, *NSRDS–NBS* **9** *(Oct. 27, 1967), $2.00.*
This survey covers the kinetics of bimolecular and thermolecular gas reactions that do not involve atoms or molecules in electronically excited states. Bimolecular reactions are here defined as reactions in which two molecules are involved as reactants, that yield two or more molecules as products. Those reactions in which two molecules combine to form one molecule are most usefully considered as the reverse of unimolecular reactions which will be dealt with in another survey. Reactions of oxygen and nitrogen atoms have been omitted as they will also form the subject of another survey.
The literature from 1954 to December 31, 1965 has been exhaustively searched and it is hoped that for this period nothing has been omitted that should have been included.
The survey of earlier work has been based on one of the writers' books on "Gas Kinetics" which covered the literature to 1954. Use of the book for over ten years has revealed few omissions and these have been included in these tables. Data for the period January to August 1966 has been included where possible.

Key Words: Chemical kinetics, gas, bimolecular, reactions, tables, rate constants, activation energies, Arrhenius equation, data.

Tabulation of data on microwave tubes, J. K. Moffitt, *Handb. 104 (Sept. 29, 1967), $1.25. Supersedes Handb. 70.*
A tabulation of microwave electron tubes with characteristics of each type has been arranged in the form of two major listings, a Numerical Listing in which the tubes are arranged by type number, and a Characteristic Listing in which the tubes are arranged by the kind of tube, and further ordered on the basis of minimum frequency and power output.

Key Words: Characteristics tabulation; microwave electron tubes; numerical.

Tabulation of data on receiving tubes, J. K. Moffitt, *Handb. 103 (Sept. 29, 1967), $1.25. Supersedes Handb. 83.*
A tabulation of Receiving-Type Electron Tubes with some characteristics of each type has been prepared in the form of two major listings, a Numerical Listing in which the tubes are arranged by type number, and a Characteristic Listing in which the tubes are arranged by tube type and further ordered on the basis of one or two important parameters. The tabulation is accompanied by a listing of similar tube types and basing connections for the listed tubes.

Key Words: Basing connections; characteristics; electron tubes; numerical; receiving-type; similar types; tabulation.

The hyperbolic character of certain experimental results which tend toward limiting values, A. F. Kirstein, *Tech. Note 435 (Nov. 1967), 15 cents.*
The hyperbolic character of certain experimental data obtained from structural and mechanical testing provides an extremely simple graphical method for use in approximating the limiting values associated with the data. The method, developed by Southwell to explain the behavior of eccentrically loaded thin elastic struts, is shown to have much wider application. A limited number of illustrations are given to describe the method and to show how it might be used as a research tool.

Key Words: Experimental, graphical solution, hyperbolic character, limiting values.

Other NBS Publications

J. Res. NBS 72B (Math. Sci.), No. 1 (Jan.–Mar. 1968), 75 cents. (Formerly Mathematics and Mathematical Physics).

Means and the minimization of errors. M. Aissen.
On Taylor's theorem. O. Shisha.
Principal submatrices III: Linear inequalities. R. C. Thompson.
The diophantine equation $P(x, y) = (xy + d)z$. C. F. Osgood.
A note on the G-transformation. H. L. Gray and T. A. Atchison.
The distribution of the sample correlation coefficient with one variable fixed. D. Hogben.
Solutions of the time-dependent Klein-Gordon and Dirac equations for a uniform electric field. V. W. Myers.

Analysis of a market split model. J. M. McLynn, A. J. Goldman, P. R. Meyers, and R. H. Watkins.

Citation searching and bibliographic coupling with remote on-line computer access. F. L. Alt and R. A. Kirsch.

Simple analytic expressions for the total Born approximation cross section for pair production in a coulomb field. L. C. Maximon.

Operations research. Proceedings of a conference for Washington area government agencies, April 20, 1966, Ed. J. A. Joseph, Misc. Publ. 294 (Dec. 1967), 25 cents.

Contribution of thermal noise to the line-width of Josephson radiation from superconducting point contacts, A. H. Silver, J. E. Zimmerman, and R. A. Kamper, Appl. Phys. Letters **11,** No. 6, 209–211 (Sept. 15, 1967).

Electron diffraction studies of active, passive, and transpassive oxide films formed on iron, C. L. Foley, J. Kruger and C. J. Bechtoldt, J. Electrochem. Soc. **114,** No. 10, 994–1001 (Oct. 1967).

Machine oriented fingerprint classification system, J. H. Wegstein and J. F. Rafferty, Proc. First Natl. Symp. Law Enforcement Science and Technology, March 7–9, 1967, Chicago, Illinois, Ed. S. A. Yefsky, 1, Chapt. V. Information Storage and Retrieval, 459–465 (Academic Press Inc., New York, N.Y., 1967).

Pair production by photons on electrons, K. J. Mork, Phys. Rev. **160,** No. 5, 1065–1071 (Aug. 1967).

Probability distribution of the radius of gyration of a flexible polymer, S. R. Coriell and J. L. Jackson, J. Math. Phys. **8,** No. 6, 1276–1284 (June 1967).

Metallo-organic polymers, E. Horowitz, Mod. Plastics **45,** No. 3, 146–148 (Nov. 1967).

Structure, isomerization, and cleavage of 1,2-bis(dichloroboryl)ethylene, T. D. Coyle and J. J. Ritter, J. Am. Chem. Soc. **89,** 5739–5740 (1967).

Analysis of rotationally misaligned stators in the rotary-vane attenuator, W. Larson, IEEE Trans. Instr. Meas. **IM-16,** No. 3, 225–231 (Sept. 1967).

Development of a method for testing and rating refrigerated truck bodies, C. W. Phillips and R. W. Penny, USDA Tech. Bull. No. 1376 (Superintendent of Documents, Government Printing Office, Washington, D.C. 20402, Sept. 1967, 15 cents).

Experimental apparatus and procedures for evaluating parameters affecting the pumping efficiency of a cryogenically cooled plane, L. O. Mullen and M. J. Hiza, J. Vacuum Sci. Technol. **4,** No. 5, 219–229 (Sept.–Oct. 1967).

Forty years of precise measurement, W. G. Brombacher, Instr. Control Systems **40,** No. 9, 87–92 (Sept. 1967).

User reaction as a system design tool at CFSTI, P. F. Urbach, Proc. Fourth Annual National Colloquium on Information Retrieval, May 3–4, 1967, Ed. A. B. Tonik, pp. 7–18 (International Information, Inc., Philadelphia, Pa., 1967).

Sapphire window mountings for low temperature spectroscopy, L. J. Schoen, Rev. Sci. Instr. **38,** No. 10, 1531–1532 (Oct. 1967).

Lunar tides in the ionosphere, S. Matsushita, Encyclopedia of Physics **XLIX/2,** 547–602 (Springer-Verlag, Berlin, Germany, 1967).

**Publications for which a price is indicated are available by purchase from the Superintendent of Documents, U.S. Government Printing Office, Washington, D.C. 20402 (foreign postage, one-fourth additional). The NBS non-periodical series are also available from the Clearinghouse for Federal Scientific and Technical Information, Springfield, Va. 22151. Reprints from outside journals and the NBS Journal of Research may often be obtained directly from the authors.*

U.S. GOVERNMENT PRINTING OFFICE : 1968 OL—293-857

JSR-A OCT 46129
UNIVERSITY MICROFILMS INC
ATTN SERIALS SECTION
300 NORTH ZEEB RD
ANN ARBOR MICH 48106

UNITED STATES
GOVERNMENT PRINTING OFFICE
DIVISION OF PUBLIC DOCUMENTS
WASHINGTON, D.C. 20402
OFFICIAL BUSINESS

POSTAGE AND FEES PAID
U.S. GOVERNMENT PRINTING OFFICE

JOURNAL OF RESEARCH of the National Bureau of Standards Vol. 72A, No. 3 May–June 1968
A. Physics and Chemistry

Contents

Page

Jump rates for point defects in special positions held by a trapping center of noncubic symmetry. H. S. Peiser and J. B. Wachtman, Jr. 231

The thermodynamics of the ternary system: water-potassium chloride-calcium chloride at 25 °C. R. A. Robinson and A. K. Covington. 239

Force field for SiF_4. Ira W. Levin and Stanley Abramowitz. 247

Blemish formation in processed microfilm. C. I. Pope. 251

Absolute isotopic abundance ratios of common, equal-atom, and radiogenic lead isotopic standards. E. J. Catanzaro, T. J. Murphy, W. R. Shields, and E. L. Garner. 261

Role of nickel in Al–10 percent Si composites containing nickel-coated sapphire whiskers. H. Yakowitz, W. D. Jenkins, and H. Hahn. 269

Publications of the National Bureau of Standards. 273

Library of Congress Catalog Card Number: 62-37059

For sale by the Superintendent of Documents, U.S. Government Printing Office, Washington, D.C. 20402. Price $1 (single copy).
Subscription price: $5 a year; $1 additional for foreign mailing.
UNITED STATES GOVERNMENT PRINTING OFFICE, WASHINGTON : 1968